Mechanistic Insights into Necroptosis of Macrophages

Erin Lauren Cessford

Thesis submitted to the
Faculty of Graduate and Postdoctoral Studies
In partial fulfillment of the requirements
For the MSc degree in Microbiology and Immunology

Department of Biochemistry, Microbiology and Immunology

Faculty of Medicine

University of Ottawa

ABSTRACT

Cell death is an imperative mechanism for the development, homeostasis and survival of an organism. Various forms of cell death have been documented and recent reports indicate that the mode of cell death elicited can have a profound influence on the development and perpetuation of inflammation. Apoptosis is the predominant, programmed pathway of cell death, which ensures physiological elimination of unwanted cells. On the other hand, another cell death pathway described as programmed necrosis (necroptosis), has recently been revealed. The induction of necroptosis and its impact in host biology is not clear. Herein I have evaluated the mechanisms of necroptosis in macrophages, an important cell type of the immune system. My experiments indicate that type I interferon (IFN-I) signaling through transcription factors STAT1, STAT2 and IRF9, collectively described as the ISGF3 complex, is indispensable for necroptosis of macrophages. Furthermore, my results indicate that IFN-I signaling promotes the sustained phosphorylation of receptor interacting protein kinase 3 (Rip3), a key protein required for the execution of necroptosis. My findings also reveal that dynamin-dependent endocytosis following IFNβ stimulation and caspase inhibition is necessary for the induction of necroptosis. The results presented in this thesis provide new insights into the molecular mechanisms of necroptosis and therefore contribute to a deeper understanding of multiple inflammatory pathologies.

ACKNOWLEDGMENTS

I would like to begin by acknowledging my supervisor Dr. Subash Sad. I want to sincerely thank you for all of your guidance and unfailing support. You have taught me many lessons, in life and in science, over the last few years and I am extraordinarily grateful. It has truly been a privilege to work in your laboratory. I would also like to extend a sincere thank you to my thesis advisory committee members Dr. Robert G. Korneluk and Dr. Kathryn Wright. I genuinely appreciate all of the support and advice provided.

To Dr. Scott McComb, your enthusiasm and passion for science is both infectious and inspiring. Your advice and patient guidance in teaching me both lab techniques and concepts of cell death has been invaluable over the course of my graduate studies. A huge thank you also to all of the Sad lab members for your thought provoking discussions and useful advice. Dr. Julie Joseph - thank you for your friendship and for also keeping me sane during times of insanity.

Lastly, I would of course like to thank all of my family and friends. I cannot put into words how unbelievably lucky I am to have such a strong support system from my parents and two sisters. Mom, Dad, Katlyn and Kristen, my success and accomplishments are a direct result of your unconditional love and encouragement – I am eternally grateful.

Research funds were provided by grants awarded to Dr, Subash Sad from the Canadian Institute of Health Research (CIHR).

TABLE OF CONTENTS

LIST OF ABBREVIATIONS

APAF-1	Apoptotic Protease Activating Factor 1
BCL-2	B-Cell Lymphoma Protein-2
BMDM	Bone Marrow Derived Macrophage
cIAP(1/2)	Cellular Inhibitor of Apoptosis
CYLD	Cylindromatosis
DAMP	Danger Associated Molecular Pattern
DD	Death Domain
DED	Death Effector Domain
ELISA	Enzyme-linked Immunosorbent Assay
FLIP	FLICE-Like Inhibitory Protein
Fn14	Fibroblast Growth Factor-Inducible 14
GAS	Gamma Activated Site
IFN	Interferon
IFN-I	Type I Interferon
IFNAR	Interferon α/β Receptor
IKK	Inhibitor of Nuclear Factor Kappa-B Kinase
IL-6	Interleukin 6
IL-10	Interleukin 10
IRF	Interferon Regulatory Factor
IRFBS	IRF Binding Site
ISG	Interferon Stimulated Gene
ISGF3	Interferon Stimulated Gene Factor 3
ISRE	Interferon-Stimulated Response Element
JAK1	Janus Kinase 1
KO	Knockout
LPS	Lipopolysaccharide
M-CSF	Macrophage Colony Stimulating Factor
MLKL	Mixed Lineage Kinase domain-Like Protein
MPT	Mitochondrial Permeability Transition
MTT	3-(4,5-dimethylthiazol-2-yl)-2,5-diphenyltetrazolium bromide
MyD88	Myeloid Differentiation Primary Response Gene 88
NEMO	NFκB Essential Modulator
NFκB	Nuclear Factor Kappa-light-chain-enhancer of Activated B Cells
NIK	NFκB Inducing Kinase
PAMP	Pathogen Associated Molecular Pattern
PBS	Phosphate Buffered Saline
PCD	Programmed Cell Death
PI	Propidium Iodide
PIP	Phosphatidylinositol Phosphate
PM	Plasma Membrane
PS	Phosphatidylserine
PolyI:C	Polyinosinic-polycytidylic Acid
PRR	Pattern Recognition Receptor

R8	RPMI with 8% Fetal Bovine Serum
RHIM	Rip Homotypic Interaction Motif Domain
RIP(1/3)	Receptor Interacting Protein Kinase
RPMI	Roswell Park Memorial Institute Medium
SBE	STAT Binding Element
SIRS	Systemic Inflammatory Response Syndrome
SM	SMAC mimetic
SMAC	Secondary Mitochondrial Activator of Cell Death
ST	*Salmonella enterica* serovar Typhimurium
STAT	Signal Transducers and Activators of Transcription
TBK1	Tank-Binding Kinase 1
TAB2	Transforming Growth Factor-Beta Activated Kinase 1 Binding Protein 2
TAK1	Transforming Growth Factor-Beta-Activated Kinase 1
TBS	Tris Buffered Saline
TBST	Tris Buffered Saline with Tween
TGF	Transforming Growth Factor
TIRAP	Toll-interleukin 1 Receptor Domain Containing Adaptor Protein
TLR	Toll Like Receptor
TNF	Tumor Necrosis Factor
TNFR	Tumor Necrosis Factor Receptor
TRADD	TNFR Associated Death Domain Protein
TRAF	TNFR Associated Factor
TRAIL	TNF Related Apoptosis Inducing Ligand
TRAM	TRIF Related Adaptor Molecule
TWEAK	TNF Like Weak Inducer of Apoptosis
TYK2	Tyrosine Kinase 2
TRIF	TIR-domain Containing Adapter Inducing IFN-ß
WT	Wild-Type
xIAP	x-Linked Inhibitor of Apoptosis
zVAD	Benzyloxycarbonyl-Val-Ala-Asp-fluoromethylketone Pan-Caspase Inhibitor

LIST OF FIGURES AND TABLES

1.0 INTRODUCTION

It is difficult to overstate the importance of cell death as the human body eliminates approximately 60 billion cells on a daily basis just to maintain homeostasis (Han and Ravichandran, 2011; Liu et al., 2013). Without cell death the existence of life would be impossible. Development, homeostasis, immunity and disease progression are only a few of the many examples in which cell death plays a vital role within complex multicellular organisms (Han et al., 2011). A delicate balance must be maintained between mitotic cell growth and programmed cell death (PCD) (Evan and Littlewood, 1998). Dysregulation of this homeostatic balance can have profound influences on the pathogenesis of various diseases. For example, insufficient PCD can result in cancer, autoimmunity and severe pathogenic infections, while enhanced PCD can lead to chronic degenerative diseases, immunodeficiency and detrimental inflammatory conditions (Danial and Korsmeyer, 2004).

The cell death research field has become one of the most intensively studied fields of biology (Clarke and Clarke, 2012). As a result, cell death research has seen dramatic advancement over the last few decades and continues to generate a high level of interest amongst scientists. Many different modes of cell death have been reported, however the two most extensively studied cell death mechanisms are apoptosis and necrosis. Morphologically and physiologically, these two modes of cell death are quite distinct. Apoptosis is generally considered to be a physiologically silent (non-inflammatory) form of cell death while necrosis ignites an extremely robust inflammatory response (Khan et al., 2014; Liu et al., 2013). For many years necrosis was seen as an accidental or uncontrolled mode of cell death occurring only in response to extreme physiochemical insults, such as heat, osmotic shock and mechanical stress (Kaczmarek et al., 2013; McCall, 2010). Interestingly however, over

the last 10 years a flurry of evidence has shed light on the existence of a genetically encoded and tightly regulated form of necrotic cell death now known as necroptosis (Degterev et al., 2005).

The discovery of this highly inflammatory programmed form of necrotic cell death has given rise to the exciting possibility of new therapeutic avenues that have the potential to prevent and even treat various inflammatory pathologies such as sepsis, rheumatoid arthritis, multiple sclerosis and ischemia reperfusion injury (Ajami et al., 2011; Degterev et al., 2005; Duprez et al., 2011; Kim and Li, 2013; Northington et al., 2011). In this thesis I will describe the work I have done to investigate the intracellular mechanisms of necroptosis in macrophages.

1.1 The Immune System

The immune system is akin to a battleground where cell death is a common occurrence that can have a major impact depending on the nature of infection or disease. The study of immunology emerged in the late 18th century when English physician Dr. Edward Jenner made the pivotal observation that exposure to cowpox, a less virulent human disease, provided protection against smallpox, a highly virulent and often lethal human disease (Murphy et al., 2008). This revolutionary discovery resulted in the advent of vaccinations and many years later eventually led to the eradication of smallpox (Murphy et al., 2008). The early findings of Jenner and many other scientists, such as Robert Koch and his discovery that microorganisms cause disease, Louis Pasteur's rabies vaccine and Elie Metchnikoff's discovery of macrophages, has led to a much deeper understanding of the immune system and has paved the way for groundbreaking immunological research (Murphy et al., 2008).

The immune system is a remarkable protective mechanism within the body that evolved in response to the harmful effects of infectious microorganisms (Medzhitov and Janeway, 1997). As a result, multicellular organisms are now equipped with an army of different cell types, molecules and structures that are able to recognize and destroy invading microbes, thereby preventing harmful infections (Medzhitov and Janeway, 1997; Murphy et al., 2008). The immune system can be segregated into two main sections: innate immunity and adaptive immunity (Medzhitov, 2007). The evolutionarily ancient innate immune response acts as one of the first lines of host defense against invading pathogens (Medzhitov, 2001). Within minutes to hours of pathogen entry, the innate immune response is alerted (Murphy et al., 2008). The innate detection process relies on germline-encoded receptors that are able to recognize common, typically invariant, molecular components conserved amongst a variety of infectious agents. More specifically, vertebrate immune cells have cell surface pattern recognition receptors (PRRs), such as toll-like receptors (TLRs), NOD-like receptors. RIG-I-like receptors and C-type lectin receptors, which broadly recognize specific pathogen associated molecular patterns (PAMPs) (Takeuchi and Akira, 2010). An example of this is lipopolysaccharide (LPS), a common cell wall component of gram-negative bacteria, which upon engagement with TLR4 on the surface of innate immune cells such as macrophages, dendritic cells, monocytes and neutrophils, leads to the induction of inflammatory responses that promote clearance of the bacteria (Dranoff, 2004).

In contrast to the innate response, the adaptive immune response is much slower, requiring several days to develop (Baxter, 2007). Instead of recognizing broadly expressed PAMPs that are common to a variety of microorganisms, the adaptive immune response is mediated by clonal selection and expansion of pathogen-specific lymphocytes, such as B cells, $CD4^+$ and $CD8^+$ T cells (Murphy et al., 2008). Unlike the germline-encoded receptors

utilized in the innate response, adaptive immunity relies on the generation of a random and extremely diverse repertoire of antigen receptors in each individual (Medzhitov, 2001; Medzhitov and Janeway, 1997). A defining characteristic of the adaptive response is the capacity to generate immunological memory (Murphy et al., 2008). Following the initial exposure to a particular pathogen, the adaptive immune response is able to generate memory lymphocytes specific to that pathogen (Murphy et al., 2008). If re-exposed to the same pathogen a rapid and extremely robust response will take place, ultimately providing long-lasting protective immunity (Murphy et al., 2008).

1.1.1 Macrophages

Macrophages are large mononuclear cells of the innate immune system, which are found ubiquitously throughout the various tissues of the body (Murphy et al., 2008; Wynn et al., 2013). Originating in the bone marrow as pluripotent hematopoietic stem cells, macrophages undergo several stages of differentiation before developing into functional tissue resident macrophages (Volkman and Gowans, 1965). Pluripotent hematopoietic stem cells differentiate into common myeloid progenitors, which have the ability to differentiate into several different cell types, such as neutrophils, eosinophils and monocytes (Gordon and Taylor, 2005; Murphy et al., 2008). Following further differentiation and release into the blood stream, the common myeloid progenitor differentiates into a monocyte, another important innate immune cell type (Murphy et al., 2008). The monocyte remains in circulation for approximately three days before entering a tissue in response to various cytokines, chemokines and stimuli to finally mature into a macrophage with a half-life ranging from a few days to several months (Gordon and Taylor, 2005; Kuroda, 2010).

Interestingly, macrophages are a heterogeneous cell type, which is largely due to the fact that macrophages can reside in a variety of microenvironments (Gordon and Taylor, 2005). Based on anatomical location, macrophages become functionally specialized in order to optimize the immune response (Gordon and Taylor, 2005). For example, alveolar macrophages highly express PRRs and scavenger receptors, as they continuously come in contact with airborne pathogens (Palecanda et al., 1999; Taylor et al., 2002; Gordon and Taylor, 2005), while macrophages localized within the gut have been shown to be highly phagocytic and bactericidal but with attenuated production of pro-inflammatory cytokines to maintain the balance between helpful and harmful bacteria and also to avoid tissue damage induced by excessive inflammation (Gordon and Taylor, 2005; Smythies et al., 2005).

Functionally, macrophages are remarkably diverse. These vital cells partake in biological processes ranging from development, to bone remodeling, and of course immunity (Morrissette et al., 1999). One of the best-known functions of a macrophage is the ability to ingest large particles (>0.5 μm) through a process called phagocytosis (Aderem and Underhill, 1999). Phagocytosis, derived from the Greek terms 'phagein', meaning to eat, 'kytos', meaning cell and 'osis', meaning process, is a dynamic actin-dependent process that involves the extension of cytoplasmic lobes (Aderem and Underhill, 1999; Russell et al., 2013). Phagocytosis typically occurs when a macrophage, which is constantly surveying the environment for particulate matter, comes in contact with an infectious microorganism or cellular debris (Aderem and Underhill, 1999). For many species, phagocytosis is a cornerstone of early innate immunity (Stuart and Ezekowitz, 2008).

Following microbial detection, the macrophage membrane and actin cytoskeleton rearrange thereby allowing the macrophage to surround and engulf the pathogen into an internal vesicle called a phagosome (Murphy et al., 2008). Once formed, the phagosome

begins to mature by undergoing a series of fusion and fission events with early and late endosomes (Aderem and Underhill, 1999). Eventually the phagosome fuses with a lysosome, an intracellular membrane enclosed vesicle comprised of granules, enzymes, proteins and peptides, forming what is called a phagolysosome (Murphy et al., 2008). Fusion with early and late endosomes traffics acid hydrolases, such as cathepsin H and S respectively, from the endocytic compartments to the phagosome, while fusion with a lysosome releases the lysosomal contents that can destroy the pathogen into the phagosome (Aderem and Underhill, 1999). Together these processes result in the generation of an acidic and hydrolytic phagolysosomal environment that is unfavorable to many harmful microorganisms without affecting macrophage integrity or homeostasis (Stuart and Ezekowitz, 2008).

1.2 Endocytosis

Endocytosis is a mechanism by which cells are able to survey the environmental milieu, pick up apoptotic bodies or debris and transduce signals intracellularly (Kumari et al., 2010). Within multicellular organisms, endocytosis is a key process for cell and tissue function (Kumari et al., 2010). In most cell types, endocytosis is a common process that is typically characterized by the import of smaller molecules (< 200 nm) (Kumari et al., 2010). In contrast to endocytosis, internalization by phagocytosis occurs at a much larger scale and has generally been considered to be restricted to a subset of immune cells with antibacterial activity (described in section 1.1.1) (Kurmari et al., 2010). Some studies however argue that phagocytic uptake can occur equally well in phagocytic cell types, such as macrophages and neutrophils, and non-phagocytic cell types lacking antibacterial activity, such as fibroblast, epithelial and endothelial cells, which rely on similar molecular mechanisms to phagocytose particulate material (Groves et al., 2008).

Broadly, two distinct yet related endocytic pathways have been identified in the eukaryotic system: bulk-phase endocytosis or pinocytosis ('cell drinking'), which is the nonspecific uptake of extracellular fluid and any molecules that happen to be present, and receptor-mediated endocytosis, which occurs following ligand-receptor binding (Russell et al., 2013). In regards to receptor-mediated endocytosis, pathways can be characterized by corresponding coat proteins that reinforce the cytoplasmic side of the membrane (Russel et al., 2013). For example, clathrin was one of the first coat proteins to be discovered and is an important component in clathrin-mediated endocytosis (Pearse, 1976; Kumari et al., 2010). In addition to clathrin, calveolin is another example of an endocytic coat protein (Rothberg et al., 1992).

Following cargo recognition and coat protein assembly, vesicles begin to form via invaginations (Kumari et al., 2010). Once a membrane bound vesicle is formed, scission from the cell surface occurs to release the newly formed endosome into the cytoplasm (Kumari et al., 2010). The large GTPase dynamin has been shown to play an essential role in the cleavage and subsequent formation of early endosomes (Macia et al., 2006). Furthermore, inhibition of dynamin by the specific cell-permeable inhibitor known as dynasore has been shown to effectively block receptor-mediated endocytosis (Macia et al., 2006). Importantly, for many signaling pathways receptor-mediated endocytosis is a requirement for signal transduction and the formation of various intracellular signaling complexes (Sorkin and Von Zastrow, 2002). Whether or not endocytosis of various necroptotic receptors is important for necroptotic signaling and necrosome formation remains unclear and is a subject of interest in this thesis.

1.3 Inflammatory Response

Following phagocytosis or endocytosis of pathogens or signaling molecules, macrophages embark on a multitude of signaling mechanisms in order to activate the transcription of key proteins involved in a variety of cellular processes. In particular, macrophages play a major role in the initiation, maintenance and resolution of inflammation through the production of inflammatory mediations, such as chemokines, pro- and anti-inflammatory cytokines, in response to infection, trauma and tissue damage (Fujiwara and Kobayashi, 2005). A very tightly regulated balance between pro- and anti-inflammatory signals must be enforced to ensure a protective rather than pathological inflammatory response. A poor inflammatory profile could lead to dampened innate immune responses that results in insufficient pathogen clearance. On the other hand, an excessive inflammatory response could lead to better pathogen clearance, but at the cost of massive inflammation, resulting in tissue pathology and systemic inflammatory responses syndrome (SIRS) (Medzhitov, 2008).

Inflammation is an intricate, complex and very active process that has been evolutionarily conserved as a host response to infection and tissue injury (Buckley et al., 2013; Medzhitov, 2008). An inflammatory response is characterized by the local accumulation of fluid, plasma proteins and white blood cells, resulting in the cardinal symptoms of inflammation: rubor (redness), dolor (pain), calor (heat), tumor (swelling) and functio laesa (loss of tissue function) around the affected area (Gaestel et al., 2009; Murphy et al., 2008; Serhan et al., 2008; Takeuchi and Akira, 2010). Inflammatory responses are important for delivering additional effector molecules and cells to the affected site, inducing local blood clotting to act as a physical barrier, thereby preventing further spreading of infection and to promote repair of the injured tissue (Murphy et al., 2008).

Initiation of inflammation occurs when macrophages at the infected or damaged site release cytokines, chemokines and other inflammatory mediators that induce the dilation of local small blood vessels (Murphy et al., 2008). More specifically, release of histamines, prostaglandins and nitric oxide cause vasodilation of surrounding blood vessels and an increase in blood flow, which is why redness and heat are symptoms that usually accompany an inflammatory response (Murphy et al., 2008; Newton and Dixit, 2012). Additionally, endothelial cells lining the blood vessel walls are activated to express selectins, important cell-adhesion molecules, thus promoting selective tethering and adhesion to the integrins and chemokine receptors on the surface of circulating leukocytes, while at the same time preventing the escape of erythrocytes (Medzhitov, 2008; Murphy et al., 2008). Once bound to the endothelium, leukocytes such as neutrophils and monocytes are able to extravasate into the tissue (Murphy et al., 2008). Within the tissue, neutrophils are active phagocytes and can also release cytotoxic granules in an attempt to kill the pathogen (Medzhitov, 2008). Monocytes entering the tissue respond to the environmental stimuli and differentiate into macrophages or dendritic cells.

As the inflammatory response progresses, other cells, such as eosinophils and lymphocytes, enter the afflicted site to further combat the infection (Murphy et al., 2008). In response to histamines and leukotrienes, permeability of surrounding blood vessels increases, which in turn loosens the normally tightly bound endothelial cells lining the blood vessels (Murphy et al., 2008; Newton and Dixit, 2012). As a result, fluid and proteins within the blood enter the tissue to aid in host defense (Murphy et al., 2008). This infiltration event accounts for the swelling and pain symptoms experienced during an inflammatory response (Murphy et al., 2008). During the final stages of inflammation, clotting of local microvessels is induced to prevent the spread of infection into the circulatory system (Murphy et al., 2008).

1.3.1 NFκB Signaling

Activation of inflammatory signaling pathways occurs through the interaction of host cell surface PRRs with foreign PAMPs or host cell-derived danger-associated molecular patterns (DAMPs) (Newton and Dixit, 2012). Once activated, PRRs oligomerize and induce a cascade of intracellular signaling events, which include protein trafficking, ubiquitination, phosphorylation and degradation, ultimately culminating in the activation of NFκB and/or interferon regulatory factor (IRF) transcription factors (Frazier et al., 2009; Medzhitov and Horng, 2009; Newton and Dixit, 2012). These particular transcription factors have been shown to induce the transcription of an assortment of pro-and anti-inflammatory genes and as a result, transcriptional control of inflammation can strongly influence the outcome of various inflammatory pathologies (Medzhitov and Horng, 2009).

1.3.2 Canonical NFκB Pathway

The canonical NFκB pathway is defined as being mediated by the NFκB Essential Modulator (NEMO)-dependent inhibitor of nuclear factor kappa-B kinase (IKK) complex and is generally considered to be a mediator of inflammatory responses, while the noncanonical NFκB pathways is considered to be more important for immune cell differentiation and maturation (Shih et al., 2011). Within the mammalian system, the NFκB family of transcription factors consists of five members, p65/RelA, cRel, RelB, p50 and p52 encoded by RELA, REL, RELB, NFKB1 and NFKB2 respectively, which are involved in dimerization, DNA binding, interaction with IκB's and nuclear translocation (Hayden and Gosh, 2008; Shih et al., 2011). Under steady state conditions, the canonical NFκB transcription factors are kept in an inactive state by association with inhibitory IκBα, IκBβ and IκBε, while the noncanonical NFκB transcription factors are kept inactive by

maintaining the p100 and p105 precursor proteins and preventing their processing into active p52 and p50 (Hayden and Gosh, 2008).

Activation of the canonical NFκB pathway occurs by engagement of proinflammatory cytokines, PAMPs or DAMPs with their corresponding receptors (Shih et al., 2011; Wullaert et al., 2011). Signals from various receptors converge upon a similar pathway involving the activation of an IKK complex to trigger canonical NFκB signaling (Sun, 2012). For example, tumor necrosis factor (TNFα) is a pleiotropic proinflammatory cytokine that is able to induce canonical NFκB signaling via the cell surface TNF receptor (TNFR) (Beug et al., 2012). Following ligand binding to TNFR, multiple signaling proteins, such as TNFR-associated death domain protein (TRADD), TNFR-associated factor 2 (TRAF2), cellular inhibitors of apoptosis proteins 1/2 (cIAP1/2) and serine/threonine kinase family member receptor-interacting protein kinase 1 (Rip1) are recruited to the cytoplasmic domain of TNFR to form an important signaling complex (Beug et al., 2012). Both cIAP1 and cIAP2 are E3 ligases and are therefore able to ubiquitinate various target proteins (Beug etl al., 2012). Importantly, cIAP1/2 positively regulate the canonical NFκB pathway (Tenev et al., 2011). More specifically, in the case of canonical NFκB activation, cIAP1/2 polyubiquitinate Rip1 with nondegradative K63-linked ubiquitin chains (Beug et al., 2012). K63 ubiquitination of Rip1 recruits TGF-beta activated kinase 1 binding protein 2 (TAB2) and transforming growth factor-beta-activated kinase 1 (TAK1) to the receptor complex, which subsequently activates the IKK complex (Beug et al., 2012). The IKK complex is comprised of IKK proteins and NFκB essential modulator (NEMO). Once activated, the IKK complex phosphorylates IκB, which is bound to p50 and RelA, so that it is degraded by the proteasome (Beug et al., 2012). Once IκB is degraded, the p50/RelA heterodimer translocates into the nucleus and induces the transcription of a vast array of NFκB target genes (Beug et al., 2012).

The canonical NFκB pathway is also commonly induced through the engagement of various TLRs. A well-studied example of TLR-mediated canonical NFκB activation is LPS binding to TLR4 (Beug et al., 2012). Engagement of TLR4 recruits four adaptor proteins, myeloid differentiation primary response gene (MyD88), toll-interleukin 1 receptor (TIR) domain containing adaptor protein (TIRAP), TIR-domain-containing adaptor-inducing interferon-β (TRIF) and TRIF-related adaptor molecule (TRAM) (Takeuchi and Akira, 2010). Association of these proteins occurs through their TIR domains located on both the adaptor proteins and TLR4 (Takeuchi and Akira, 2010). Importantly, TLR4 stimulation can activate two distinct adaptor protein-mediated signaling pathways (Beug et al., 2012). More specifically, MyD88 induces canonical NFκB signaling whereas TRIF induces the production of interferon β (IFNβ) (Takeuchi and Akira, 2010). MyD88 is required for downstream signaling of most TLRs, with TLR3 being an exception (Takeuchi and Akira, 2010). Following recruitment of MyD88 to TLR4, a complex made up of interleukin 1 receptor associated kinases (IRAKs) and the E3 ligase TRAF6 is formed (Takeuchi and Akira, 2010). Once formed, this complex interacts with a complex comprised of TAK1 and TAB1-3, resulting in the activation of the IKK complex and subsequent translocation of p65/RelA into the nucleus to activate the transcription of specific target genes (Takeuchi and Akira, 2010).

As previously mentioned, in addition to MyD88-mediated canonical NFκB activation, stimulation of TLR4 also induces TRIF-mediated IFNβ production (Takeuchi and Akira, 2010). A detailed study performed by Kagan et *al.* (2008) focused on the mechanisms of TLR4 signaling and demonstrated that MyD88-mediated canonical NFκB activation occurs at the cell surface following LPS binding to TLR4, while TRIF-mediated IFNβ production occurs only after receptor-mediated endocytosis of the TLR4 complex. Once localized inside

an early endosome, TRIF and TRAM are able to interact with TRAF3 to induce the phosphorylation of IRF3 (Kagan et al., 2008). Phosphorylated IRF3 can then translocate into the nucleus and induce the expression of type I IFN genes (Takeuchi and Akira, 2010). Additionally, TLR3 is also able to induce the production of type I IFNs via TRIF and IRF3 (discussed in greater detail in section 1.3) (Cusson-Hermance et al., 2005).

1.3.3 Noncanonical NFκB Pathway

The noncanonical NFκB pathway is generally defined as being NEMO–independent (Shih et al., 2011). Activation of the noncanonical NFκB pathway can occur through various cell surface receptors, including CD40, fibroblast growth factor-inducible 14 (Fn14) and TNFR2 (Beug et al., 2012; Rauert et al., 2009). Under resting conditions, the noncanoncial NFκB pathway is suppressed through constitutive proteasomal degradation of NFκB inducing kinase (NIK), which is induced by TRAF3-mediated k48-linked ubiquitination of NIK (Beug et al., 2012). Engagement of CD40 with CD40 ligand (CD40L) or Fn14 with TNF-like weak inducer of apoptosis (TWEAK) results in the assembly of a cytoplasmic signaling complex made up of cIAP1/2, TRAF2/3 and NIK (Shih et al., 2011). Under resting conditions, TRAF2/3 suppress constitutive noncanoncial NFκB activation through the ubiquitintation and degradation of NIK (Beug et al., 2012). Once activated, cIAP1/2 ubiquitinate TRAF3 with K48-linked ubiquitin chains, which results in proteasomal degradation of TRAF3 (Beug et al., 2012). Since NIK expression is negatively regulated by TRAF3, degradation of TRAF3 results in the subsequent accumulation of NIK (Shih et al., 2011). Elevated NIK expression leads to the phosphorylation p100 and activation of IKKα (Shih et al., 2011). Additional phosphate groups are added to p100 by a phosphorylated IKKα homodimer to induce the processing or partial degradation of p100 into p52 by the proteasome (Shih et al.,

2011). A p52/RelB heterodimer translocates to the nucleus and activates the transcription of various genes (Shih et al., 2011). In the context of TNFR2-mediated activation of the noncanoncial NFκB pathway less is known about the molecular mechanisms. TNFR2 mutants have however been shown to induce p100 processing and translocation of p52/RelB into the nucleus (Rauert et al., 2009).

A crucial role for noncanonical NFκB signaling in the regulation of adaptive immunity and lymphoid organ development has been well established, however it was not until recently that a role for noncanonical NFκB signaling in the regulation of innate immunity was revealed (Jin et al., 2014). Jin and colleagues (2014) demonstrated that genetic ablation of noncanonical signaling components, such as NIK, resulted in hyperinduction of type I interferons (IFN-Is) (IFN-Is discussed in section 1.4). This study unveiled an interesting, previously unidentified relationship between the noncanonical NFκB pathway and the production of IFN-Is in response to RNA viruses and TLR ligands (Jin et al., 2014). More specifically, a novel function for noncanonical NFκB signaling involving the suppression of IFN-I production was exposed (Jin et al., 2014).

1.3.4 Sterile Inflammation

Inflammation is not an exclusive response to infection. For many years heavy interest has been concentrated on the concept of sterile inflammation, which is defined as inflammation in the absence of any detectable infection (Chen and Nuñez, 2010). Sterile inflammation occurs in response to physical trauma, ischemia-reperfusion injury or chemical insult and plays an important role in tissue repair (Chen and Nuñez, 2010). The same inflammatory PRRs stimulated by infectious microorganisms can alternatively be stimulated by non-microbial signals such as DAMPs (Chen and Nuñez, 2010). Several studies have implicated

sterile inflammation in pathologies such as gout, atherosclerosis, Alzheimer's, ischemia-reperfusion injury resulting from a stroke or myocardial infarction, tumor progression and cancer (Chen et al., 2007; Chen and Nuñez, 2010; Coussens and Werb, 2012; Jaeschke, 2006; Ross, 1999). At present, the underlying mechanisms of injury induced sterile inflammation remain elusive and certainly warrant further investigation.

1.4 Type I Interferons

IFNs are critically important cytokines with a variety of functions ranging from antiviral immunity to tumor surveillance and cell death (De Weerd and Nguyen, 2012; Robinson et al., 2012). IFNs were the first cytokines to be discovered and have been the subject of extensive research for over half a century (Decker et al., 2005; Pestka et al., 2004). The initial discovery of IFN emerged in 1957 when Isaacs and Lindenmann reported that virally infected cells secreted an 'activity' that protected other cells from becoming infected (Decker et al., 2005). IFNs have since been classified into three distinct types, type I, II and III, based on their corresponding cell surface receptors (De Weerd and Nguyen, 2012). The type I IFN (IFN-I) family is comprised of multiple members, namely 12 IFNα subtypes, IFNβ, IFNε, IFNκ, and IFNω (González-Navajas et al., 2012). All IFN-Is signal through the type I IFN α/β receptor (IFNAR), which is widely expressed on the surface of many different cell types (Decker et al., 2005). In contrast to the larger type I IFN family, IFNγ is the only member of the type II IFN family and signals through the IFNγ receptor (IFNGR) (González-Navajas et al., 2012). Lastly the type III IFN family is made up of IFNλ1, IFNλ2 and IFNλ3 (González-Navajas et al., 2012). The corresponding receptor for type III IFNs is the IFNλ receptor (IFNLR) (Gad et al., 2009).

Of pertinence to this thesis are IFN-Is, particularly IFNβ. Various receptors, including TLR3, TLR4, and TNFR, are able to induce the production of IFNβ through the activation of different IRFs (see Fig. 1) (Yarilina et al., 2008). Once produced, IFNβ signals through IFNAR in an autocrine or paracrine fashion (Gao et al., 1998). The IFNAR is comprised of two subunits, IFNAR1 and IFNAR2, which are constitutively bound to tyrosine kinase 2 (Tyk2) and janus kinase 1 (JAK1), respectively (Decker et al., 2005). Classically, stimulation of IFNAR results in the activation of JAK and Tyk2 leading to the phosphorylation of tyrosine residues on the receptor and thereby providing a docking site for signal transducer and activator of transcription 1 (STAT1) and STAT2 (Decker et al., 2005). Phosphorylated STAT1/2 heterodimers can then associate with IRF9 to form interferon stimulated gene factor 3 (ISGF3), a trimolecular complex that translocates to the nucleus, binds to its cognate IFN-stimulated response element (ISRE) and induces the transcription of a distinct set of interferon stimulated genes (ISGs) (Ivashkiv and Donlin, 2014). Furthermore, in the absence of STAT1/2 phosphorylation, an unphosphorylated ISGF3 (U-ISGF3) can also form. Similar to ISGF3, U-ISGF3 can enter the nucleus and activate the transcription of a specific set of U-ISGF3 regulated ISGs (See Fig. 2) (Cheon et al., 2013).

Intriguingly, low levels of IFNβ have been documented within the milieu of a variety of murine tissues in the absence of any infection, suggesting that some cells, such as macrophages, constitutively secrete small amount of IFNβ as a mechanism to maintain homeostasis (Gough et al., 2012). Tonic IFNβ signaling has also been reported to prime cells in an attempt to ensure a rapid and robust immune response against future challenges (Gough et al., 2012). Further research demonstrated that constitutive low level IFNβ signaling is needed to maintain adequate basal expression of various ISGs, such as STAT1, STAT2, IRF1 and IRF9 (Gough et al., 2012). Impaired tonic IFNβ signaling causes enhanced

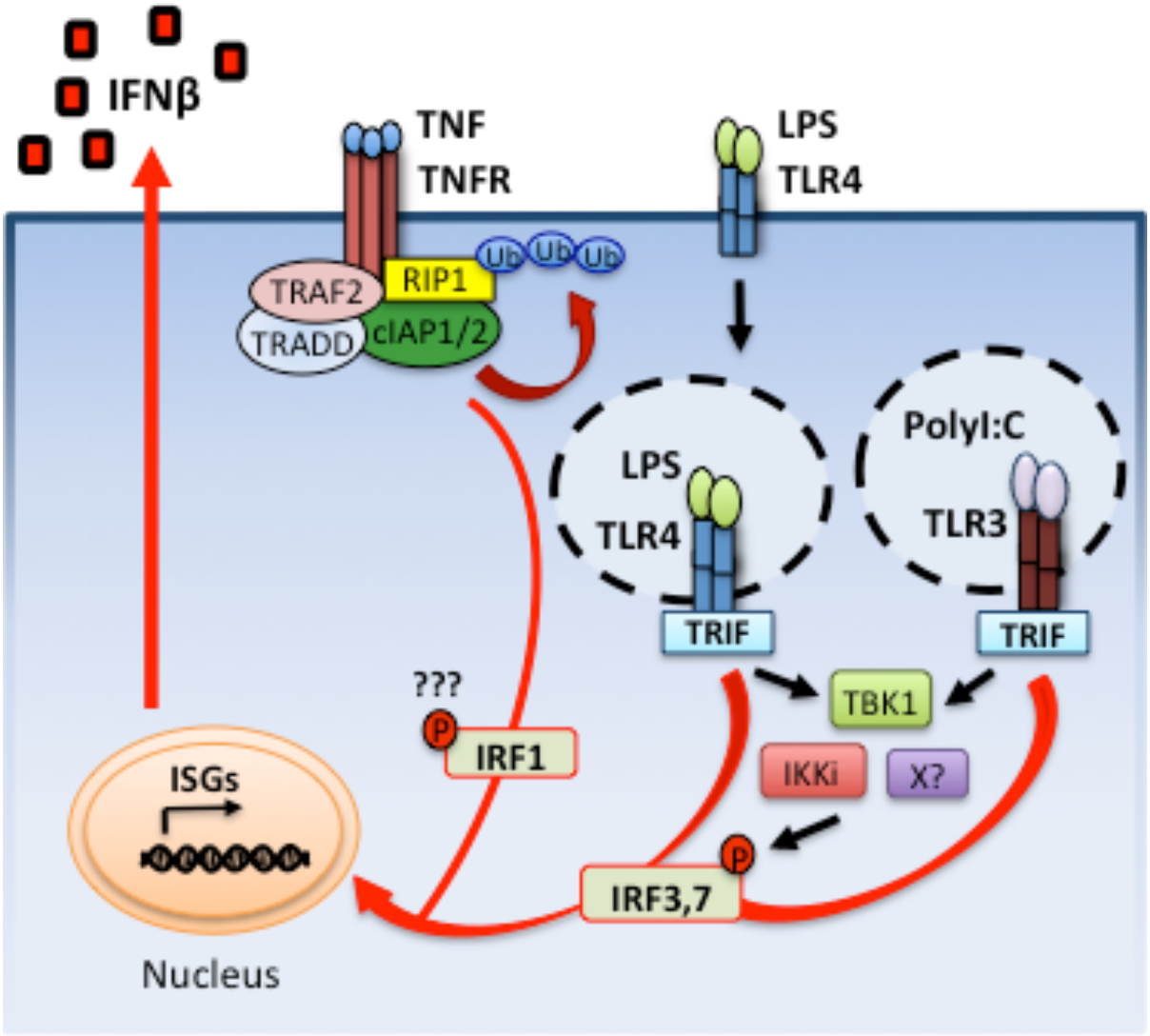
IFNβ
TNF
TNFR
LPS
TLR4
Ub
Ub
Ub
TRAF2
RIP1
TRADD
cIAP1/2
LPS
TLR4
Poly I:C
TLR3
TRIF
TRIF
???
P
IRF1
TBK1
IKKi
X?
P
IRF3,7
ISGs
Nucleus

Figure 1. *IFN-I production.* Several different signaling pathways can induce the production of IFN-Is. Signaling through TNFR can induce the production of IFNβ via IRF1, however the mechanism of IRF1 activation is not clear. Several studies have suggested that post-translational modifications, such as phosphorylation, activate IRF1. Endosomal TLR3 and TLR4 induce IFN-I production through TRIF activation, which activates kinases, such as tank-binding kinase 1 (TBK1), IKKi or a presently unknown kinase, to phosphorylate IRF3 or IRF7. Once phosphorylated, IRF3 or IRF7 migrate into the nucleus and bind to an IRF-binding site (IRFBS) to induce the transcription of IFN-Is, which can signal in an autocrine or paracrine fashion.

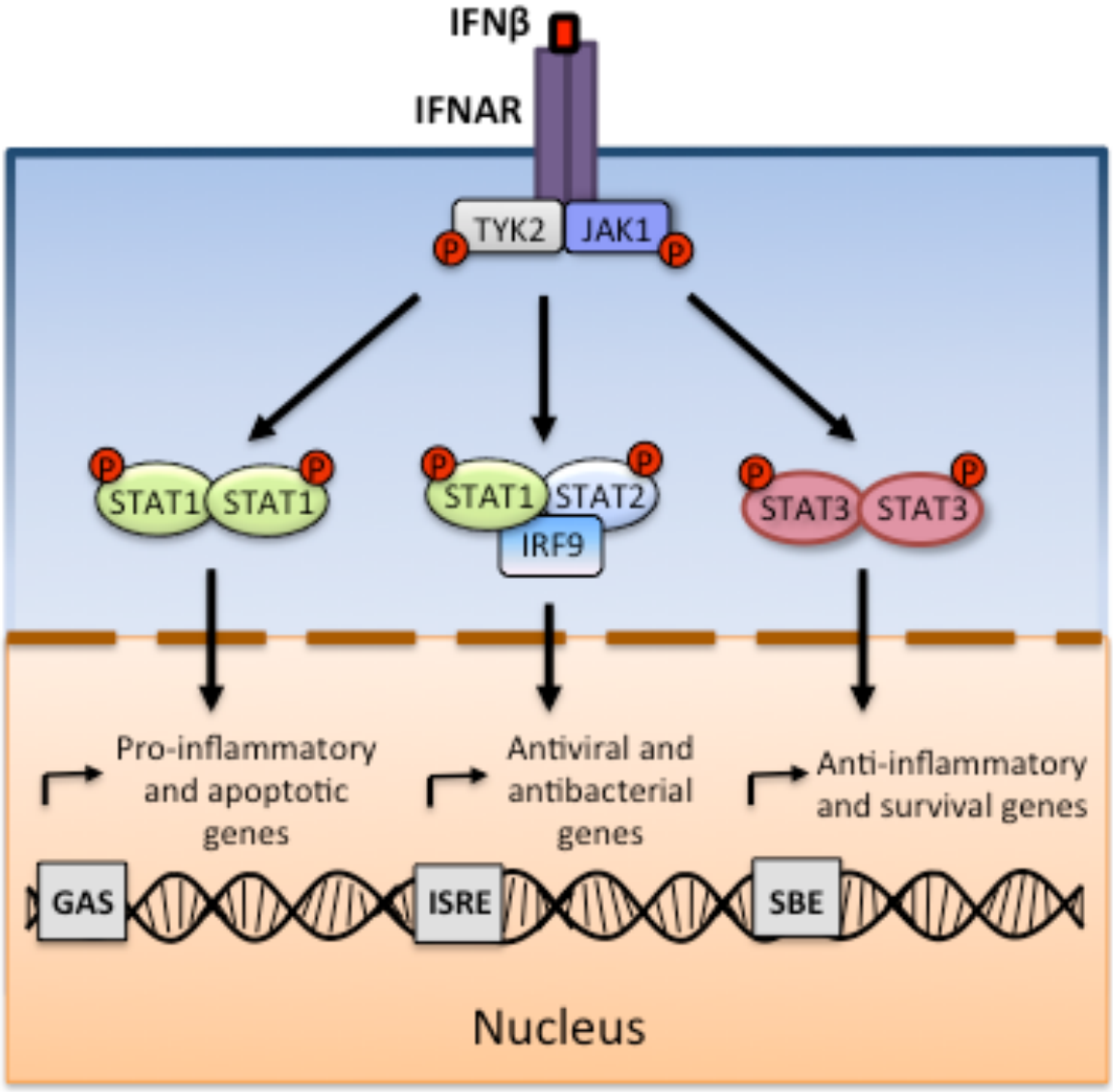
IFNβ
IFNAR
TYK2
JAK1
P
STAT1
STAT1
STAT1
STAT2
IRF9
STAT3
STAT3
Pro-inflammatory and apoptotic genes
Antiviral and antibacterial genes
Anti-inflammatory and survival genes
GAS
ISRE
SBE
Nucleus

Figure 2. *Classical IFN-I signaling pathways.* Binding of IFN-Is to IFNAR results in the phosphorylation of JAK1 and Tyk2. Phosphate groups on JAK1 and Tyk2 allow STATs to interact with the receptor complex. Phosphorylated STAT1 is able to form a homodimer, enter the nucleus and bind to a gamma activated site (GAS) to promote the production of pro-inflammatory and apoptotic proteins. IFN-Is can also elicit the formation of phosphorylated STAT1/STAT2 heterodimers that associate with IRF9 to form the ISGF3 complex. ISGF3 enters the nucleus and binds to the corresponding ISRE to drive the production of anti-viral and anti-bacterial proteins. Finally, IFN-Is can also mitigate the formation of phosphorylated STAT3 homodimers, which can migrate into the nucleus, bind a STAT3-binding element (SBE) and induce the transcription of genes important for survival, proliferation and anti-inflammatory responses.

susceptibility to infection, inadequate hematopoietic stem cell mobilization and increased bone resorption, thereby highlighting the importance of constitutive secretion of low levels of IFNβ (Gough et al., 2012).

It has been very well established that IFN-Is play a critical protective role for the host in the context of viral infections (González-Navajas et al., 2012). With respect to bacterial infections however, a clear consensus as to whether IFN-Is are beneficial or counterproductive for the host has yet to be established. Most bacterial infections induce the production of IFN-Is, whether or not it is helpful or harmful seems to rely heavily on the specific bacterium (i.e intracellular vs extracellular pathogens) (Decker et al., 2005). For example, our lab demonstrated a detrimental role of IFN-Is for the host during an infection with *Salmonella enterica* serovar Typhimurium (ST) (Robinson et al., 2012). Furthermore, ST promoted the production of IFN-Is, which enhanced macrophage necroptosis (Robinson et al., 2012). In contrast, IFN-Is are beneficial for the host response to many extracellular pathogens such as *Escherichia coli* (Mancuso et al., 2007).

1.5 Programmed Cell Death

Programmed cell death (PCD) is a genetically regulated process that plays an imperative role in almost every aspect of organismal life (Ameisen, 2002). Early questions surrounding physiological cell suicide began in the 19th century from development and metamorphosis studies on tadpoles and insects (Lockshin and Zakeri, 2001). In 1842 Carl Vogt reported his observation of cell death in the notochord and adjacent cartilage in toads undergoing metamorphosis (Clarke and Clarke, 1996). These preliminary studies generated a basic understanding of organismal cell death, however experimental examination did not occur until the mid-20th century when various scientific techniques, such as microscopy and

histology, saw major improvements (Lockshin and Zakeri, 2001). Beginning in the early 1960s, studies began to recognize cell death as a biologically controlled process (Lockshin and Zakeri, 2001). By 1990, the Nobel Prize winning work of Sydney Brenner, Robert Horvitz and John Sulston led to further advancements in the understanding of the mechanisms of PCD using the nematode *Caenorhabditis elegans*. More specifically, this work illuminated some of the central machinery of PCD (caspase-3, B-cell lymphoma protein-2 (bcl-2) and Fas) and provided the first evidence of a genetic basis in some forms of cellular demise (Ellis and Horvitz, 1986; Lockshin and Zakeri, 2001; Meier et al., 2000).

To date, additional forms of programmed cell death have been identified, such as caspase-1-mediated pyroptosis and iron-dependent ferroptosis, however the two most dominant and studied forms of cell death are apoptosis and necrosis (Duprez et al., 2009; Green and Victor, 2012). Intriguingly, the particular mode of cell death elicited has been suggested to have different consequences, both beneficial and detrimental, for the host (Green and Victor, 2012). More specifically, necrotic cell death is considered to be highly immunogenic, resulting in a robust inflammatory response, while apoptosis is a quieter non-inflammatory form of death (Discussed in further detail in sections 1.2.1 and 1.2.4). Dysregulation of PCD can have catastrophic effects for the host (Pettigrew and Cotter, 2009). It is therefore important to thoroughly understand the signaling events and specific mechanisms of cell death in order to develop therapeutic strategies and drug targets for a variety of cell death-related pathologies ranging from cancer to sepsis (Duprez et al., 2009).

1.5.1 Apoptosis

One of the best-characterized forms of PCD is apoptosis. Derived from Ancient Greek texts, the literal translation of apoptosis is “falling off”, as in leaves falling from a tree during

autumn (Lawen, 2003). In 1972, Kerr and colleagues (Kerr et al., 1972) identified some of the hallmark morphological features of apoptosis, including cytoplasmic shrinkage, nuclear condensation and plasma membrane (PM) blebbing (Kerr et al., 1972; Wyllie et al., 1980). The apoptotic process involves distinct biochemical and physical modifications involving the cytoplasm, nucleus and plasma membrane (Lawen, 2003). These modifications occur as a result of a proteolytic system involving a family of cysteine proteases known as caspases (Thornberry and Lazebnik, 1998). An apoptotic cell is able to very neatly break itself down by releasing small membrane bound vesicles containing fragments of cellular contents through a process known as membrane blebbing (Lawen, 2003). As the cell is gradually breaking down without actual rupturing of the PM, 'eat me' signals such as phosphatidylserine (PS) are translocated to the outside of the cell surface, which results in recognition and phagocytosis by resident phagocytes including macrophages, neutrophils and/or dendritic cells by a process described as efferocytosis (Lawen, 2003; Maeda and Fadeel, 2014). Induction of apoptotic cell death can occur through intrinsic or extrinsic signals (Lawen, 2003).

1.5.2 Intrinsic Apoptotic Pathway

Intrinsic apoptosis is regulated by internal stimuli, such as DNA damage, oxidative stress, toxins and hypoxia (Elmore, 2007). Intrinsic apoptotic signaling can occur in response to both positive and negative signals (Elmore, 2007). Negative signals, such as deficient growth factors and cytokines, can prevent a cells ability to suppress PCD, thereby inducing a cell death program such as apoptosis (Elmore, 2007). Alternatively, positive signals, such as radiation, hypoxia and infection, can activate cell death signaling pathways (Elmore, 2007). Collectively, both positive and negative signals for intrinsic apoptosis alter the inner

mitochondrial membrane so that the mitochondrial permeability transition (MPT) pore opens and releases pro-apoptotic proteins, such as cytochrome c, secondary mitochondria-derived activator of caspases (SMAC), Bcl2-associated x protein (BAX), Bcl2 antagonist/killer (BAK) and BH3 interacting domain death agonist (BID), into the cytosol (Elmore, 2007; Saelen et al., 2004).

Once cytochrome c is released from the mitochondria due to a loss of mitochondrial membrane potential it binds to apoptotic protease activating factor 1 (Apaf-1) in the presence of dATP or ATP (Riedl et al., 2007). Binding of cytochrome c induces the heptamerization of Apaf-1, which subsequently forms the apoptosome; an important ring shaped signaling complex located within the cytosol (Riedl et al., 2007). Following apoptosome formation, a caspase cascade is activated (Riedl et al., 2007). The apoptosome binds, cleaves and activates initiator pro-caspase-9 (Shi, 2004). Activation of initiator caspases, such as caspase-9, irreversibly commits the cell to death (Qin et al., 1999). Active caspase-9 goes on to cleave the executioner caspases-3 and 7 at specific internal aspartic acid residues (Qin et al., 1999; Shi, 2004). Active caspase-3 and 7 then cleave a variety of important substrates to finalize cellular suicide (Hakem et al., 1998). Based on studies that have disrupted the genes corresponding to cytochrome c, Apaf-1 and caspase-9, all three proteins play an essential role in the intrinsic apoptotic pathway (Saelens et al., 2004).

1.5.3 Extrinsic Apoptotic Pathway

Extrinsic apoptosis is induced by various death receptors on the cell surface, such as TNFα, FasL and TNF related apoptosis inducing ligand (TRAIL). Apoptotic transmembrane receptors involved in the extrinsic pathway are members of the TNFR gene superfamily and contain a cytosolic death domain (DD), which plays a central role in the transduction of

apoptotic signals (Elmore, 2007; Schmitz et al., 2000). Ligation of preassociated homotrimeric death receptors, such as FasL binding to the FasR, results in a conformational change that leads to the recruitment of multiple proteins to the intracellular domain of the receptor to form a multiprotein death inducing signaling complex (DISC) (Peter and Krammer, 2003).

Following stimulation, the first cytoplasmic protein to associate with the receptor is Fas associated DD containing protein (FADD) via homotypic interactions between the DDs (Dickens et al., 2012). Association with pro-caspase-8 and 10 ensues through death effector domain (DED) interactions with FADD (Dickens et al., 2012). Caspase-8 is typically considered to be the main initiator of extrinsic apoptosis (Peter and Krammer, 2003). The association of procaspase-8 with FADD results in autoproteolytic cleavage and subsequent activation of caspase-8 (Peter and Krammer, 2003). Active caspase-8 is released from the DISC and cleaves (and activates) the executioner caspase-3 thereby leading to endonuclease activation, degradation of nuclear and cytoplasmic proteins and the formation of apoptotic bodies, which culminates in apoptotic cell death (Elmore, 2007).

1.5.4 Necrosis and Secondary Necrosis

Necrosis is a highly inflammatory mode of cell death that is morphologically characterized by cellular and organelle swelling (a process known as oncosis), membrane rupture and loss of intracellular content (Kroemer et al., 2008). As a general notion, necrosis is considered to be an accidental, uncontrolled mode of cell death that occurs in response to environmental perturbations, such as chemical or physical trauma (Kroemer et al., 2008). Initial reports of necrotic cell death can be traced back to the work of Galen in ancient Greek texts (Majno and Joris, 1995). The term necrosis originated from the Greek word ‘nekros’,

which means ‘dead body’ (Vanlangenakker et al., 2012). During the mid-nineteenth century, various studies began correlating necrosis with the presence of dying tissues (Fink and Cookson, 2005). In 1858, German pathologist and biologist Rudolph Virchow contributed to the understanding of necrotic cell death by identifying necrosis as an appreciable form of cellular demise, which he believed to strictly occur only under pathological conditions (Clarke and Clarke, 2012; Linkermann and Green, 2014). For example, Virchow commonly referred to necrosis in situations such as gangrene (Clarke and Clarke, 2012).

In addition to necrosis, studies have reported a phenomenon referred to as secondary necrosis (Vanden Berghe et al., 2010). Following apoptosis, apoptotic blebs are rapidly phagocytosed by phagocytic cells via a process known as efferocytosis (Silva, 2010). When the clearance of dead or dying cells is impaired following apoptosis, cells rupture causing the intracellular debris to be dissipated into the extracellular milieu, thus inducing an inflammatory phenotype (Vanden Berghe et al., 2010) Many studies have argued that secondary necrosis is not necessarily physiologically relevant and may instead be an *in vitro* artifact due to the lack of phagocytosis (Vanden Berghe et al., 2010). Secondary necrosis may however have a (patho)physiological role when there is extensive apoptosis overwhelming the phagocytic system (Vaden Berghe et al., 2010).

1.5.5 Necroptosis

A flurry of recent evidence has unveiled the existence of a highly regulated genetically programmed form of necrosis now commonly known as necroptosis (Degterev et al., 2005). Morphologically, necroptosis is identical to unregulated necrosis (see section 1.5.4). A major difference between necroptosis and necrosis lies in the kinetics of death (Vanden Berghe et al., 2010). Necroptosis is receptor-mediated and occurs at a slower rate than necrosis since it

relies on an intricate signaling pathway to initiate and execute death (Vanden Berghe et al., 2010). In contrast, necrosis lacks a signaling phase and therefore occurs at a faster rate with cell beginning to disintegrate immediately after exposure to extreme stress (Vanden Berghe et al., 2010).

The initial discovery of necroptosis originated with experiments using the pan-caspase inhibitor benzyloxycarbonyl-Val-Ala-Asp (OMe) fluoromethylketone (zVAD) (Slee et al., 1996). Early studies performed on THP1 monocytes and Jurkat T-cells demonstrated that zVAD interferes with the processing of pro-caspases to active caspases, which consequently inhibits apoptotic cell death (Chow et al., 1995; Slee et al., 1996; Zhu et al., 1995). Subsequently, Vercammen and colleagues made the seminal observation that death receptor stimulation in combination with zVAD treatment induced necrotic death in L929 fibrosarcoma cells. This study established a negative role for caspases in TNF-mediated necrotic cell death (Vercammen et al., 1998). Additionally, a second paper from the same group demonstrated that caspases also negatively regulate Fas-mediated necrotic death (Vercammen et al., 1998). These publications not only debunked the notion that necrosis is a solely unregulated form of cell death but also revealed a fundamental difference between these two different forms of death with respect to the role of caspases.

A major breakthrough in the study of programmed necrosis was achieved in a study examining Fas, TRAIL and TNF-mediated necroptosis in primary T cells (Holler et al., 2000). Holler and colleagues demonstrated that necroptosis is negatively regulated by caspase-8 and reliant on the kinase activity of Rip1 for necroptotic signal transduction and subsequent death (Holler et al., 2000). This study better established the molecular dichotomy between apoptosis, which is caspase-8-dependent, and necroptosis, which is caspase-8 independent and Rip1-mediated, when initiated by the same death receptor. Structurally Rip1

is comprised of three domains: an amino-terminal kinase domain important for phosphorylating various target proteins, an intermediate Rip homotypic interaction motif (RHIM) domain important for NFκB signalling and homotypic interactions and a carboxyl-terminal death domain important for homologous interactions with death receptors (Degterev et al., 2008; Ofengeim and Yuan, 2013). In 2005, a pivotal study by the Yuan group coined the term necroptosis and also developed the Rip1 kinase inhibitor nectrostatin-1 (nec-1), which provided researchers with an important tool for investigating necroptosis *in vivo* and *in vitro* (Degterev et al., 2005). It was later confirmed by the same group that nec-1 co-treatment with zVAD and death receptor stimuli inhibits necroptosis, emphasizing the importance of Rip1 kinase activity in necroptotic cell death (Degterev et al., 2008).

1.5.6 Necrosome Formation

Necroptosis has been mainly studied from the context of TNF-signaling (see Fig. 3). Similar to extrinsic apoptosis, stimulation of the TNFR results in the recruitment of a number of different proteins to the cytosolic domain of the death receptor including TRADD, TRAF2, cIAP1/2 and Rip1. In most cell types, TNFR stimulation results in the activation of NFκB signaling via cIAP1/2-mediated K63-linked polyubiquitination of Rip1 (Vanlangenakker et al., 2011). If however protein synthesis is inhibited, for example with the translational inhibitor cyclohexamide, TNF signaling converts a pro-survival signal to a pro-death signal (Vanlangenakker et al., 2011). The type of cell death induced largely depends on caspase activity. If caspases are functional, Rip1 and Rip3 are inactivated by proteolytic cleavage and a pro-apoptotic caspase cascade is induced (Feng et al., 2007; Lin et al., 1999; Vanlangenakker et al., 2011). Under conditions of caspase inhibition, deubiquitination of

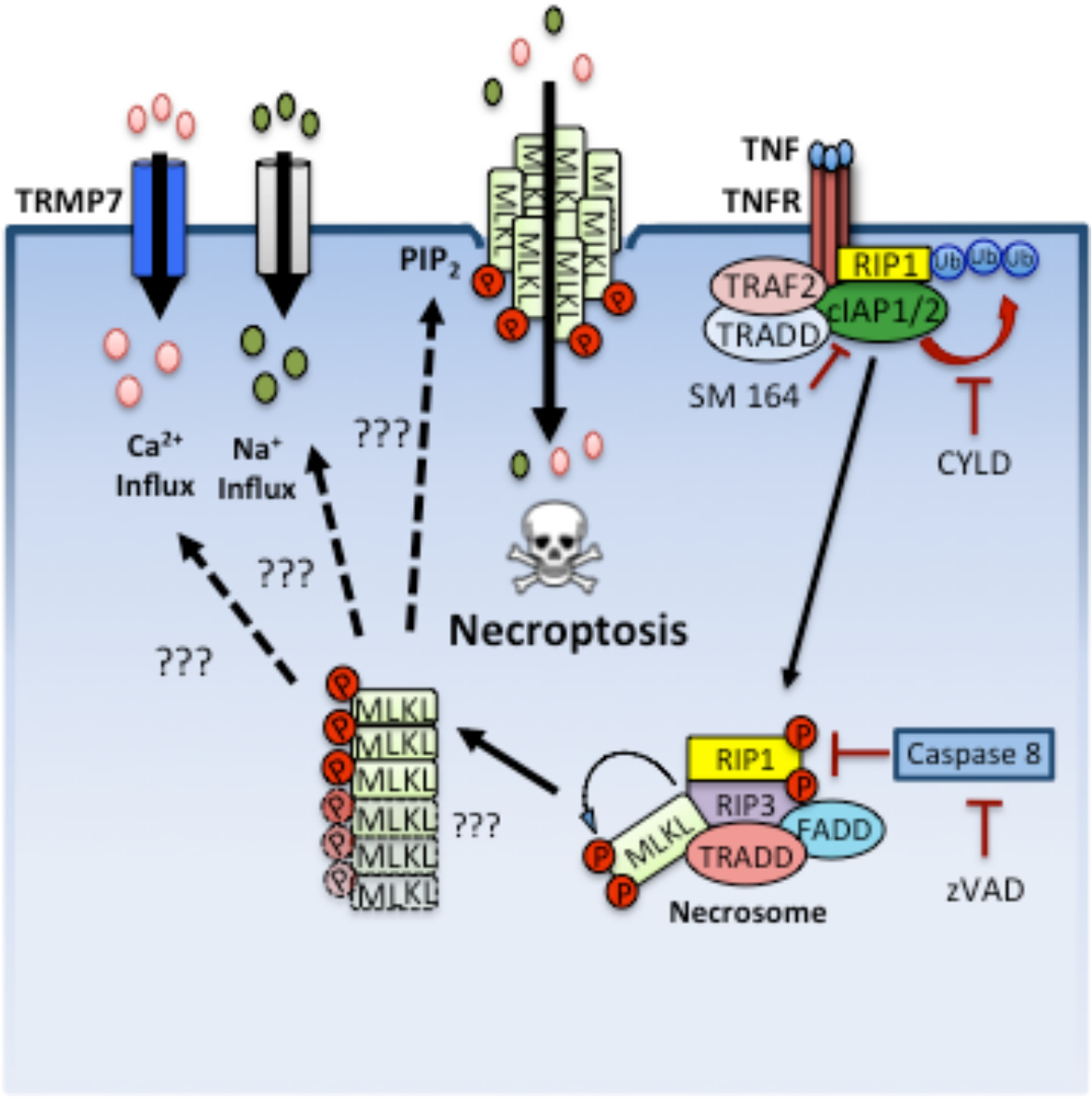
TRMP7
PIP2
TNF
TNFR
RIP1
Ub
Ub
Ub
TRAF2
cIAP1/2
TRADD
SM 164
CYLD
Ca2+
Influx
Na+
Influx
???
???
???
Necroptosis
MLKL
MLKL
MLKL
MLKL
MLKL
MLKL
???
RIP1
RIP3
MLKL
TRADD
FADD
Caspase 8
zVAD
Necrosome

Figure 3. *TNF-mediated necroptosis signaling pathway.* TNF binding to TNFR induces the formation of an intracellular multiprotein signaling complex, composed of cIAP1/2, Rip1, FADD and TRAF2, at the cytoplasmic domain of the receptor. Under conditions of caspase inhibition, Rip1 will become phosphorylated and associate with Rip3, leading to Rip3 phosphorylation and necrosome formation. Within the necrosome, active Rip3 transiently interacts with and phosphorylates pseudokinase MLKL. Phosphorylated MLKL forms homo-oligomers (the exact number of monomers that associate is currently under debate) and translocates to the PM where three separate hypotheses have been reported. First, MLKL has been shown to interact with calcium channels to induce calcium influx, thereby disrupting ionic homeostasis and causing an osmotic imbalance resulting in oncosis and PM rupture. Second, phosphorylated MLKL oligomers have been shown to interact with sodium channels instead of calcium channels but with the same outcome. Lastly, MLKL oligomers associate within the PM by interacting with PIP_2 to create a pore. Further investigation is needed to decipher the executioner mechanisms of TNF-mediated necroptosis.

Rip1 by the deubiquitinases cylindromatosis (CYLD) or A20 allows Rip1 to dissociate from the receptor complex and associate into a cytoplasmic signaling complex referred to as the necrosome. The specific components of the necrosome are currently not fully understood and are a subject of great interest. It is however well established that the two major components comprising the backbone of the necrosome are Rip1 and Rip3.

Necrosome formation is highly regulated by ubiquitination and phosphorylation events (Vandenabeele et al., 2010). In particular, the phosphorylation of Rip1 and Rip3 strongly influence necrosome signaling, which in part is mediated by the association of Rip1 and Rip3 via homologous RHIM domain interactions. How exactly Rip1 becomes phosphorylated following necroptotic stimulation is not well understood. Additionally, it is unclear how Rip1 mediates downstream Rip3 phosphorylation; does the Rip1/3 interaction recruit a separate kinase to the necrosome or does this induce Rip3 autophosphorylation (Cho et al., 2009)? Importantly, using knockout mice and cells researchers have demonstrated that Rip3 plays an indispensible role in necroptosis (Cho et al., 2009). The importance of Rip1 in necroptosis has proven to be more difficult to fully understand as genetically knocking out Rip1 results in embryonic lethality. In addition, a Rip3-dependent and Rip1-independent necroptosis pathway has recently been identified, again questioning the importance of Rip1 to necroptosis (Dillon et al., 2014).

1.5.7 Execution of Necroptosis

Significant progress has been made in the understanding of upstream necroptotic signaling events, however for many years the signaling events downstream of the necrosome remained elusive. In 2012 a library of ~ 200,000 necroptosis blocking chemical inhibitors was tested and necrosulfonamide was identified to target mixed lineage kinase domain like

(MLKL) protein, which is a downstream Rip3 interacting partner (Sun et al., 2012). Another study published around the same time also demonstrated a pro-necroptotic role of MLKL through small interfering RNA experiments (Zhao et al., 2012). MLKL is a pseudokinase, meaning that it contains a kinase-like domain, however lacks two of the three conserved catalytic residues required for a functional kinase domain (Murphy et al., 2013). The presence of a kinase-like domain allows MLKL to associate with the kinase domain of Rip3 (Sun et al., 2012). Importantly, Sun and colleagues also conclusively demonstrated that Rip3 directly phosphorylates MLKL in response to necroptotic stimuli.

Shortly after the discovery of MLKL as a critical necroptotic protein, MLKL-deficient mice were generated to define the role of MLKL in a physiological setting (Murphy et al., 2013). Similar to mice lacking Rip3, MLKL null mice appear phenotypically normal (Murphy et al., 2013). Initially MLKL was implicated as a core necrosome member along with Rip1/3, however it now appears that Rip3 and MLKL instead transiently interact to allow for the phosphorylation of MLKL, suggesting an interaction more typical to that of an enzyme and substrate (Murphy et al., 2013). Once Rip3 phosphorylates MLKL it forms cytoplasmic homo-oligomers (Cai et al., 2014; Chen et al., 2014; Wang et al., 2014). The stoichiometry of these homo-oligomers remains unclear as Cai et al. reported MLKL trimers, Chen et al. reported tetramers and Wang et al. reported hexamers. Following homo-oligomerization, MLKL relocates to the PM via interactions with positively charged amino acids on the surface of MLKL with PM phosphatidylinositol phosphates (PIPs) (Dondelinger et al., 2014). Once at the cell surface, there are discrepancies with respect to the functional role of MLKL. In the first study, MLKL was reported to interact with a calcium channel to induce the influx of calcium and disrupt osmotic homeostasis resulting in oncosis (Cai et al., 2014). In a second study, PM localized MLKL was instead connected to a sodium channel,

inducing sodium influx to rupture the PM (Chen et al., 2014). It has now recently been suggested that once at the PM, MLKL homo-oligomers assemble into a pore that disrupts osmotic homeostasis resulting in oncosis, PM rupture and subsequent necroptotic demise, suggesting a more direct pore-forming function of MLKL rather than an indirect function through ion channels (Dondelinger et al., 2014). While these studies mark a major milestone in necroptosis research, further exploration is required to determine the exact mechanism of necroptotic execution.

1.5.8 Necroptosis by PAMPs

TLR3 and TLR4 have been shown to induce Rip3-mediated necroptosis in macrophages (He et al., 2011) (see Fig. 4). Engagement of TLR3 with polyinosinic-polycytidylic acid (polyI:C), a double stranded RNA mimetic, or TLR4 with LPS in the absence of functional caspases results in the association of TRIF and Rip3 through RHIM domain interactions (He et al., 2011). The signaling events downstream of TRIF/Rip3 are currently unclear. PRR-mediated necroptosis is important for antimicrobial innate immune responses, especially under conditions of pathogen induced apoptotic inhibition (He et al., 2011). More specifically, some viruses have evolved cell death inhibitors as a mechanism to subvert the host immune response (Ekert et al., 1999). For example, cowpox virus-encoded protein, cytokine response modifier A (CrmA), inhibits mammalian caspases as a mechanism to prevent apoptosis of infected cells (Gillet and Brun, 1996). To circumvent this issue, necroptosis provides the host with an alternative pathway to remove infected cells. With this being said, the evolutionary arms race between host and pathogen continues as viral inhibitors of necroptosis have been recently reported (Upton et al., 2010). For example, viral M45-encoded inhibitor of Rip activation (vIRA) is a murine cytomegalovirus (MCMV)

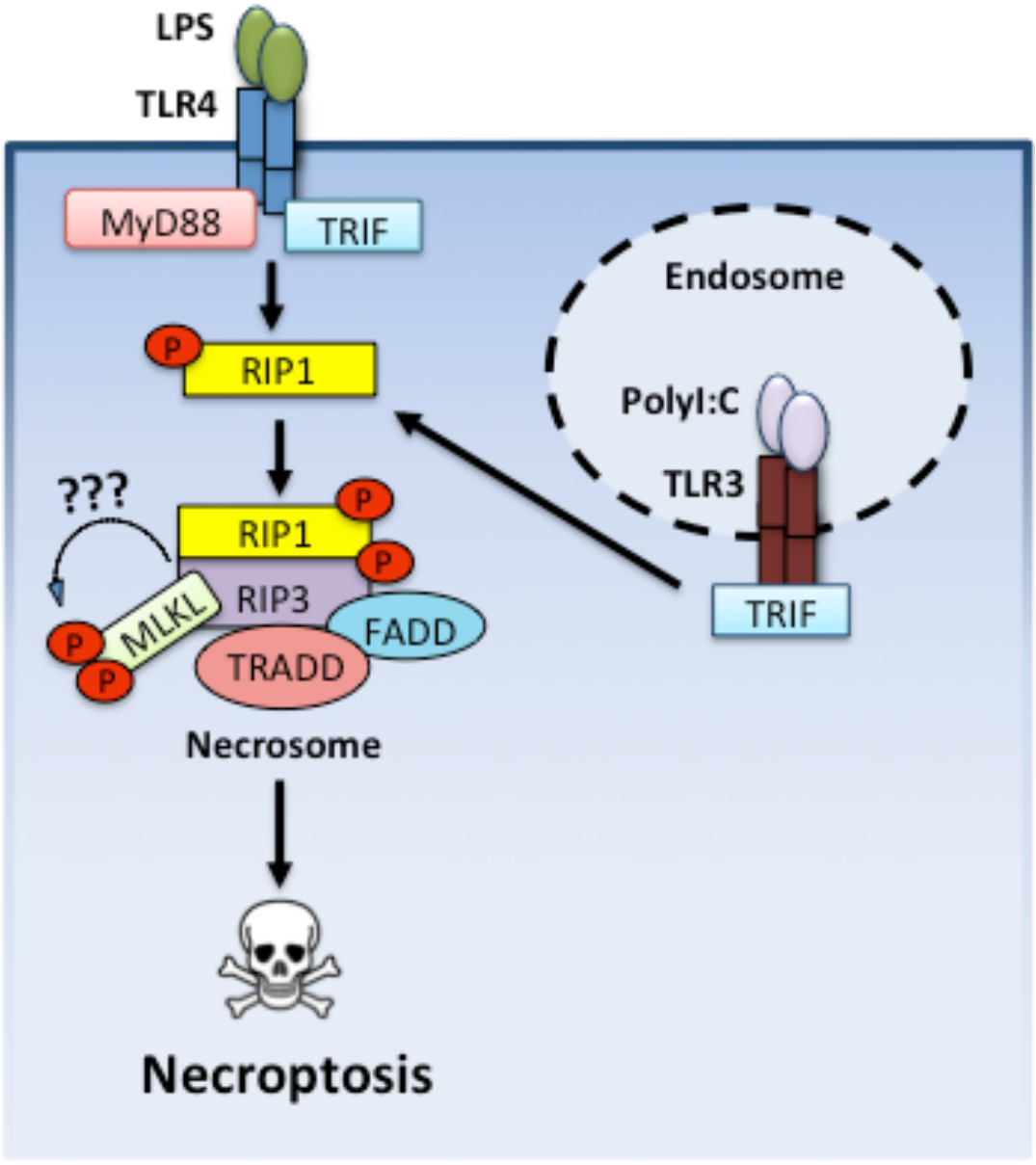
LPS
TLR4
MyD88
TRIF
P
RIP1
???
P
RIP1
P
RIP3
MLKL
FADD
P
P
TRADD
Necrosome
Endosome
PolyI:C
TLR3
TRIF
Necroptosis

Figure 4. *LPS and PolyI:C-mediated necroptosis signaling pathways.* Engagement of TLR4 with LPS recruits signal transducing adapter proteins MyD88 and TRIF to the cytosolic domain of TLR4. Endosomal TLR3 interacts with TRIF following stimulation with double stranded RNA mimetic PolyI:C. Stimulation of TLR3 or TLR4 leads to Rip1 phosphorylation, however the mechanism of Rip1 phosphorylation is unclear. In the presence of zVAD, Rip1 induces Rip3 phosphorylation via homologous RHIM domain interactions between TRIF, Rip1 and Rip3. Very little work has been done to fully characterize TLR-mediated necroptotic signaling pathways. Presumably necrosome formation and subsequent phosphorylation of MLKL (similar to what occurs in TNF-mediated necroptosis) follows Rip3 activation.

protein that targets Rip3 and inhibits necroptosis (Upton et al., 2010). The discovery of viral inhibitors of necroptosis provides further support for the notion that this immunogenic form of death evolved in higher vertebrates as a defense mechanism against invading pathogens (Linkermann and Green, 2014).

1.5.9 Necroptosis and IFN-I signaling

For many years IFN-I signaling and necroptotic cell death were considered to be separate, non-related events. It was not until a recent study investigating mechanisms of cancer resistance in blind mole rats that this notion began to change (Gorbunova et al., 2010). Intriguingly, Gorbunova and colleagues (2010) discovered a unique anti-cancer adaptation involving massive necrotic cell death, which appeared to occur in response to IFNβ secreted by proliferating cells. A few years later, Robinson et al. (2012) provided further insight into the role of IFN-I signaling in necroptosis by examining macrophages infected with *Salmonella enterica* serovar Typhimurium (ST). Importantly, Robinson and colleagues (2012) demonstrated that IFN-Is are required for ST-induced necroptosis of macrophages. More specifically, IFN-Is were shown to induce Rip1 phosphorylation, unveiling a previously unidentified role for IFN-Is in programmed necrosis of macrophages (Robinson et al., 2014). Robinson and colleagues (2012) added another important piece to the puzzle of necroptosis, however the mechanistic relationship between IFN-I signaling and necroptosis remained unclear. Additionally, a study by Thapa et al. (2013) demonstrated that type II IFNs mediate necroptosis of MEFs via RNA-responsive protein kinase R (PKR) and in the absence of FADD, which provided further support for an important necroptotic role for IFNs.

2.0 SUMMARY AND HYPOTHESIS

2.1 Rationale: Necroptosis has been implicated in the pathogenesis of a variety of human diseases ranging from ischemic-reperfusion injury to sepsis (Vandenabeele et al., 2010). It is therefore critically important to gain a thorough understanding of the mechanisms of necroptosis in order to develop therapies to suppress detrimental necrotic cell death and subsequent inflammatory pathology (Degterev et al., 2005). In addition, necroptosis may provide a promising avenue in the fight against apoptotic resistant cancer cells (Gorbunova et al., 2010).

2.2 Hypothesis: Intracellular type I interferon signaling induces the maintenance of Rip3 phosphorylation leading to macrophage necroptosis.

2.3 Objectives:

1. **To identify how the necroptotic signal is transmitted following ligand-receptor binding using murine bone marrow derived macrophages.**
    a. Experiments using dynasore, an inhibitor of dynamin-mediated endocytosis, will be performed to determine if the necroptotic signal is transmitted at the cell surface or intracellularly following receptor-mediated endocytosis.
    b. Exploration into the effects of dynasore on key necroptotic proteins Rip1 and Rip3 will be performed.
    c. The impact of dynasore treatment on the inflammatory phenotype consequent of necroptosis will be explored.
    d. Implications of NFκB signaling on necroptosis will be investigated.

2. **To investigate the intracellular mechanisms of IFNβ-mediated necroptosis.**
    a. IFNAR1 knockout mice will be utilized to explore the function of IFN-Is in macrophage necroptosis.
    b. The role of IFN-I signaling in Rip1/3 activation will be evaluated.
    c. Mechanisms of necrosome formation in response to necroptotic stimuli will be explored.
    d. Various knockout mice and chemical inhibitors will be utilized to delineate key components of the necroptotic signaling pathway.

3.0 MATERIALS AND METHODS

3.1 Animals: Mice were housed under specific pathogen-free conditions at the University of Ottawa Animal Facility. All mice were maintained in accordance with CCAC guidelines. Protocols and procedures were approved and monitored by the University of Ottawa Animal Care Committee and Ethics Board. Strains of mice utilized for experiments are listed in Table 1. All mice were age and sex-matched for experiments. Unless stated otherwise, all knockout mice were on a C57BL/6 genetic background.

3.2 Generation of Bone Marrow Derived Macrophages: Primary murine bone marrow derived macrophages were used for the majority of experiments. Following CO_2 euthanasia mice were thoroughly coated with 70% ethanol. Scissors and tweezers were used to remove fur surrounding the fore and hindlimbs prior to limb excision. Muscles and tissue was carefully removed from bones using scissors, tweezers and paper towel soaked in 70% ethanol. Once thoroughly cleaned bones were placed in RPMI + 8% FBS + 55 μM 1000X β-mercaptoethanol (2ME) + 50 ng/ml gentamycin (R8+gentamycin). To harvest pluripotent hematopoietic stem cells, a small gauge needle was used to flush bones with R8+gentamycin. Bone marrow was flushed through a 100 nm cell strainer and into a 50 ml falcon tube. A small 10 μl aliquot was taken to count the number of cells while remaining cells were centrifuged at 1600 RPM for 7 minutes. 50 mm plastic Petri dishes were coated with macrophage colony stimulating factor (M-CSF) at 5 ng/ml. To prevent macrophages from clumping in culture, M-CSF was spread evenly over the bottom of the Petri dish using an L spreader. Following centrifugation, the cell pellet was resuspended in R8+gentamycin and approximately $14x10^6$ cells were added to each Petri dish. R8 + gentamycin was added to Petri dishes for a final volume of 10 ml. Petri dishes were incubated at 37°C for 6 days to

Table 1. Mouse strains used for experiments.

Mouse Strain	Source	Other Information
C57BL/6	Jackson Laboratories	Stock #000664
129S6	Taconic	Stock: 129SVE-F
IFNAR1-/-	A kind gift from Dr. Kaja Murali-Krishna (Emory University, USA)	Mice were backcrossed to C57BL/6 for 14 generations as described by Kolumam et *al.* (2005) from mice generated as described by Müller et *al.* (1994)
Rip3-/-	A kind gift from Dr. Vishva Dixit (Genentech, USA)	Generated as described by Newton et *al.* (2004)
TRIF-/-	Jackson Laboratories	Stock #005037
MyD88-/-	Jackson Laboratories	Stock #009088
IRF3-/-	Bones provided by Dr. Karen Mossman (McMaster University, Canada)	Generated as described by Sato et *al.* (2000)
IRF7-/-	Bones provided by Dr. Karen Mossman (McMaster University, Canada)	Generated as described by Honda and Taniguchi (2006)
IRF3/7-/-	Bones provided by Dr. Karen Mossman (McMaster University, Canada)	Generated as described by Daffis et *al*. (2009)
IRF9-/-	Bones provided by Dr. Karen Mossman (McMaster University, Canada)	Generated as described by Kimura et *al.* (1996)
STAT1-/-	Taconic	129S6 genetic background Generated as described by Meraz et *al.* (1996) Stock: 2045-F
STAT2-/-	Bones provided by collaborator Dr. Ana Gamero (Temple University, USA)	Mice were backcrossed to C57BL/6 for 11 generations Generated as described by Park et *al.* (2000)
TNFR1/2-/-	Jackson Laboratories	Stock #003243

allow macrophage differentiation to occur. The purity of macrophages was confirmed by flow cytometry (CD11b+/F4/80+).

3.3 *In vitro* Inhibitor Assays: BMDMs were treated with many different small molecule inhibitors and agonists as listed in Table 2. Techniques varied for each experiment and details will be provided in the text. In general, BMDMs were plated after remaining in culture with M-CSF for 6 days. In a 96-well flat bottom tissue culture plate (Falcon), macrophages were seeded at $7x10^4$ cells/well one day before treatment with inhibitors and agonists to ensure adherence and prevent treatment of macrophages in a pre-stressed state from plating. Following treatment with appropriate concentrations of inhibitors and agonists, macrophages were usually left for 24 hours before cell death or viability was measured.

3.4 Cell viability assay (MTT assay): Cell viability was assessed using the 3-(4,5-dimethylthiazol-2-yl)-2,5-diphenyltetrazolium bromide (MTT) assay. In a reservoir, the MTT reagent was mixed into R8+gentamycin at a final concentration of 0.5 mg/ml. Cell supernatant was collected and frozen for future experiments or aspired and discarded. 100 µl of MTT + R8+gentamycin was added to the cells, which were then incubated at 37°C for 2 hours. Cells were lysed by adding 5mM HCl in isopropyl alcohol and vigorously mixed to solubilize the MTT crystals. Optical density values were obtained by measuring absorption at 570 nm with a reference wavelength of 650 nm on a Molecular Devices Emax plate reader. Data was analyzed using SoftMax Pro and Graphpad Prism software. Unless otherwise stated, cells were normalized to the corresponding stimulated control in the absence of zVAD (i.e. LPS+zVAD treated cells were normalized to LPS treated cells while TNFα+zVAD treated cells were normalized to TNFα).

Table 2. Inhibitors and agonists used for experiments.

Inhibitor/Agonist	Source	Notes	Concentrations
zVAD	EMD Millipore (Cat. # 627610)	Pan-caspase inhibitor	10-50 μM
Necrostatin-1 (Nec-1)	Sigma-Aldrich (Cat. # 9037)	Inhibitor of Rip1 kinase activity	30 μM
Dynasore Hydrate	Sigma-Aldrich (Cat. # D7693)	Dynamin inhibitor preventing dynamin-mediated endocytosis	40-80 μM
Lactacystin	Sigma-Aldrich (Cat. # L6785)	Irreversible proteasome inhibitor	10 μg/ml
Ultra pure LPS from E. coli 0111:B4	Sigma-Aldrich (Cat. # L3024)	Cell wall component of gram negative bacteria used to stimulate TLR4	100 ng/ml
PolyI:C	Sigma-Aldrich (Cat. # P1530)	dsRNA mimetic used to stimulate TLR3	20 μg/ml
Recombinant mouse TNFα	R&D Systems (Cat. # 410-MT)	TNFR agonist	50 μg/ml
Recombinant mouse IFNβ	PBL InterferonSource (Cat. # 12400-1)	IFNAR agonist	100 U/ml
SM-164	A gift from Dr. Shaomeng Wang, (University of Michigan)	xIAP, cIAP1 and cIAP2 inhibitor	1000-5000 nM

Note: All inhibitors and agonist were diluted in R8+gentamycin from stock.

3.5 Western blotting: In a 24-well plate, BMDMs were seeded at $3x10^5$ cells/well after 6 days in culture with M-CSF. The following day macrophages were treated with inhibitors and agonists at different time points to perform a time course. Supernatants were collected and frozen for cytokine analysis and macrophages were washed with PBS. PBS was aspirated and cells were directly lysed in 1% SDS lysis buffer with 1% β-mercaptoethanol. Samples were boiled immediately in an attempt to minimize protein degradation and frozen for future use. Standard protocol for western blot analysis was followed. Lysates were run on a 1.5 mm 10- or 15-well 6%, 8% or 10% polyacrylamide gel depending on the size of the proteins of interest. Gels were typically loaded with 25 µl of lysate and run at 120 V for one hour and 20 minutes.

A PVDF membrane was soaked with methanol, rinsed with water and then incubated with 20% methanol transfer buffer for minutes before setting up the transfer. The transfer was run at 400 mA for an hour and 15 minutes. An ice pack was added to the transfer cassette to prevent overheating. Once transferred, the membrane was blocked in 5% skim milk in Tris Buffered Saline Solution (TBS – 0.5M Tris, 1.5 NaCl pH 7) with 0.5% Tween-20 (TBST) or 5% bovine serum albumin (BSA) depending on the manufacturers protocol for one hour at room temperature on the rocker. Primary antibodies were diluted in appropriate blocking buffer (5% milk or BSA), added to the membrane and incubated overnight on the rocker at 4°C. Antibodies and corresponding dilutions used are listed in Table 3. Diluted primary antibody was kept for up to one month by adding 0.2% sodium azide to milk (no sodium azide was added to BSA diluted antibodies). Membranes were then washed with TBST three times at ten minutes/wash before adding secondary antibody diluted in the appropriate blocking buffer (5% milk or BSA) for one hour. Secondary antibody was

Table 3. Primary and secondary antibodies used for western blot analysis.

Antibody	Source	Dilution Used
Mouse anti-Rip1	BD Transduction Laboratories (Cat. # 610458)	1:1000 in 5% milk
Mouse anti-Actin	Santa Cruz Biotechnology (Cat. # 47778)	1:1000 in 5% milk
Mouse anti-PKR	Santa Cruz Biotechnology (Cat. # 6282)	1:1000 in 5% milk
Rabbit anti-Rip3	ProSci Inc. (Cat. # 2283)	1:1000 in 5% milk
Rabbit anti-STAT1	Cell Signaling (Cat. # 9172)	1:1000 in 5% milk
Rabbit anti-phosphorylated STAT1	Cell Signaling (Cat. # 9167)	1:1000 in 5% milk
Rabbit anti-STAT2	Cell Signaling (Cat. # 4597)	1:1000 in 5% milk
Rabbit anti-p65	Cell Signaling (Cat. # 8242)	1:1000 in 5% BSA
Rabbit anti-phosphorylated p65	Cell Signaling (Cat. # 3033)	1:1000 in 5% BSA
Rabbit anti-cIAP1/2	Cyclex (Cat. # CY-P1041)	1:1000 in 5% milk
Rat anti-MLKL	EMD Millipore (Cat. # MABC604)	1:1000 in 5% milk
Rabbit anti-phosphorylated PKR	EMD Millipore (Cat. # 07-886)	1:1000 in 5% milk
Goat anti-mouse HRP conjugated secondary antibody	Santa Cruz Biotechnology (Cat. # 2005)	1:1000 in 5% milk
Goat anti-rabbit HRP conjugated secondary antibody	Santa Cruz Biotechnology (Cat. # 2004)	1:1000 in 5% milk
Sheep anti-rat HRP conjugated secondary antibody	EMD Millipore (Cat. # AP510P)	1:1000 in 5% milk

discarded and membranes were washed five times at ten minute/wash. Membranes were visualized using either luminol ELC substrate (Thermo Scientific #32106) or the highly sensitive West Femto ECL substrate (Thermo Scientific #34095) depending on protein expression. Photosensitive film (Sigma-Aldrich, Carestream Heath 785019) was used to examine protein expression. Results were quantified using Image-J software to perform densitometic analyses.

3.6 Lambda Phosphatase Assay: Some antibodies, such as Rip1 and Rip3, do not have a phospho-specific antibody counterpoint that is commercially available. Importantly, the Rip1 and Rip3 antibodies used in this thesis detect a slower migrating band located just above the targeted protein. Previous reports have suggested that these bands with a slightly higher molecular weight are phosphorylated proteins of interest. To confirm this, a lambda phosphatase experiment was performed to dephosphorylate proteins. BMDMs were plated after 6 days of being in culture with M-CSF at $3x10^5$ cells/well in a 24-well plate. 24 hours later macrophages were treated with inhibitors and agonists (described in the text) and lysed with RIPA buffer containing protease inhibitors (Roche Applied Science, 04693132001). Phosphatase treatments included 500 units of lambda phosphatase (Santa Cruz Biotechnology, 2000312) for 30 minutes at 30°C. SDS lysis buffer was added to samples, which were then boiled for 5 minutes at 100°C before western blot analysis.

3.7 Immunofluorescence: BMDMs were plated at $7x10^4$ cells/well in a 96-well plate after differentiating for 6 days in culture. 24 hours later, macrophages were treated with corresponding reagents as described in the text. Following another 24 hour incubation, media was aspirated and 100 μl/well of clear RPMI lacking phenol was added to the cells. Macrophages were stained with Hoechst (2.5 μg/ml; Invitrogen 33342) and propidium iodide (PI) (1:10 dilution; BD Pharmingen, 550825) and incubated at 37°C for 25 minutes prior to

being examined by immunofluorescence microscopy. A Zeiss AxioObserver.D1 microscope was used and the AxioVision Rel. 4.8 program was used to analyze images. Cells were quantitated using the Lumenera Infinity Analyze program.

3.8 Cytokine Analysis: Enzyme linked immunosorbant assays (ELISAs) were used to measure the concentration of cytokines produced in response to various inhibitors and agonists as described in the text. Murine IL-10 (BD Biosciences, 555252) and TNFα (BD Biosciences, 560478) were measured using a kit while IL-6 was measured using a primary and secondary IL-6 antibody pair (eBioscience, 14-7061-81, 13-7062-85). Briefly, microwell 96-well plates were coated with 50 µl /well of diluted capture antibody, sealed and incubated at 4°C overnight. The following day plates were aspirated and washed 3 times with PBST (washing buffer). Plates were blocked with 100 µl/well of assay diluent, sealed and incubated at room temperature for 1 hour. Plates were then aspirated and washed 3 times with washing buffer. 50 µl of standard and sample were added to the plates, which were sealed and incubated at room temperature for 2 hours. Plates were aspirated and washed 5 times with washing buffer. 50 µl/well of working detector (detection antibody+Steptavidin-HRP) was added to IL-10 and TNFα plates before sealing and incubating at room temperature for 1 hour. For IL-6 plates, 50 µl/well of detection antibody was added and plates were sealed and incubated at room temperature for 1 hour. After washing 3 times, 50 µl/well of Steptavidin was added to the IL-6 plates, which were then sealed and incubated at room temperature for 30 minutes. All plates were washed 7 times and 50 µl of substrate solution (mixed at a 1:1 ratio) was added to each well. Plates were sealed and incubated in the dark for varying amounts of time depending on the development of standards. 25µl of stop solution (2N H_2SO_4) was added to each well and absorbance was read at 450 nm – 570 nm on a Molecular Devices Emax plate reader. Data were analyzed using SoftMax Pro and Graphpad Prism.

3.9 IFNβ production: IFNβ expression was assessed using an L929 cell line (obtained from Dr. Bruce Beutler, USA) with a luciferase reporter gene cloned under the regulation of an ISRE promoter. A frozen stock of ISRE-L929 cells was revived in 10% FBS + 2ME + Dulbecco's Modified Eagle's Medium (DMEM) and incubated at 37°C for several days to allow cells to proliferate. ISRE-L929 cells were seeded at $5x10^4$ cells/well in a 96-well flat bottom plate and incubated with 40 µl of BMDM culture supernatant for 4 hours. Cells were quickly rinsed with PBS and then lysed with 20 µl/well of 1X lysis buffer supplied in the luciferase assay system kit (Promega, E1500). 100 µl of luciferase assay reagent was added to each well containing lysed cells and luminescence was measured using a Molecular Devices Emax plate reader. Data were analyzed using SoftMax Pro and Graphpad Prism.

3.10 LDH Assay: In addition to examining cell viability via MTT assay, cell death was measured using a commercial lactate dehydrogenase (LDH) release assay (Sigma-Aldrich, TOX7) according to the manufacturers protocol. Briefly, supernatants were collected from BMDMs treated with various reagents as described in the text. Equal parts of LDH substrate, LDH dye and LDH cofactor were mixed together prior to adding a 1:1 ratio of LDH mixture to supernatants. This solution was incubated at room temperature in the dark for approximately 30 minutes before the reaction was stopped with a 1/10 volume of 1N HCl. The signal was then measured at 490 nm with a reference of 650 nm on a Molecular Devices Emax plate reader. Data were analyzed using SoftMax Pro and Graphpad Prism.

4.0 RESULTS

4.1 Dynamin-mediated endocytosis plays a role in necroptosis of macrophages

4.1.1 Stimulation and caspase inhibition are required for the induction of necroptosis in macrophages

To investigate the upstream necroptotic signaling events, murine macrophages were treated with various stimuli and incubated with 3-(4,5-dimethylthiazol-2-yl)-2,5-diphenyltetrazolium bromide (MTT) to measure cell viability. Live cells reduce MTT into formazan crystals resulting in higher optical density (OD) values, while dead cells are unable to perform this conversion and therefore display much lower OD values. Cell viability was also assessed by immunofluorescence imaging after adding propidium iodide (PI) and Hoechst to macrophages. WT C57BL/6 murine bone marrow derived macrophages (BMDMs) were generated and plated as described in experimental methods. BMDMs were treated with various stimuli for 24 hours. WT BMDMs did not die in response to treatment with cytokines, such as TNFα or IFNβ, or PAMPs, such as LPS or PolyI:C. Instead, cytokine or PAMP treatment resulted in much higher OD values, indicative of very little cell death occuring (Fig. 5A-C). Only in the combined presence of the pan-caspase inhibitor zVAD and stimulant did macrophages die by necroptosis (Fig. 5B-C). Additionally, caspase inhibition with zVAD treatment alone enhanced metabolic activity and did not induce detectable cell death (Figure 6A). Macrophages died by necroptosis in response to LPS+zVAD, TNFα+zVAD, IFNβ+zVAD and PolyI:C+zVAD treatment, a phenotype that was inhibited in the presence of Rip1 kinase inhibitor necrostatin-1 (Nec-1) (Fig. 6A). These results demonstrate that cytokines/PAMPs and zVAD are needed for necroptosis of murine BMDMs.

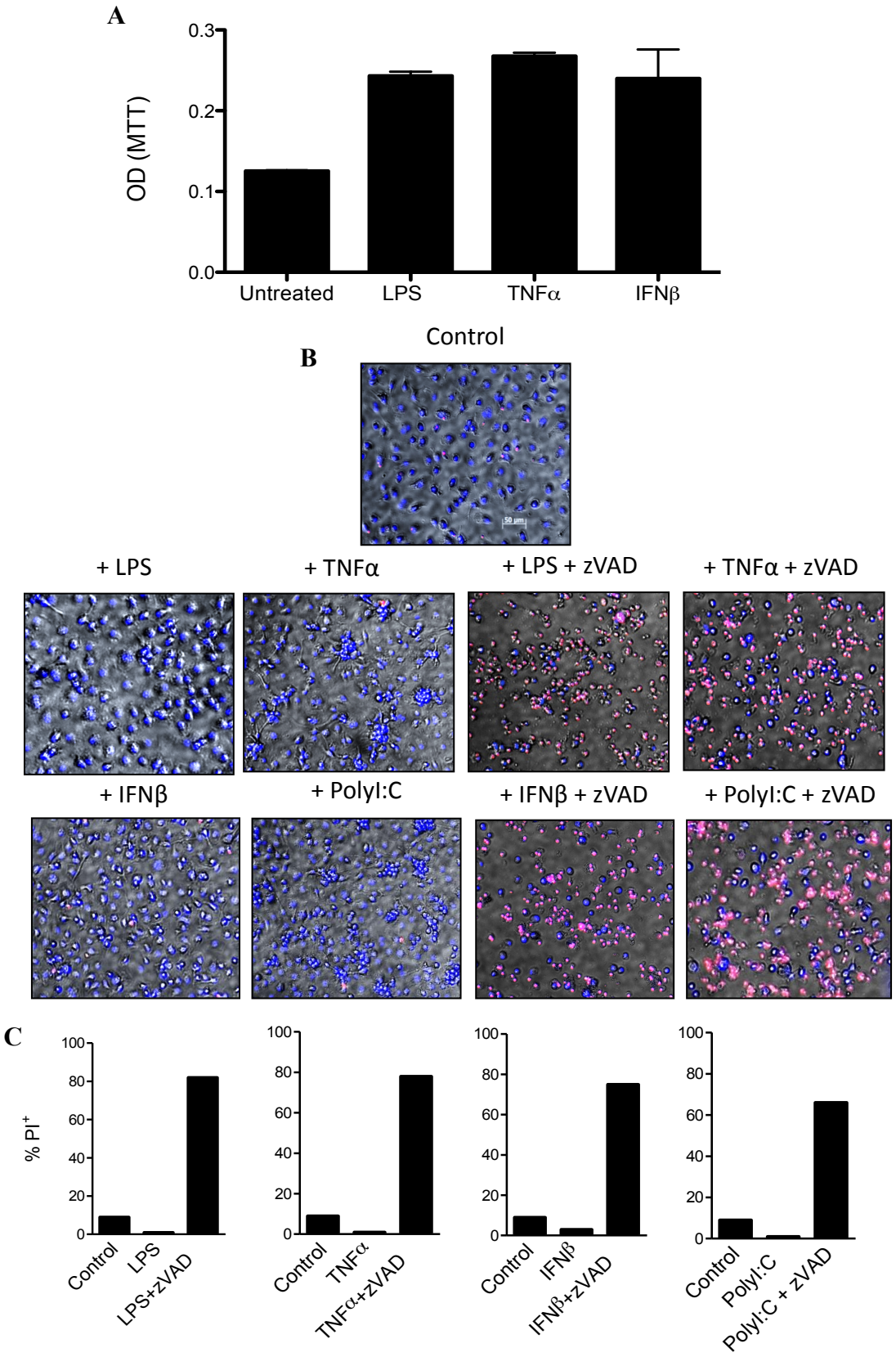
A
OD (MTT)
0.3
0.2
0.1
0.0
Untreated
LPS
TNFα
IFNβ
B
Control
+ LPS
+ TNFα
+ LPS + zVAD
+ TNFα + zVAD
+ IFNβ
+ PolyI:C
+ IFNβ + zVAD
+ PolyI:C + zVAD
C
% PI+
100
80
60
40
20
0
Control
LPS
LPS+zVAD
TNFα
TNFα+zVAD
IFNβ
IFNβ+zVAD
PolyI:C
PolyI:C + zVAD

Figure 5. *Stimulation of necroptosis inducing receptors in the absence of zVAD does not induce death.* BMDMs from WT C57BL/6 mice were treated with various stimuli including LPS (100ng/ml), TNFα (50 ng/ml), IFNβ (100 U/ml) and PolyI:C (20 μg/ml) for 24 hours before measuring cell viability by MTT assay (**A**). WT BMDMs were treated as mentioned above and cell viability was assessed by immunofluorescence using Hoescht (blue) and Propidium Iodide (PI) (red) co-staining (**B**). Images were taken and analyzed using AxioVision Rel. 4.8 program and the percentage of dead (PI^+) cells were quantitated using the Lumenera Infinity Analyze program (**C**). Data representative of at least three independent experiments.

A

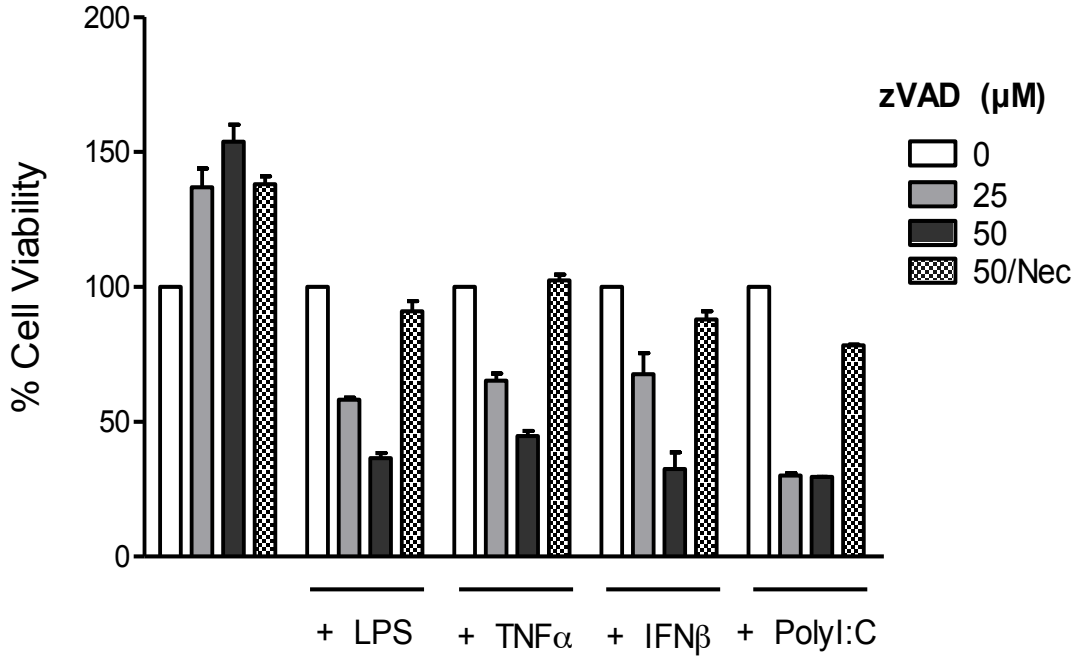
200
150
100
50
0
% Cell Viability
zVAD (μM)
0
25
50
50/Nec
+ LPS
+ TNFα
+ IFNβ
+ PolyI:C

Figure 6. *zVAD alone does not kill macrophages.* WT BMDMs were treated with different combinations of zVAD (25-50 μM), Nec-1 (30 μM), LPS (100ng/ml), TNFα (50 ng/ml), IFNβ (100 U/ml) and PolyI:C (20 μg/ml) for 24 hours before measuring cell viability by MTT assay (**A**). Graph shows % cell viability mean ± SEM relative to cells treated with corresponding stimuli in the absence of zVAD and are representative of at least 3 independent experiments performed in triplicate.

4.1.2 Necroptotic signaling results in Rip1 and Rip3 phosphorylation

As a measure of necroptotic activation, lysates from WT BMDMs treated with LPS/zVAD were collected to examine Rip1 and Rip3 phosphorylation by western blot (Fig. 7A). Antibodies specific to mouse phosphorylated Rip1 and Rip3 are currently unavailable commercially, however, the two particular Rip1 and Rip3 antibodies employed in my experiments detect both phosphorylated and unphosphorylated bands for Rip1 and Rip3 (Fig. 7A). Following LPS/zVAD stimulation, Rip1 was rapidly activated with the phosphorylated band appearing within 10 minutes post treatment, while the phosphorylated Rip3 band was detectable at a much later time point (Fig. 7A). To confirm the presence of phosphorylated Rip1 and phosphorylated Rip3 I treated extracts with lambda phosphatase (as described in experimental methods) to dephosphorylate proteins (Fig. 7B). Importantly, the slower migrating Rip1 and Rip3 bands disappeared when treated with lambda phosphatase, thus confirming the upper bands to be phosphorylated forms of Rip1 and Rip3 (Fig. 7B).

4.1.3 Blockage of dynamin-mediated endocytosis dramatically reduces cytokine production and STAT1 phosphorylation.

The first aim of this thesis was to investigate how the necroptotic signal is transmitted following ligand-receptor binding. Since ligand-receptor binding in the case of PAMPs and cytokines occurs at the cell surface I was interested in blocking endocytosis to examine the impact on cytokine production and necroptosis in response to stimuli known to induce both. Dynasore is a potent inhibitor of dynamin and dynamin dependent endocytosis (Macia et al., 2006). I treated BMDMs with dynasore to evaluate the impact on cytokine expression and necroptosis. Supernatants from BMDMs treated with LPS/zVAD (Fig. 8A), TNFα/zVAD (Fig. 8B) and IFNβ/zVAD (Fig. 8C) with and without dynasore for 6 and 24 hours were

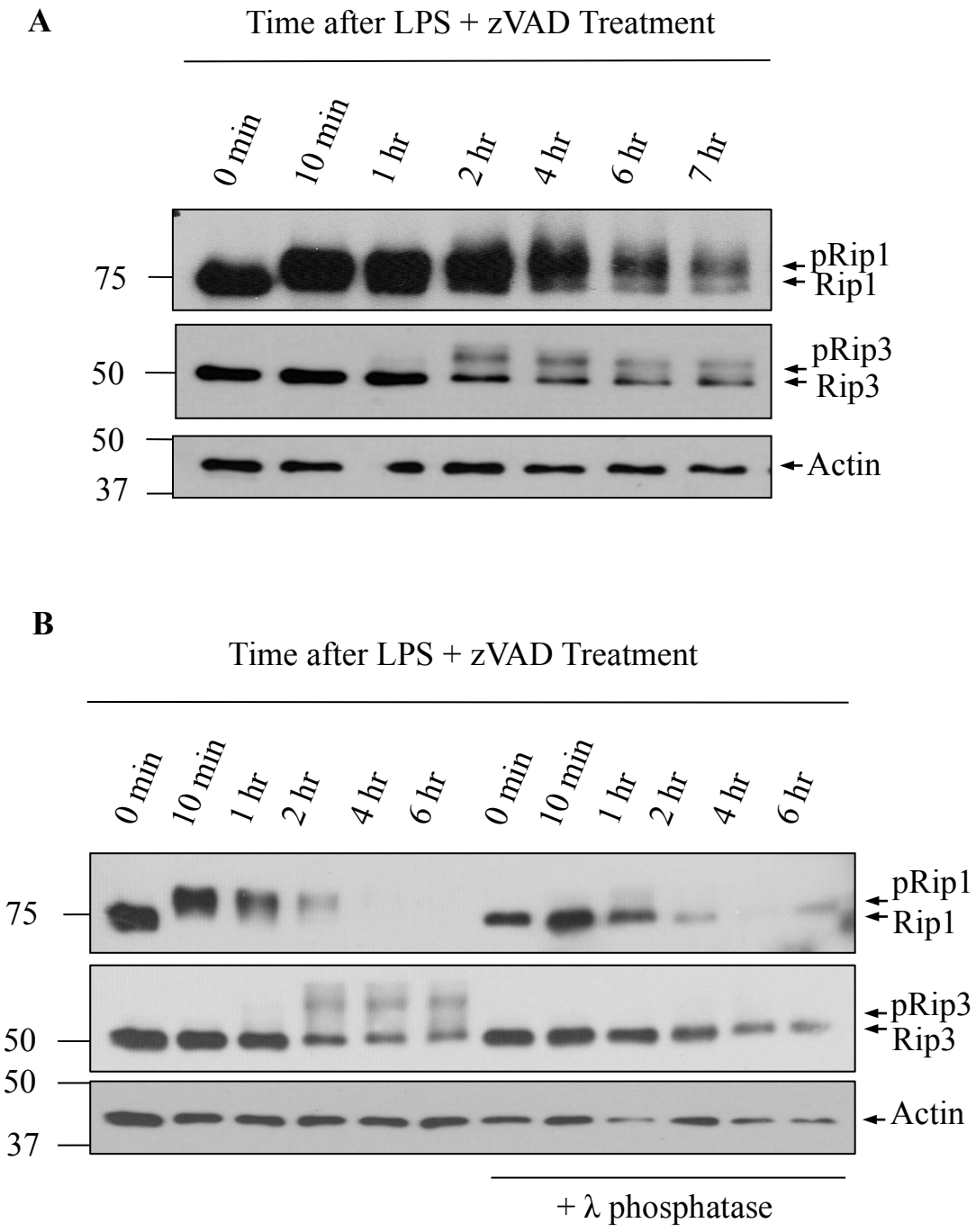
A
Time after LPS + zVAD Treatment
0 min
10 min
1 hr
2 hr
4 hr
6 hr
7 hr
75
pRip1
Rip1
50
pRip3
Rip3
50
37
Actin
B
Time after LPS + zVAD Treatment
0 min
10 min
1 hr
2 hr
4 hr
6 hr
0 min
10 min
1 hr
2 hr
4 hr
6 hr
75
pRip1
Rip1
50
pRip3
Rip3
50
37
Actin
+ λ phosphatase

Figure 7. *Necroptotic activation can be assessed by Rip1 and Rip3 phosphorylation*. Lysates were collected from LPS (100 ng/ml)/zVAD (50 μM) treated WT BMDMs to examine by western blot (**A**). To confirm the presence of phosphorylated Rip1 and phosphorylated Rip3, lysates were treated as mentioned above with and without lambda phosphatase (500 units) as described in experimental methods (**B**). Data representative of at least three independent experiments.

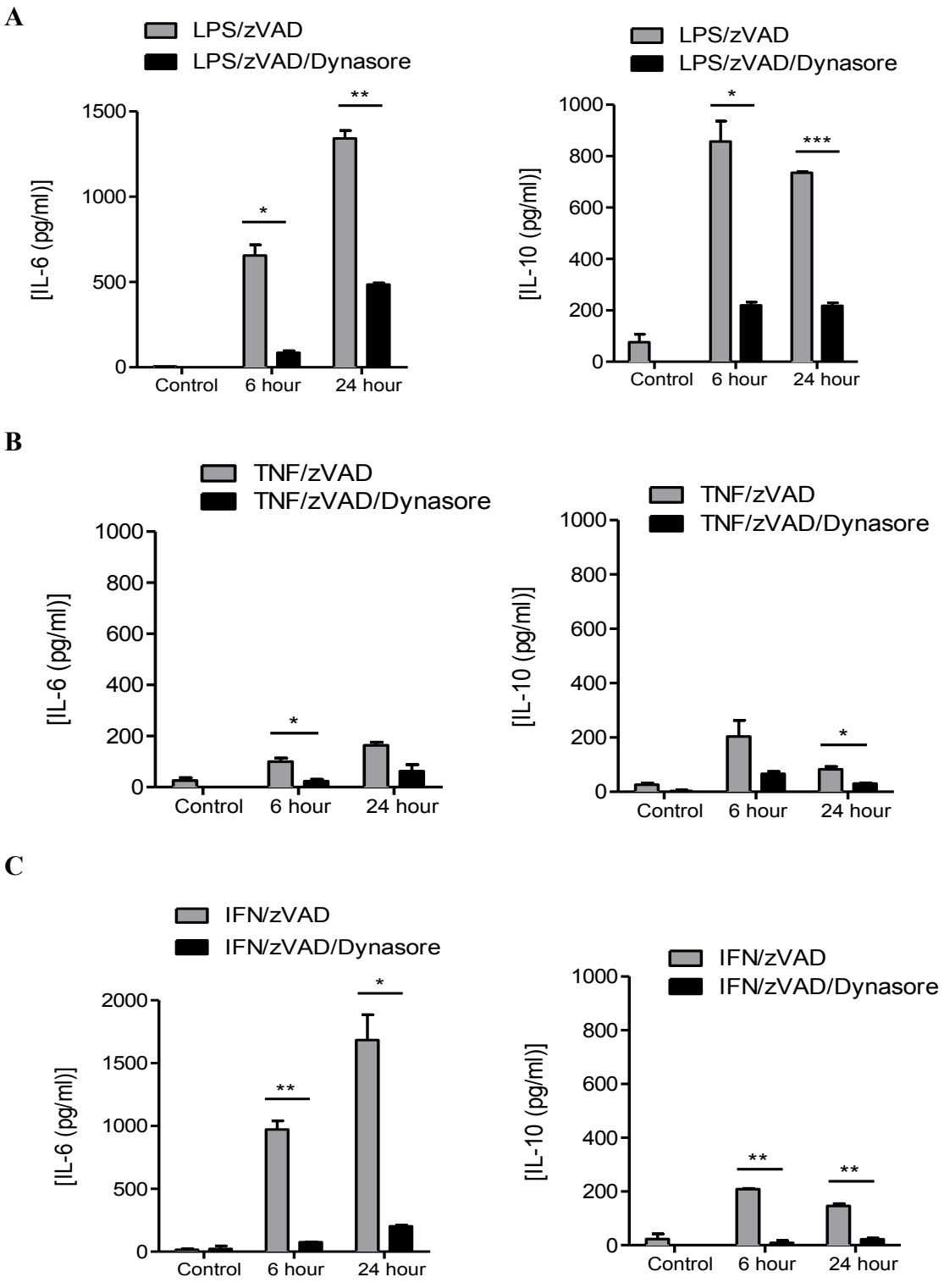
A
LPS/zVAD
LPS/zVAD/Dynasore
[IL-6 (pg/ml)]
1500
1000
500
0
*
**
Control
6 hour
24 hour
[IL-10 (pg/ml)]
1000
800
600
400
200
0
*
***
Control
6 hour
24 hour
B
TNF/zVAD
TNF/zVAD/Dynasore
[IL-6 (pg/ml)]
1000
800
600
400
200
0
*
Control
6 hour
24 hour
[IL-10 (pg/ml)]
1000
800
600
400
200
0
*
Control
6 hour
24 hour
C
IFN/zVAD
IFN/zVAD/Dynasore
[IL-6 (pg/ml)]
2000
1500
1000
500
0
**
*
Control
6 hour
24 hour
[IL-10 (pg/ml)]
1000
800
600
400
200
0
**
**
Control
6 hour
24 hour

Figure 8. *Dynasore treatment significantly reduces IL-6 and IL-10 production.* WT BMDMs were treated with and without dynasore (80 μM) in addition to LPS/zVAD, TNFα/zVAD and IFNβ/zVAD. Supernatants were collected from LPS/zVAD +/- dynasore (A), TNFα/zVAD +/- dynasore (B) and IFNβ/zVAD +/- dynasore (C) at 6 and 24 hours and analyzed by ELISA for IL-6 and IL-10 production. Graphs show mean ± SEM and are representative of at least 3 independent experiments performed in duplicate. Statistical analyses done by unpaired students t-test *$P<0.05$, **$P<0.001$ and ***$P<0.0001$.

collected to measure cytokine expression. Pre-treatment with dynasore resulted in significantly less IL-6 and IL-10 production in response to LPS/zVAD, TNFα/zVAD and IFNβ/zVAD relative to groups without dynasore (Fig. 8A-C). To further validate whether cell signaling was attenuated with dynasore treatment, I evaluated the impact on IFNβ induced phosphorylation of transcription factor STAT1. Lysates from WT BMDMs treated with IFNβ/zVAD with and without dynasore for different time intervals were collected and examined by western blot (Fig. 9A). Inhibition of dynamin-mediated endocytosis resulted in strongly reduced levels of phosphorylated signal transducer and activator of transcription 1 (STAT1) (Fig. 9A). These results indicate that although the receptor interactions happen at the cell surface, dynamin dependent endocytosis is required for cell signaling by IFNβ and suggest that the same is true for LPS and TNFα signaling.

4.1.4 The role of dynamin-mediated endocytosis in necroptosis of macrophages

After observing a marked decrease in cytokine production as a result of inhibiting dynamin-mediated endocytosis I next wanted to determine if there was an impact on necroptosis of macrophages. WT BMDMs were treated with necroptotic stimuli, varying concentrations of zVAD, Nec-1 and with and without dynamin inhibitor dynasore. For every experiment, all cells treated with dynasore were pre-treated for 30 minutes prior to the addition of other reagents. Cell viability was assessed 24 hours after treatment via MTT assay. Interestingly, dynasore treatment did not inhibit LPS/zVAD induced necroptosis of macrophages. Rather, there was a slight, yet significant, exacerbation of necroptosis in response to dynasore, LPS and zVAD treatment (Fig. 10A). In contrast, dynasore treatment had the opposite effect on TNFα and IFNβ-mediated necroptosis in which case there was a potent inhibition of necroptosis (Fig. 10B,C). No effect was observed in cells treated with

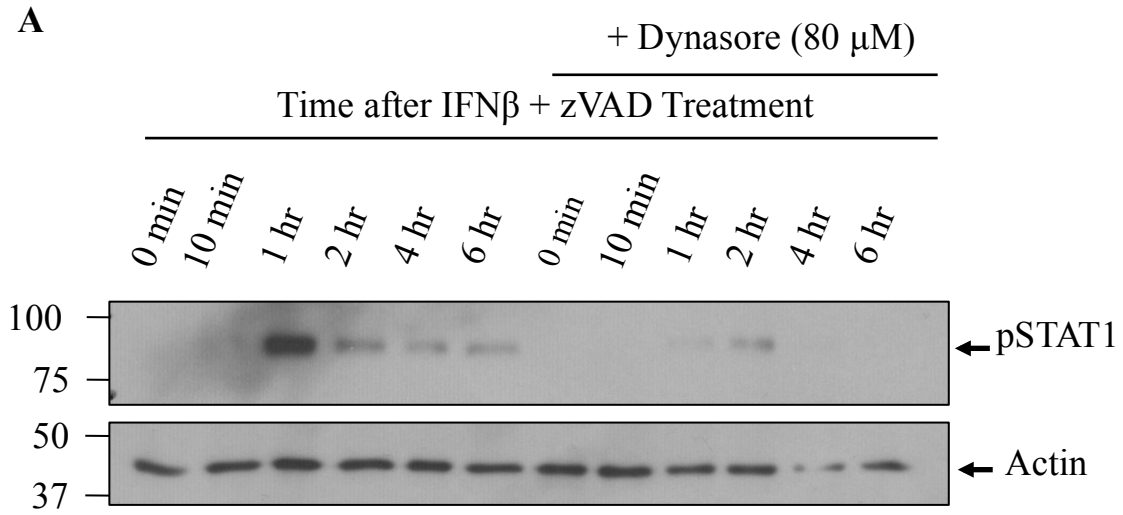
A
+ Dynasore (80 μM)
Time after IFNβ + zVAD Treatment
0 min
10 min
1 hr
2 hr
4 hr
6 hr
0 min
10 min
1 hr
2 hr
4 hr
6 hr
100
75
50
37
pSTAT1
Actin

Figure 9. *Dynasore treatment significantly reduces STAT1 phosphorylation.* Lysates were collected from WT BMDMs treated with IFNβ (100 U/ml)/zVAD (50 μM) +/- dynasore (80 μM) to measure STAT1 phosphorylation by western blot (A). Data representative of at least 3 independent experiments.

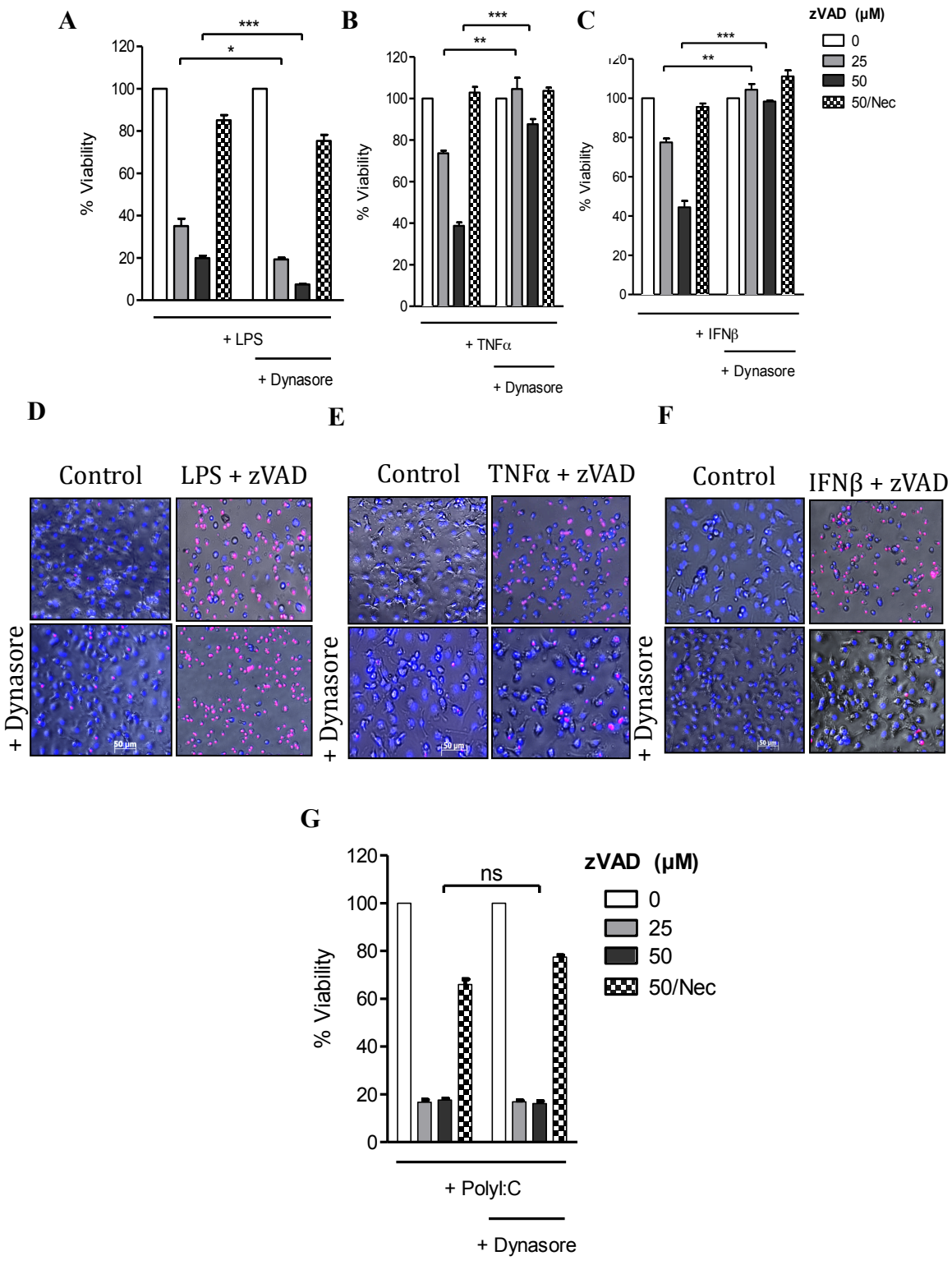
A
B
C
zVAD (μM)
0
25
50
50/Nec
% Viability
+ LPS
+ TNFα
+ IFNβ
+ Dynasore
D
E
F
Control
LPS + zVAD
TNFα + zVAD
IFNβ + zVAD
+ Dynasore
G
ns
+ Polyl:C

Figure 10. *Dynamin-mediated endocytosis is required for TNFα and IFNβ-mediated necroptosis.* BMDMs from WT mice were treated with different concentrations of zVAD, +/- dynasore (80 μM) and various stimuli including LPS (100ng/ml) (**A**), TNFα (50 ng/ml) (**B**) and IFNβ (100 U/ml) (**C**) and PolyI:C (**G**). Each group was also treated with and without Nec-1 (30 μM). Macrophages were left for 24 hours before assessing cell viability by MTT assay and/or immunofluorescence using Hoescht (blue) and Propidium Iodide (red) co-staining (**A-G**). Graphs show % cell viability mean ± SEM relative to cells treated with corresponding stimuli in the absence of zVAD and are representative of at least 3 independent experiments performed in triplicate. Statistical analyses done by unpaired students t-test *P<0.05, **P<0.001 and ***P<0.0001.

PolyI:C+zVAD+dynasore (Figure 10G). Providing further support for this data, cell viability was alternatively measured by staining BMDMs with Hoechst and PI and analyzed by immunofluorescence microscopy, which indeed demonstrated that inhibition of dynamin-mediated endocytosis prevented TNFα and IFNβ-mediated necroptosis while slightly enhancing LPS-mediated necroptosis (Figure 10D-F).

4.1.5 The role of dynamin-mediated endocytosis in necroptosis may be specific to macrophages

A murine embryonic fibroblast (MEF) cell line, which was generated by immortalizing primary MEFs by E1A/Ras transformation, was maintained in 10% FBS + 2ME + Dulbecco's Modified Eagle's Medium (DMEM) and used to examine the role of endocytosis in necroptosis within a cell type other than macrophages. MEFs were plated at $3x10^4$ cells/well in a 96-well flat bottom plate the day prior to treatment. Cells were treated with various reagents for 24 hours and cell viability was measured by MTT assay. MEFs were only susceptible to necroptosis in response to TNF+zVAD treatment, which was rescuable by Nec-1 (Fig. 11A). Similar to dynasore treated BMDMs, MEFs were pre-treated with different concentrations of dynasore for 30 minutes prior to the addition of TNF, varying concentrations of zVAD and Nec-1 (Fig. 11B). Inhibition of dynamin-mediated endocytosis did not rescue MEFs from necroptotic cell death. These results stand in direct contrast to the role of dynamin-mediated endocytosis in necroptosis of macrophages. Hence it is likely that there are substantial differences in the signaling mechanisms employed by various cell types as they respond to necroptotic stimuli.

A

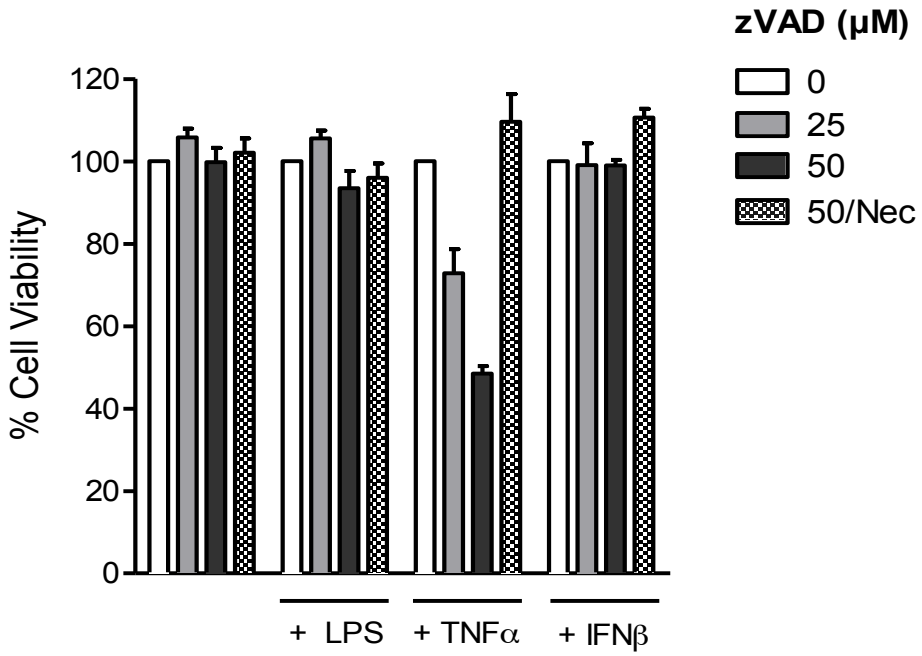
zVAD (μM)
0
25
50
50/Nec
% Cell Viability
120
100
80
60
40
20
0
+ LPS
+ TNFα
+ IFNβ

B

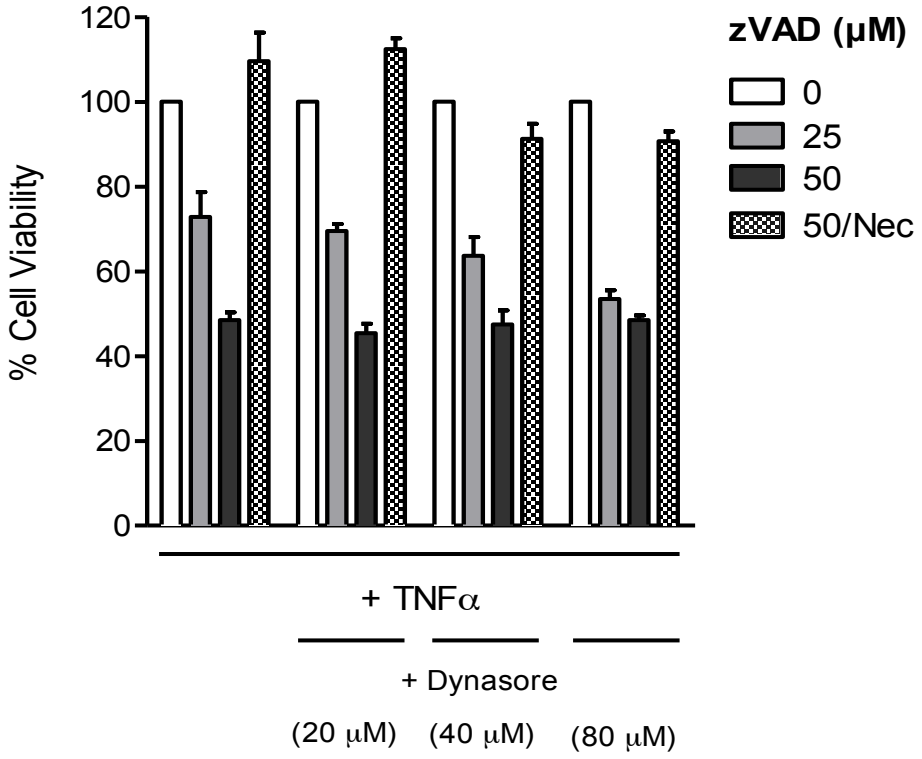
zVAD (μM)
0
25
50
50/Nec
% Cell Viability
120
100
80
60
40
20
0
+ TNFα
+ Dynasore
(20 μM)
(40 μM)
(80 μM)

Figure 11. *Necroptosis of MEFs occurs independently of dynamin-mediated endocytosis.* MEFs were treated with different concentrations of zVAD, with and without Nec-1 (30 μM), LPS (100ng/ml), TNFα (100 ng/ml) and IFNβ (100 U/ml) (**A**). MEFs were treated with TNF/zVAD with and without different concentrations of dynasore (**B**). Graphs show % cell viability mean ± SEM relative to cells treated with corresponding stimuli in the absence of zVAD and are representative of at least 3 independent experiments performed in triplicate.

4.1.6 Inhibition of dynamin dependent endocytosis strongly impairs TNFα induced necroptotic and canonical NFκB signaling

To further investigate why dynasore treatment inhibits TNFα-mediated necroptosis I collected lysates from WT BMDMs treated with TNFα+zVAD at varying time intervals over the course of 6 hours for western blot analysis of Rip1 and Rip3 activation. Interestingly, dynasore treatment did not impact Rip1 phosphorylation but dramatically reduced the phosphorylation of Rip3 and activation of NFκB (Fig. 12A). To quantify western blots, densitometric analysis of phosphorylated Rip1 to total unphosphorylated Rip1 (pRip1/Rip1), pRip3/Rip3 and p-p65/p65 ratios were measured (Fig. 12B-D).

4.2 Type I interferon signaling is required for necroptosis of macrophages

4.2.1 Signaling through IFNAR1 is required for necroptosis

Having evaluated the upstream signaling events of macrophage necroptosis, I was next interested in examining the downstream intracellular necroptotic signaling events, particularly in the context of IFN-I signaling. To explore the second aim of my thesis, many different experiments were performed using IFNAR1-/- mice. These mice lack one of the two subunits of the IFN-I receptor and therefore have impaired IFN-I signaling. BMDMs were generated from WT and IFNAR1-/- mice as described in experimental methods. Macrophages were plated at $7x10^4$ cells/well in a 96-well flat bottom plate. Necroptotic stimuli and inhibitors were added to macrophages for 24 hours. Cell viability was measured by MTT assay and immunofluorescence. Interestingly, IFNAR1-/- BMDMs were highly resistant to LPS/zVAD, TNFα/zVAD, PolyI:C/zVAD and IFNβ/zVAD induced necroptosis relative to WT macrophages (Fig. 13A-E).

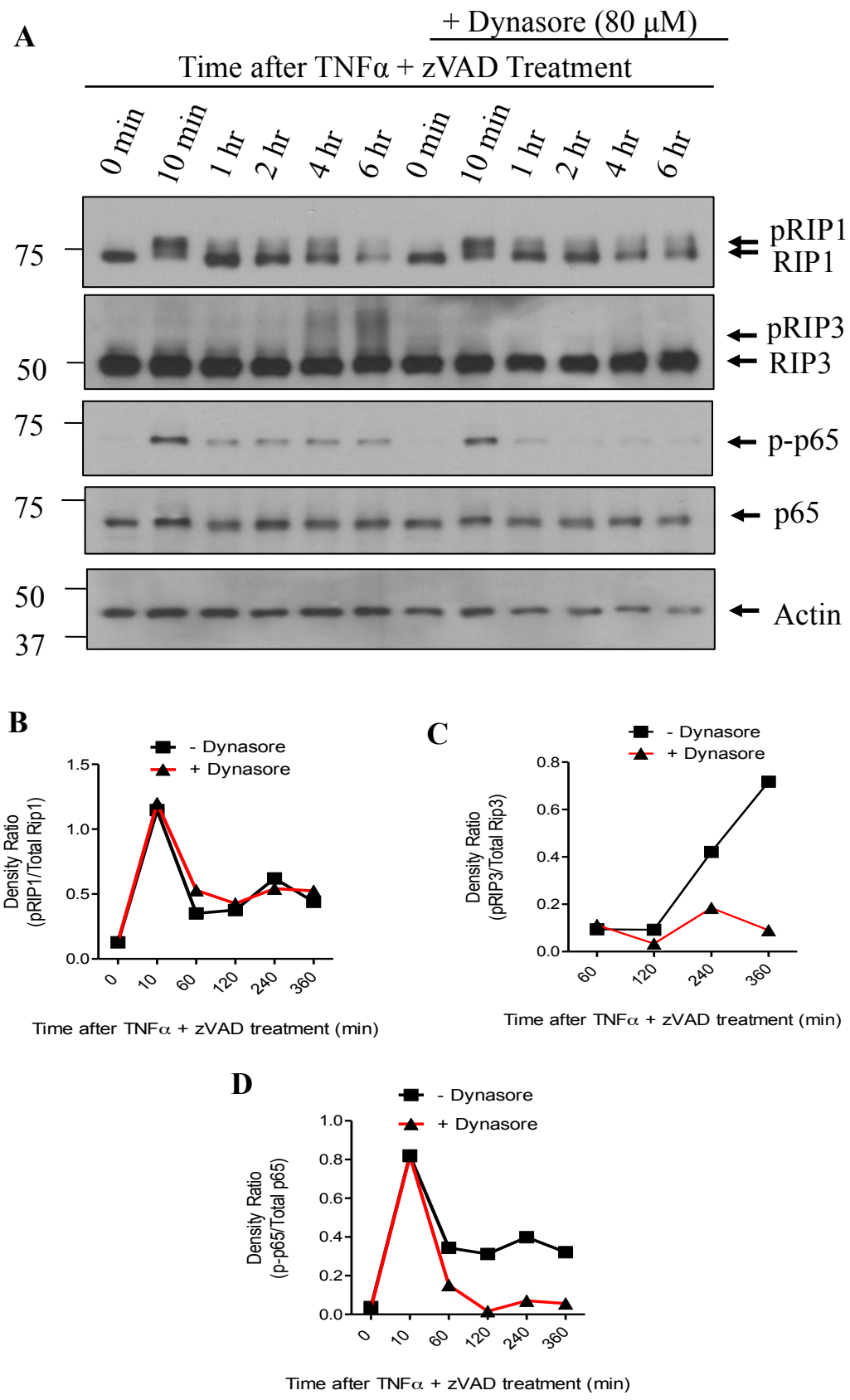
A
+ Dynasore (80 μM)
Time after TNFα + zVAD Treatment
0 min
10 min
1 hr
2 hr
4 hr
6 hr
0 min
10 min
1 hr
2 hr
4 hr
6 hr
75
50
75
75
50
37
pRIP1
RIP1
pRIP3
RIP3
p-p65
p65
Actin
B
- Dynasore
+ Dynasore
Density Ratio (pRIP1/Total Rip1)
1.5
1.0
0.5
0.0
0
10
60
120
240
360
Time after TNFα + zVAD treatment (min)
C
- Dynasore
+ Dynasore
Density Ratio (pRIP3/Total Rip3)
0.8
0.6
0.4
0.2
0.0
60
120
240
360
Time after TNFα + zVAD treatment (min)
D
- Dynasore
+ Dynasore
Density Ratio (p-p65/Total p65)
1.0
0.8
0.6
0.4
0.2
0.0
0
10
60
120
240
360
Time after TNFα + zVAD treatment (min)

Figure 12. *Inhibition of TNFR endocytosis strongly reduces Rip3 phosphorylation and hinders NFκB signaling.* Lysates from WT BMDMs treated with LPS (100 ng/ml) and zVAD (50 μM) with and without dynasore (80 μM) for different time intervals over the course of 6 hours were collected and examined by western blot (**A**). Densitometry ratios of phosphorylated Rip1 to unphosphorylated Rip1 (pRip1/Rip1), pRip3/Rip3 and p-p65/p65 were calculated (**B-D**). Data are representative of at least three independent experiments.

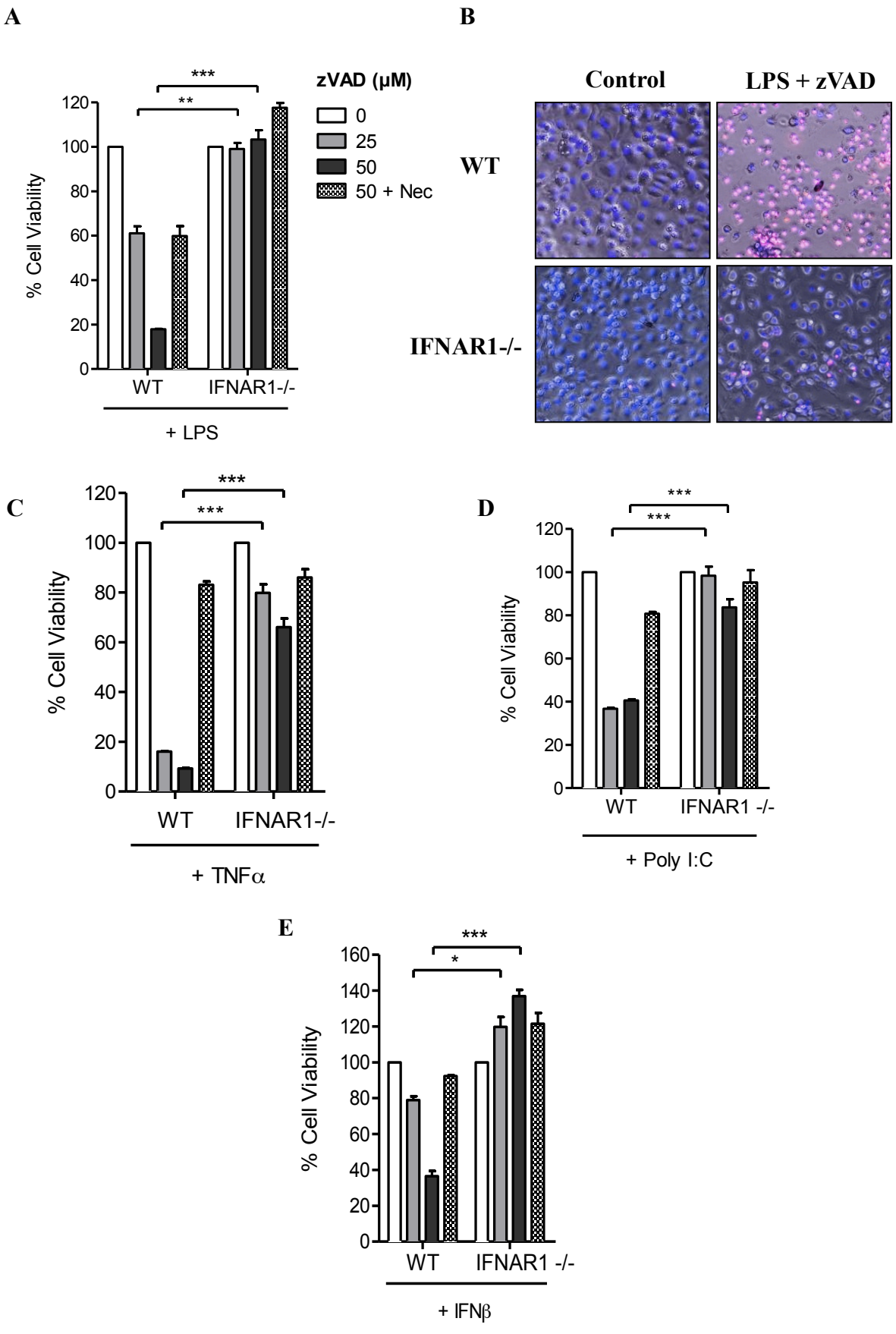
A
B
zVAD (μM)
0
25
50
50 + Nec
% Cell Viability
WT
IFNAR1-/-
+ LPS
Control
LPS + zVAD
WT
IFNAR1-/-
C
% Cell Viability
WT
IFNAR1-/-
+ TNFα
D
% Cell Viability
WT
IFNAR1 -/-
+ Poly I:C
E
% Cell Viability
WT
IFNAR1 -/-
+ IFNβ

Figure 13. *Type I interferon signalling is required for LPS, TNFα and PolyI:C-mediated necroptosis in macrophages*. WT and IFNAR1 deficient BMDMs were treated with LPS/zVAD, TNFα/zVAD, PolyI:C/zVAD and IFNβ/zVAD, all with and without Nec-1, for 24 hours before measuring cell viability by MTT assay or immunofluorescence using Hoechst (blue) and PI co-staining (red) (**A-E**). LPS was used at a concentration of 100 ng/ml, zVAD at 25-50 μM, TNFα at 50 ng/ml, IFNβ at 100 U/ml, PolyI:C at 20 μg/ml and Nec-1 at 30 μM. Graphs show % cell viability mean ± SEM relative to cells treated with corresponding stimuli in the absence of zVAD and are representative of at least 3 independent experiments performed in triplicate. Statistical analyses done by unpaired students t-test *P<0.05, **P<0.001 and ***P<0.0001.

To test whether mice lacking both subunits of the TNFR (TNFR1/2 -/-), were also resistant to necroptosis induced by other pathways, the same cell viability experiments were performed. While TNFR1/2-/- BMDMs were resistant to TNFα induced necroptosis, they were still susceptible to several other inducers of necroptosis (Fig. 14A-D), suggesting that signaling through IFNAR1 is a dominant necroptotic mechanism. The same cell viability experiments were also performed in Rip3 null BMDMs and as expected, Rip3 knockout (KO) macrophages were completely resistant to necroptosis (Fig. 15A-D). Taken together these results demonstrate that IFN-I signaling, as oppose to TNF signaling, is the predominant mechanism of necroptosis of macrophages.

4.2.2 IFN-I signaling is required for prolonged Rip3 activation

In order to determine the mechanism behind reduced necroptosis in IFNAR1-/- macrophages, I collected lysates from WT and IFNAR-/- BMDMs treated with LPS/zVAD at varying time intervals for up to 12 hours (Fig. 16A). Interestingly, Rip1 activation initially occurred similarly in WT and IFNAR1-/- macrophages, however phosphorylated Rip1 levels decreased more rapidly in IFNAR1-/- macrophages (Fig 16A) A stronger difference was observed with Rip3 phosphorylation, which was strongly attenuated in the absence of IFN-I signaling (Fig. 16A). To quantify Rip1 and Rip3 expression in WT and IFNAR1-/- macrophages, densitometry was performed and averaged on at least three independent western blots (Fig. 16B, C). Densitometric analysis revealed significant impairment in Rip1 and Rip3 phosphorylation in IFNAR1-/- macrophages (Fig. 16B,C). Phosphorylation of STAT1 was also evaluated to decipher the mechanism involved. While phosphorylation of STAT1 was detected in WT BMDMs at approximately 2 hours post stimulation with LPS/zVAD, no detectable phosphorylated STAT1 was observed in IFNAR1-/- macrophages

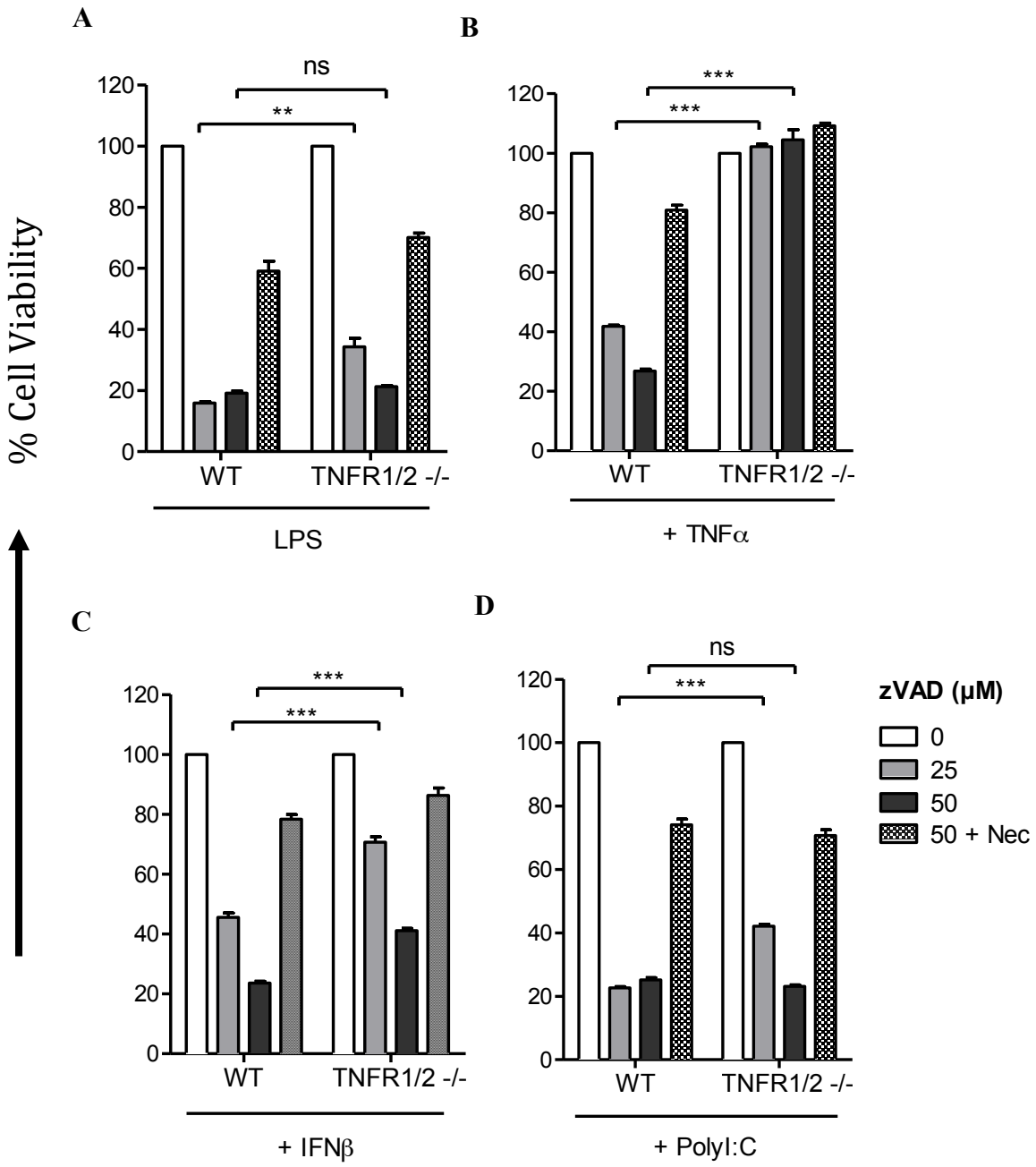
A
B
C
D
% Cell Viability
ns
**
***
***
***
***
ns
120
100
80
60
40
20
0
WT
TNFR1/2 -/-
LPS
+ TNFα
+ IFNβ
+ PolyI:C
zVAD (μM)
0
25
50
50 + Nec

Figure 14. *TNF signaling is not required for LPS, IFNβ or PolyI:C-mediated necroptosis.* TNFR1/2 -/- BMDMs were treated with LPS/zVAD, TNFα/zVAD, PolyI:C/zVAD and IFNβ/zVAD, all with and without Nec-1, for 24 hours before measuring cell viability by MTT assay (**A-D**). LPS was used at a concentration of 100 ng/ml, zVAD at 25-50 μM, TNFα at 50 ng/ml, IFNβ at 100 U/ml, PolyI:C at 20 μg/ml and Nec-1 at 30 μM. Graphs show % cell viability mean ± SEM relative to cells treated with corresponding stimuli in the absence of zVAD and are representative of at least 3 independent experiments performed in triplicate. Statistical analyses done by unpaired students t-test **P<0.001 and ***P<0.0001.

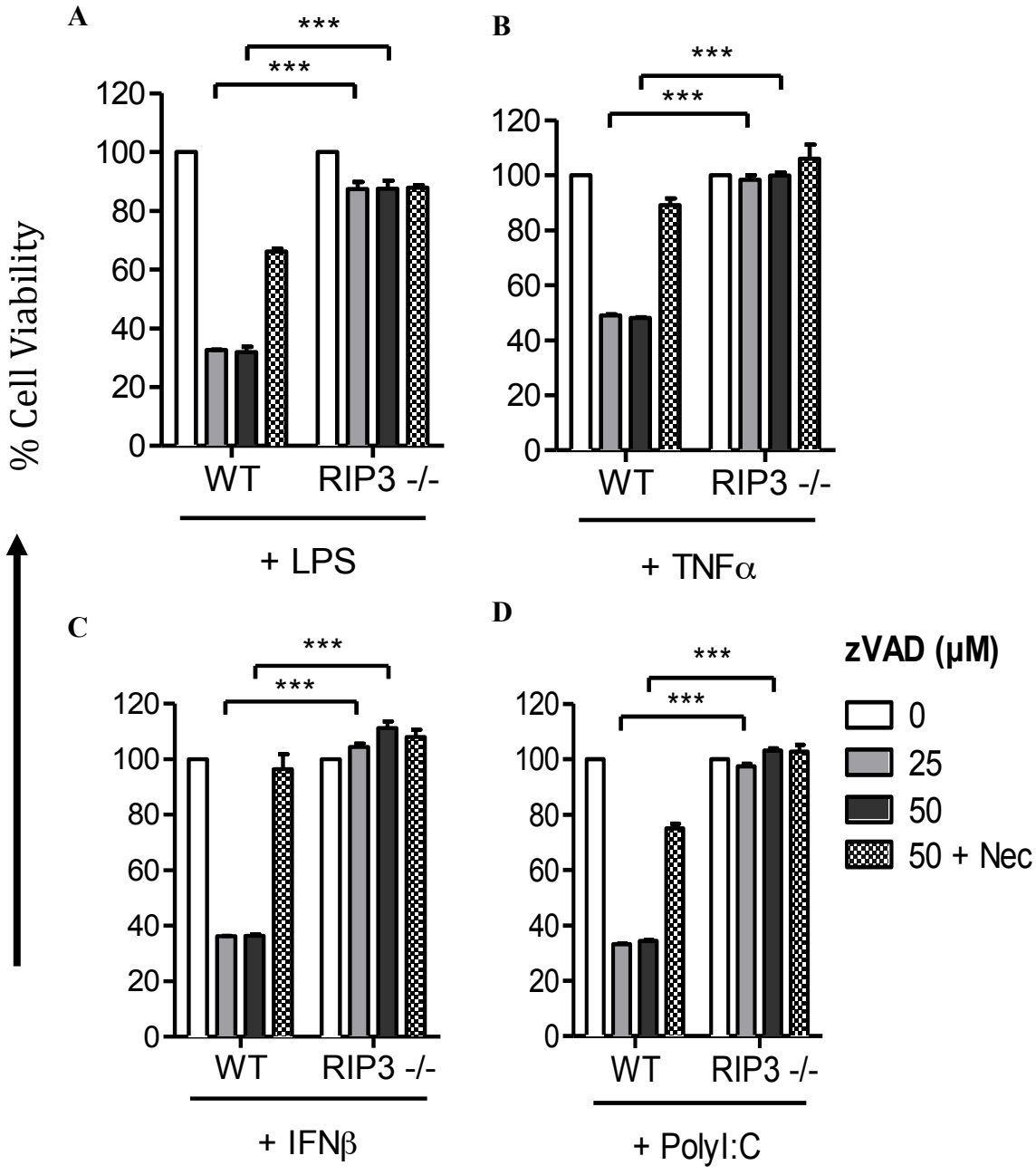
A
B
C
D
% Cell Viability
120
100
80
60
40
20
0
***
***
WT
RIP3 -/-
+ LPS
+ TNFα
+ IFNβ
+ PolyI:C
zVAD (μM)
0
25
50
50 + Nec

Figure 15. *Necroptosis of macrophages is Rip3 dependent.* Rip3 -/- BMDMs were treated with LPS/zVAD, TNFα/zVAD, PolyI:C/zVAD and IFNβ/zVAD, all with and without Nec-1, for 24 hours before measuring cell viability by MTT assay (**A-D**). LPS was used at a concentration of 100 ng/ml, zVAD at 25-50 μM, TNFα at 50 ng/ml, IFNβ at 100 U/ml, PolyI:C at 20 μg/ml and Nec-1 at 30 μM. Graphs show % cell viability mean ± SEM relative to cells treated with corresponding stimuli in the absence of zVAD and are representative of at least 3 independent experiments performed in triplicate. Statistical analyses done by unpaired students t-test *P<0.05, **P<0.001 and ***P<0.0001.

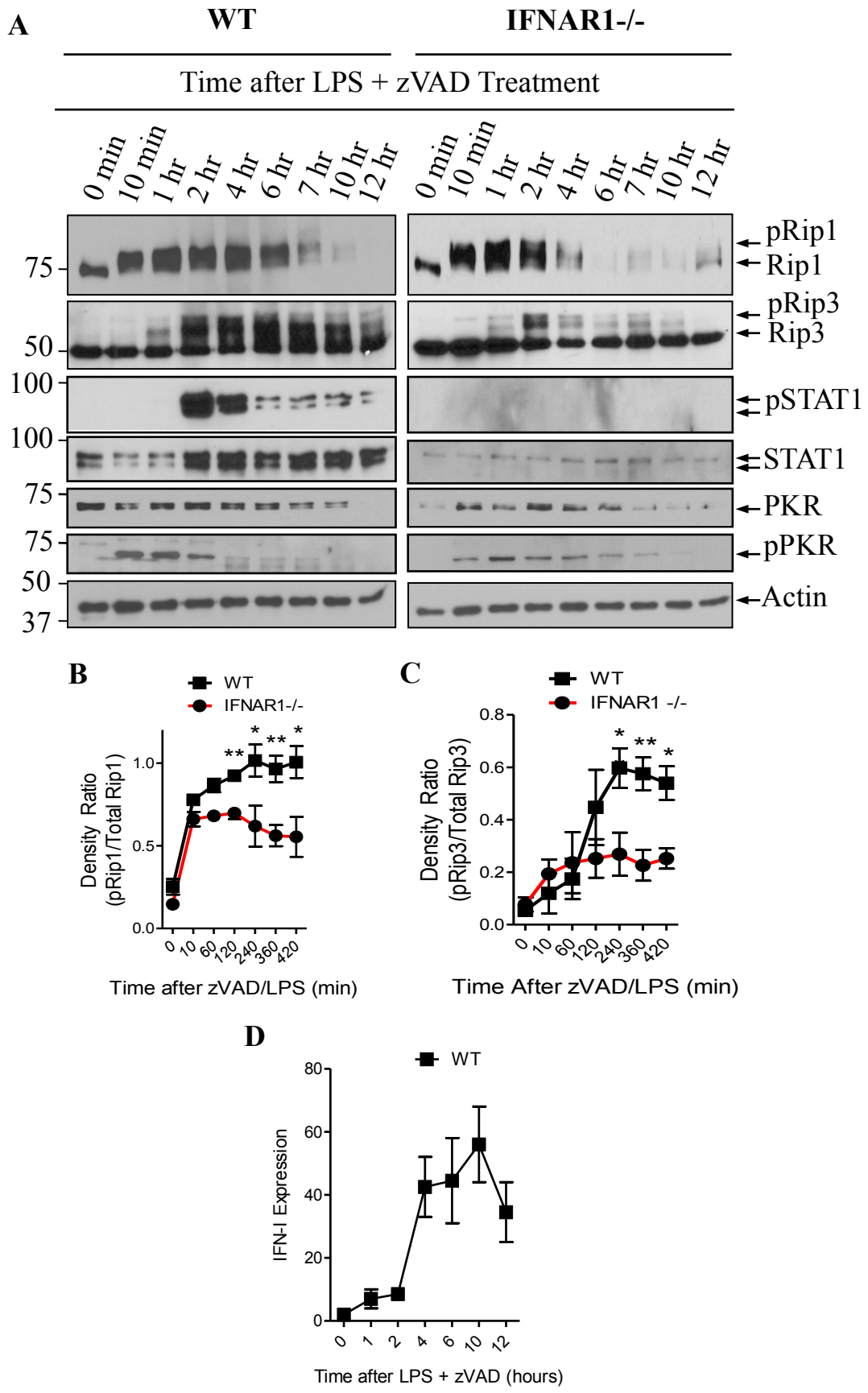
A
WT
IFNAR1-/-
Time after LPS + zVAD Treatment
0 min
10 min
1 hr
2 hr
4 hr
6 hr
7 hr
10 hr
12 hr
75
50
100
100
75
75
50
37
pRip1
Rip1
pRip3
Rip3
pSTAT1
STAT1
PKR
pPKR
Actin
B
WT
IFNAR1-/-
Density Ratio (pRip1/Total Rip1)
1.0
0.5
0.0
0
10
60
120
240
360
420
Time after zVAD/LPS (min)
C
WT
IFNAR1 -/-
Density Ratio (pRip3/Total Rip3)
0.8
0.6
0.4
0.2
0.0
Time After zVAD/LPS (min)
D
WT
IFN-I Expression
80
60
40
20
0
0
1
2
4
6
10
12
Time after LPS + zVAD (hours)

Figure 16. *IFNAR1 signaling is needed to sustain Rip3 phosphorylation.* Lysates from WT and IFNAR1-/- BMDMs were treated with LPS (100 ng/ml) + zVAD (50 μM) for different time intervals over the course of 12 hours were collected to examine by western blot (**A**). To quantitate the average ratio of pRip1 to Rip1 and pRip3 to Rip3 over at least three independent experiments a densitometric analysis was performed (**B-C**). Supernatants from the WT BMDM 12 hour LPS/zVAD western blot time course were collected and IFNβ was measured using an ISRE L929 cell line as described in experimental methods (**D**). Western blot data representative of at least 3 independent experiments. IFNβ luciferase data pooled from two independent experiments. Statistical analyses done by unpaired students t-test *$P<0.05$ and **$P<0.001$.

(Fig. 16A). I evaluated the relative timing and extent of IFN-I expression after stimulation of macrophages with LPS/zVAD, and noted that the expression of IFN-I increases substantially after the first few hours of stimulation (Fig. 16D).

4.2.3 TRIF-dependent signaling is needed for Rip3 activation and LPS-mediated necroptosis

To delve further into the LPS-mediated necroptotic pathway, I performed various experiments focusing on the two key adaptor proteins involved in TLR4 signaling, TRIF and MyD88. TRIF and MyD88 null macrophages were generated as described in experimental methods and treated with LPS/zVAD +/- Nec-1, TNFα/zVAD +/- Nec-1, IFNβ/zVAD +/- Nec-1 and PolyI:C/zVAD +/- Nec-1 for 24 hours before measuring cell viability by MTT assay (Fig. 17A-D). Interestingly, TRIF deficient macrophages were significantly resistant to LPS-mediated necroptosis and PolyI:C-mediated necroptosis (Fig. 17A,D). In response to TNFα/zVAD and IFNβ/zVAD treatment TRIF null macrophages remained susceptible to necroptosis (Fig. 17B,C). MyD88 -/- macrophages responded similarly to WT macrophages in response to all necroptotic stimuli, however a very slight rescue was observed in response to PolyI:C/zVAD treatment (Fig. 17A-D).

After observing necroptotic resistance in TRIF-/- BMDMs, I was interested in understanding the mechanisms responsible. Lysates were collected from WT, TRIF-/- and MyD88-/- BMDMs treated with LPS/zVAD at different time points over several hours (Fig. 18A). Subtle differences in Rip1 activation were observed between the three groups, demonstrating that Rip1 activation occurs though TRIF and MyD88-dependent pathways (Fig. 18A). A repeated WT, TRIF-/- and MyD88-/- western blot from a separate experiment more clearly demonstrated the differences in Rip1 activation between the three groups (Fig.

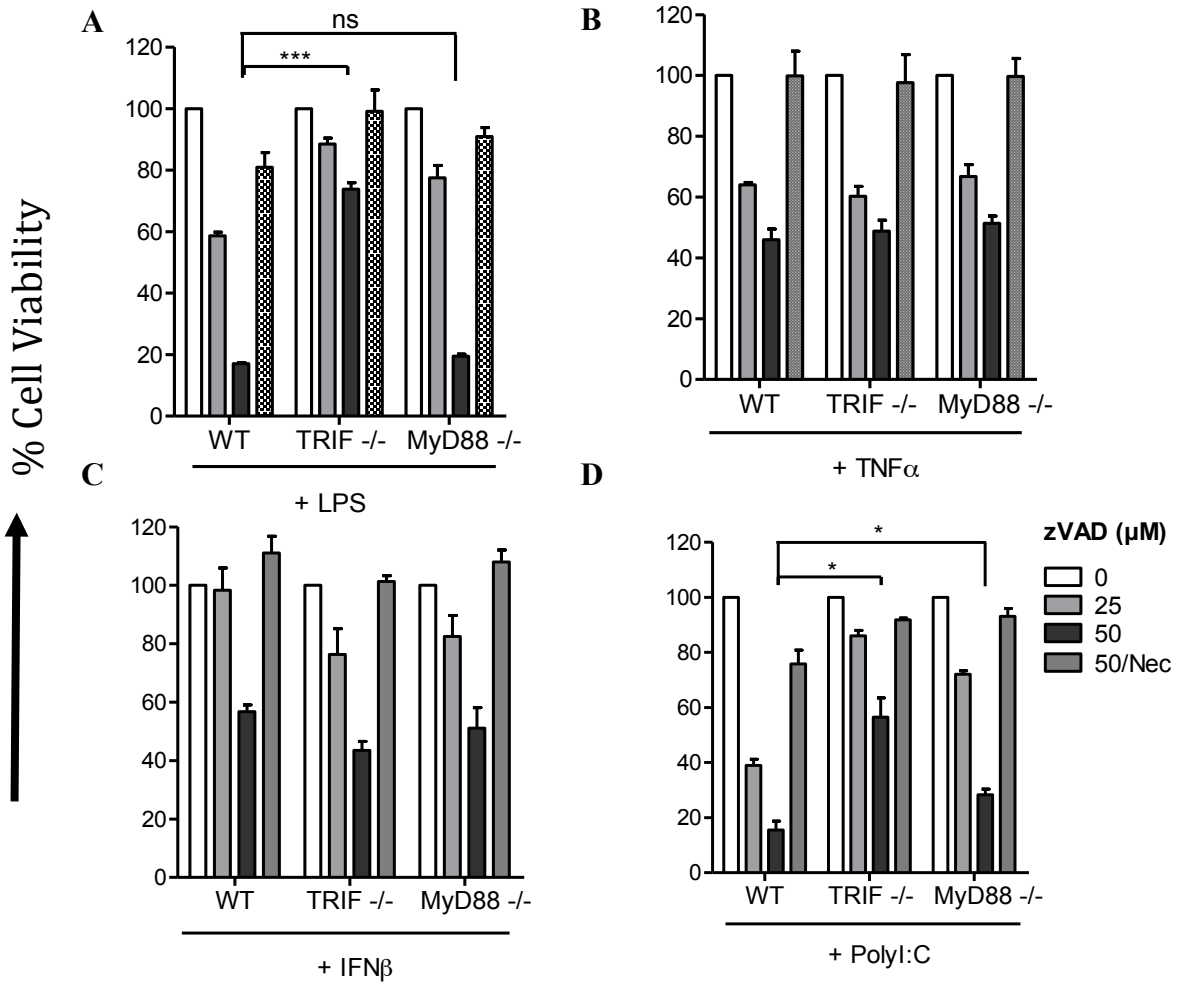
A
ns
***
120
100
80
60
40
20
0
WT
TRIF -/-
MyD88 -/-
+ LPS
B
+ TNFα
C
+ IFNβ
D
*
*
+ PolyI:C
% Cell Viability
zVAD (μM)
0
25
50
50/Nec

Figure 17. *TLR4 signaling through TRIF is important for LPS- and PolyI:C-mediated necroptosis.* WT, TRIF-/- and MyD88-/- BMDMs were treated with LPS/zVAD, TNFα/zVAD, PolyI:C/zVAD and IFNβ/zVAD, all with and without Nec-1, for 24 hours before measuring cell viability by MTT assay (**A-D**). LPS was used at a concentration of 100 ng/ml, zVAD at 25-50 μM, TNFα at 50 ng/ml, IFNβ at 100 U/ml, PolyI:C at 20 μg/ml and Nec-1 at 30 μM. Graphs show % cell viability mean ± SEM relative to cells treated with corresponding stimuli in the absence of zVAD and are representative of at least 3 independent experiments performed in triplicate. Statistical analyses done by unpaired students t-test *P<0.05, **P<0.001 and ***P<0.0001.

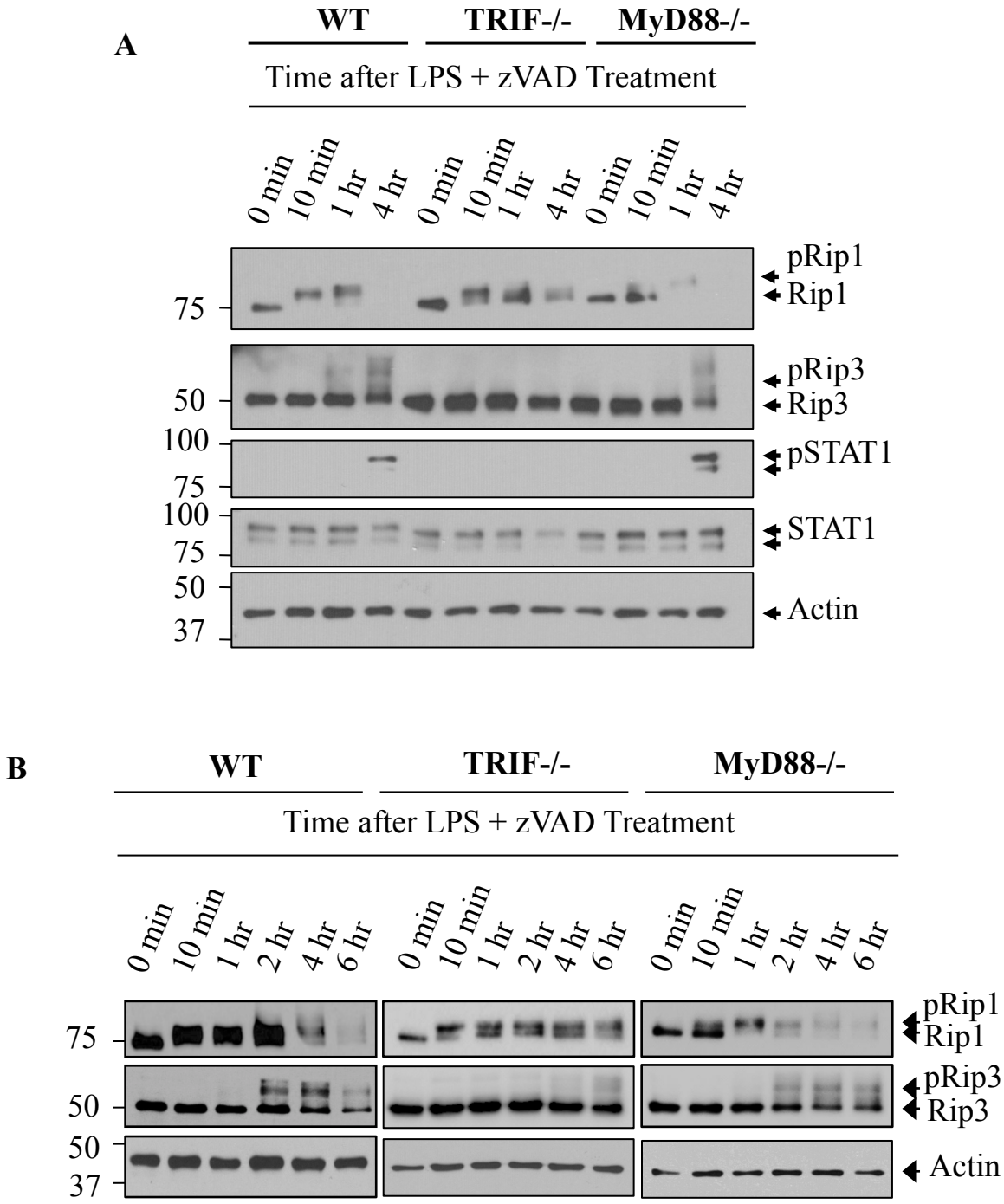
A
WT
TRIF-/-
MyD88-/-
Time after LPS + zVAD Treatment
0 min
10 min
1 hr
4 hr
pRip1
Rip1
pRip3
Rip3
pSTAT1
STAT1
Actin
75
50
100
37
B
WT
TRIF-/-
MyD88-/-
Time after LPS + zVAD Treatment
0 min
10 min
1 hr
2 hr
4 hr
6 hr
pRip1
Rip1
pRip3
Rip3
Actin
75
50
37

Figure 18. *TLR4 signaling through TRIF is needed for IFN-I production and Rip3 activation.* Lysates for western blot analysis were collected from WT, TRIF-/- and MyD88-/- BMDMs treated with LPS (100 ng/ml)/zVAD (50 μM) for different time intervals up to 4 and 6 hours (**A,B**). Data representative of at least three independent experiments.

18B). More specifically, TRIF-/- macrophages show rapid induction of Rip1 while MyD88-/- macrophages show delayed Rip1 activation (Fig. 18B). Interestingly, TRIF deficient macrophages showed strongly attenuated phosphorylation of Rip3 and no STAT1 activation (Fig. 18A). Rip3 and STAT1 activation in macrophages lacking MyD88 was comparable to that observed in WT macrophages (Fig. 18A).

4.2.4 IRF1, IRF3 and IRF7 promote macrophage necroptosis

Interferon regulatory factors (IRFs) are a family of nine transcription factors involved in the induction of genes that encode IFN-Is (Honda and Taniguchi, 2006). To investigate the role of various IRFs in necroptosis of macrophages I generated BMDMs from several different IRF KO mice. WT and IRF1 BMDMs were treated with necroptotic stimuli for 24 hours before measuring cell viability by MTT assay (Fig. 19A-C). A significant rescue from TNFα-mediated necroptosis and a partial yet significant rescue from LPS-mediated necroptosis was observed in IRF1 deficient macrophages (Fig. 19A,B). In response to IFNβ/zVAD treatment, no significant difference was observed between WT and IRF1 null macrophages (Fig. 19C). In addition to IRF1, I also investigated the role of IRF3, IRF7 and IRF3/7 on necroptosis of macrophages. IRF3, IRF7 and IRF3/7 BMDMs were partially resistant to LPS/zVAD, TNFα/zVAD and IFNβ/zVAD induced necroptosis (Fig. 20A-C). The strongest rescue was seen with IRF3 knockout macrophages, while IRF3/7 double KO macrophages did not display a cumulative rescue, suggesting that IRF3 and IRF7 have redundant roles in IFN-I induced necroptosis (Fig. 20A-C).

4.2.5 IRF9 is essential for sustained Rip3 activation and necroptosis

In addition to IRF1, IRF3 and IRF7, I also examined the importance of IRF9 in macrophage necroptosis. In contrast to the function of most IRFs, which is to induce the

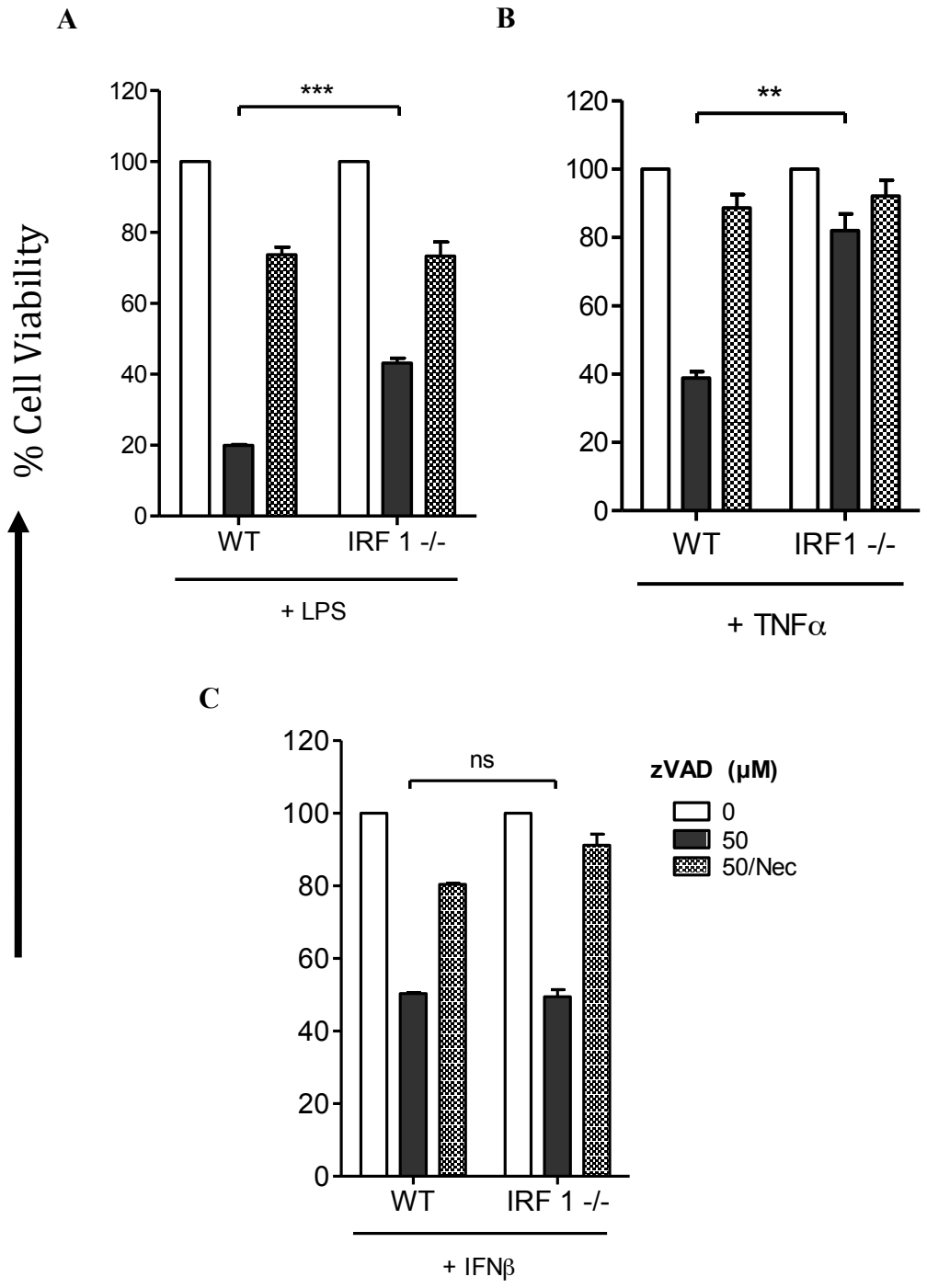
A
B
C
% Cell Viability
120
100
80
60
40
20
0
***
**
ns
WT
IRF 1 -/-
IRF1 -/-
+ LPS
+ TNFα
+ IFNβ
zVAD (μM)
0
50
50/Nec

Figure 19. *IRF1 plays a role in LPS- and TNFα-mediated necroptosis.* WT and IRF1-/-, BMDMs were treated with LPS/zVAD +/- Nec-1, TNFα/zVAD +/- Nec-1 and IFNβ/zVAD +/- Nec-1 for 24 hours before measuring cell viability by MTT assay (**A-C**). LPS was used at a concentration of 100 ng/ml, zVAD at 25-50 μM, TNFα at 50 ng/ml, IFNβ at 100 U/ml and Nec-1 at 30 μM. Graphs show % cell viability mean ± SEM relative to cells treated with corresponding stimuli in the absence of zVAD and are representative of at least 3 independent experiments performed in triplicate. Statistical analyses done by unpaired students t-test *P<0.05, **P<0.001 and ***P<0.0001.

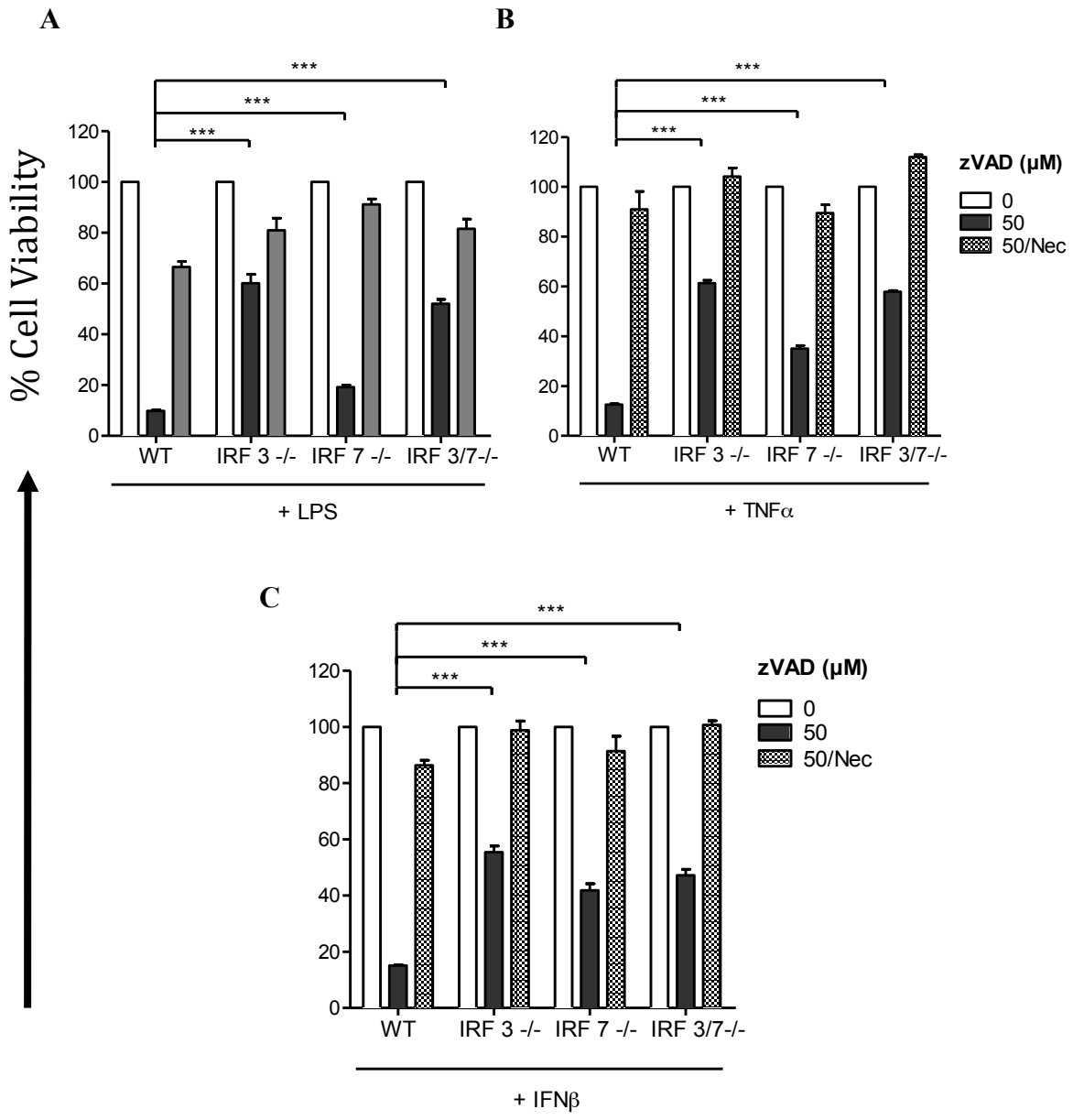
A
B
C
% Cell Viability
***
***
***
120
100
80
60
40
20
0
WT
IRF 3 -/-
IRF 7 -/-
IRF 3/7-/-
+ LPS
+ TNFα
+ IFNβ
zVAD (μM)
0
50
50/Nec

Figure 20. *IRF3 and IRF7 promote macrophage necroptosis.* WT, IRF3-/-, IRF7-/- and IRF3/7-/- BMDMs were treated with LPS/zVAD +/- Nec-1, TNFα/zVAD +/- Nec-1 and IFNβ/zVAD +/- Nec-1 for 24 hours before measuring cell viability by MTT assay (**A-C**). LPS was used at a concentration of 100 ng/ml, zVAD at 25-50 μM, TNFα at 50 ng/ml, IFNβ at 100 U/ml and Nec-1 at 30 μM. Graphs show % cell viability mean ± SEM relative to cells treated with corresponding stimuli in the absence of zVAD and are representative of at least 3 independent experiments performed in triplicate. Statistical analyses done by unpaired students t-test *P<0.05, **P<0.001 and ***P<0.0001.

production of IFN-Is, IRF9 is key for facilitating the downstream response to IFN-Is. WT and IRF9-/- BMDMs were treated with LPS/zVAD, TNFα/zVAD, IFNβ/zVAD and PolyI:C/zVAD for 24 hours before measuring cell viability by MTT assay (Fig. 21A-D). Interestingly, IRF9 deficient macrophages were highly resistant to LPS, TNFα and IFNβ-induced necroptosis but only partially resistant to PolyI:C-induced necroptosis (Figure 20A-D). I performed an LPS/zVAD 6-hour western blot time course in WT and IRF9-/- BMDMs to examine the impact of IRF9 deficiency on Rip1 and Rip3 phosphorylation (Fig. 22A). Density ratios were calculated for pRip1/Rip1 and pRip3/Rip3, which were normalized to actin (Figure 22B,C). Similar to what was observed with IFNAR1-/- macrophages, Rip3 activation was dramatically reduced in IRF9-/- macrophages (Figure 22A).

4.2.6 IFN-I signaling through ISGF3 is required for necroptotic cell death

After observing strong necroptotic resistance in macrophages lacking IRF9, I was interested in further exploring the mechanisms involved. After IFN-I stimulation, IRF9, STAT1 and STAT2 have been shown to form a transcriptional complex known as interferon stimulated gene factor 3 (ISGF3), which promotes the transcription of various interferon stimulated genes (ISGs) (Fink et al., 2013). To evaluate the role of ISGF3 in necroptosis, I treated STAT1 and STAT2 deficient macrophages with necroptotic stimuli for 24 hours before measuring cell viability by MTT assay. Consistent with IRF9 KO macrophage results, BMDMs that were deficient in STAT1 were also significantly resistant to necroptosis (Fig. 23A-D). It is important to mention that STAT1 KO mice were maintained on a 129S6 genetic background as oppose to a C57BL/6 background and the appropriate 129S6 WT mice were used as controls for STAT1 null experiments. To ensure the results from 129S6 mice were comparable to my other results from C57BL/6 mice, I performed similar cell

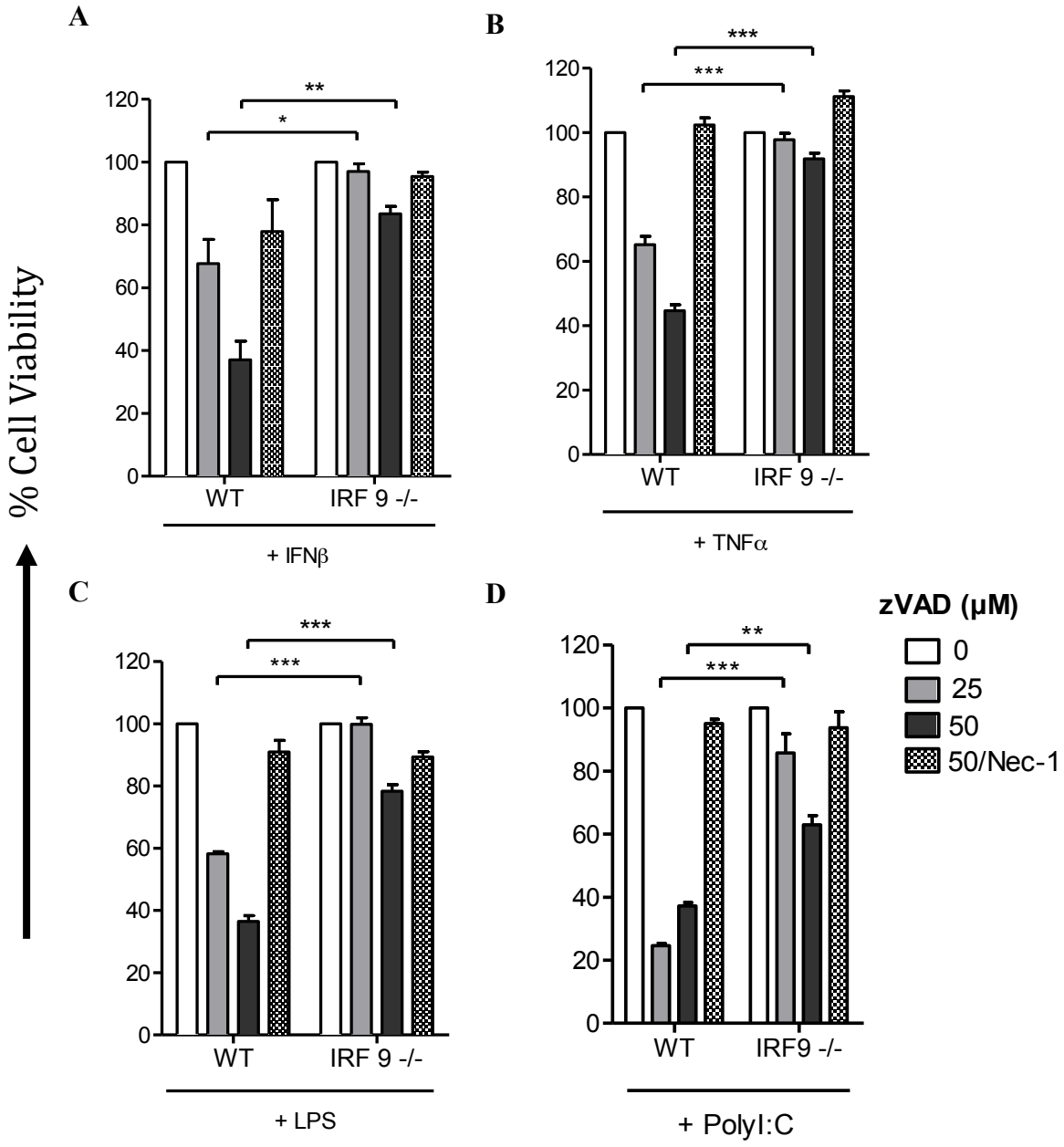
A
B
C
D
% Cell Viability
WT
IRF 9 -/-
IRF9 -/-
+ IFNβ
+ TNFα
+ LPS
+ PolyI:C
zVAD (μM)
0
25
50
50/Nec-1

Figure 21. *IRF9 plays a critical role in necroptosis.* WT and IRF9 -/- BMDMs were treated with LPS/zVAD, TNFα/zVAD, IFNβ/zVAD and PolyI:C/zVAD, all with and without Nec-1, for 24 hours before measuring cell viability by MTT assay (**A-D**). LPS was used at a concentration of 100 ng/ml, zVAD at 25-50 μM, TNFα at 50 ng/ml, IFNβ at 100 U/ml and Nec-1 at 30 μM. Graphs show % cell viability mean ± SEM relative to cells treated with corresponding stimuli in the absence of zVAD and are representative of at least 3 independent experiments performed in triplicate. Statistical analyses done by unpaired students t-test *P<0.05, **P<0.001 and ***P<0.0001.

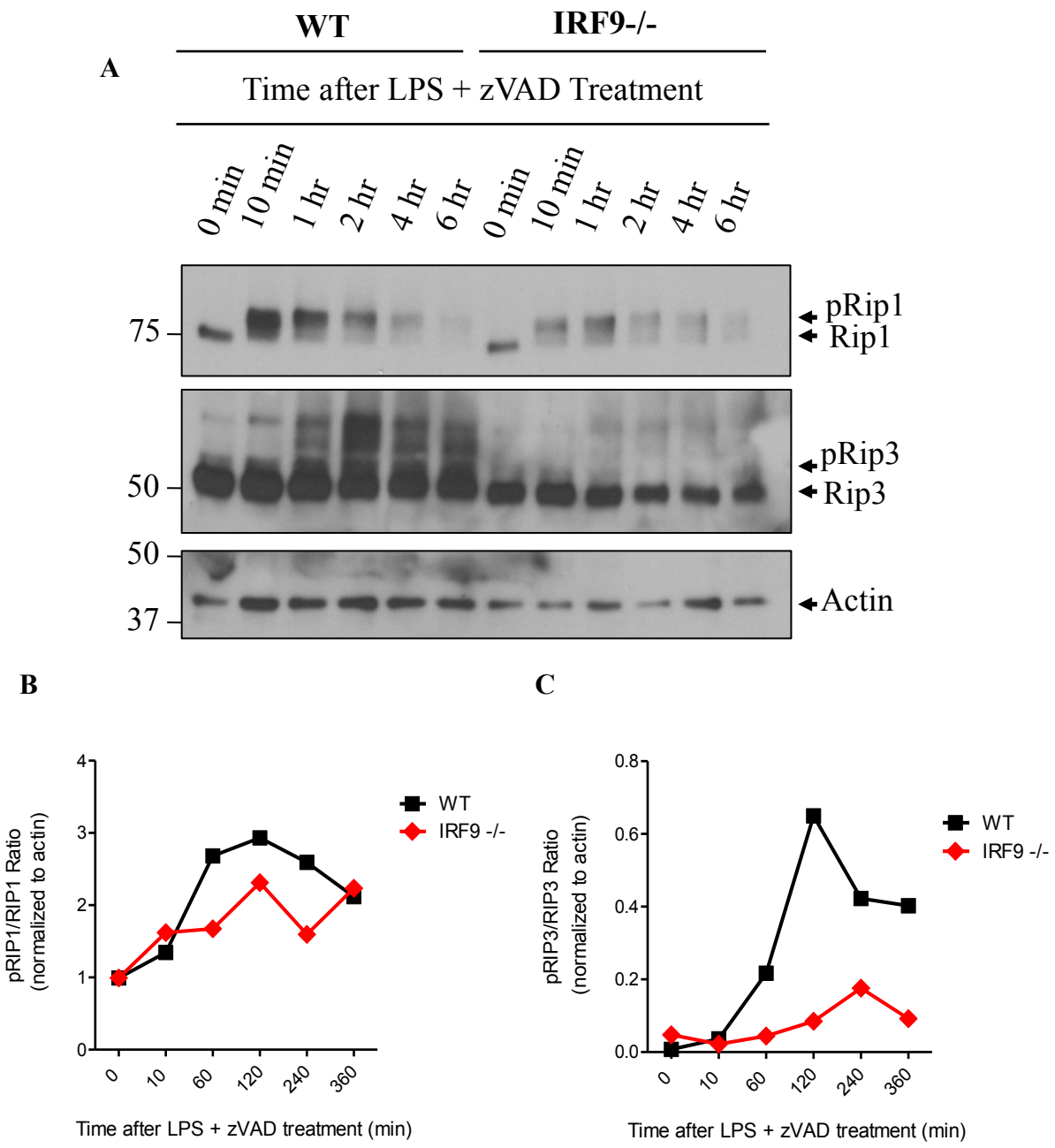
A
WT
IRF9-/-
Time after LPS + zVAD Treatment
0 min
10 min
1 hr
2 hr
4 hr
6 hr
0 min
10 min
1 hr
2 hr
4 hr
6 hr
75
pRip1
Rip1
50
pRip3
Rip3
50
37
Actin
B
pRIP1/RIP1 Ratio (normalized to actin)
WT
IRF9 -/-
Time after LPS + zVAD treatment (min)
C
pRIP3/RIP3 Ratio (normalized to actin)
WT
IRF9 -/-
Time after LPS + zVAD treatment (min)

Figure 22. *IRF9 deficiency impairs Rip3 phosphorylation.* Lysates for western blot analysis were collected from WT and IRF9-/- macrophages treated with LPS (100 ng/ml)/zVAD (50 μM) for different time intervals up to 6 hours (**A**). Quantification of western data done by graphing density ratios of pRip1/Rip1 and pRip3/Rip3 (**B,C**). Data are representative of at least three independent experiments.

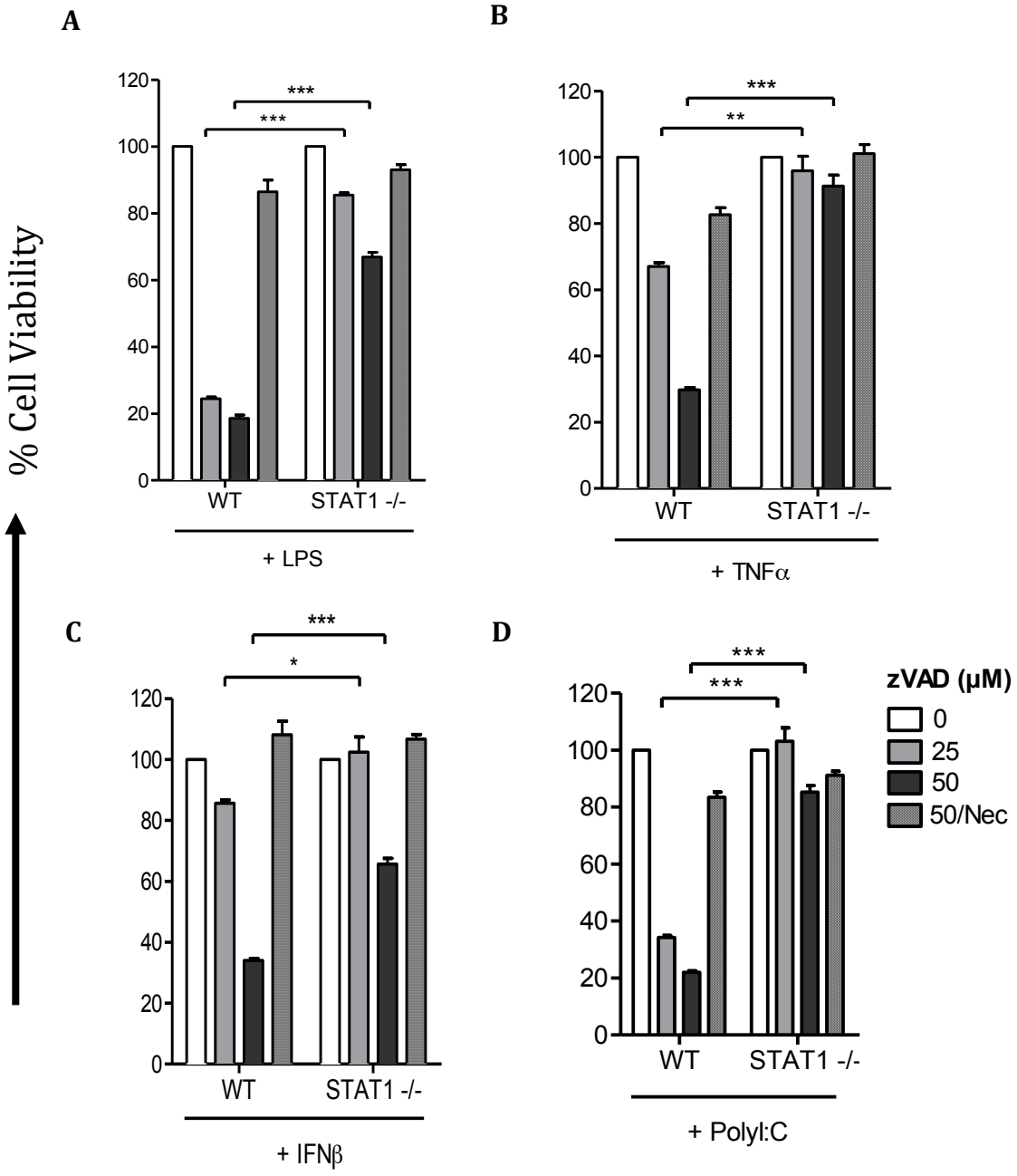
A
B
C
D
% Cell Viability
120
100
80
60
40
20
0
***
**
*
WT
STAT1 -/-
+ LPS
+ TNFα
+ IFNβ
+ Polyl:C
zVAD (μM)
0
25
50
50/Nec

Figure 23. *STAT1 is important for necroptotic death of macrophages.* BMDMs from WT 129S6 and STAT1-/- mice on a 129S6 background were treated with LPS/zVAD, TNFα/zVAD, IFNβ/zVAD and PolyI:C/zVAD, all with and without Nec-1, for 24 hours before measuring cell viability by MTT assay (**A-D**). LPS was used at a concentration of 100 ng/ml, zVAD at 25-50 μM, TNFα at 50 ng/ml, IFNβ at 100 U/ml and Nec-1 at 30 μM. Graphs show % cell viability mean ± SEM relative to cells treated with corresponding stimuli in the absence of zVAD and are representative of at least 3 independent experiments performed in triplicate. Statistical analyses done by unpaired students t-test *P<0.05, **P<0.001 and ***P<0.0001.

viability experiments on IFNAR1-/- mice maintained on a 129S6 background (Fig. 24A-C). Importantly, IFNAR1-/- mice on a 129S6 genetic background displayed a similar necroptotic resistant phenotype to IFNAR1-/- mice on a C57BL/6 background (Fig. 24A-C). Providing further support for the importance of ISGF3 in macrophage necroptosis, STAT2 null macrophages were also strongly resistant to necroptotic stimuli (Fig. 25A-D). LPS/zVAD time course western blots from STAT1-/- and STAT2-/- macrophage lysates demonstrated attenuated Rip3 phosphorylation (Fig. 26A,B). Collectively, these results demonstrate a pro-necroptotic role for ISGF3 within macrophages.

4.2.7 Functional ISGF3 is needed to maintain basal levels of STAT1 and STAT2

Studies examining macrophages and cytokine production have shown that constitutive low level IFNβ production promotes tonic signaling through ISGF3, which is important for maintaining basal levels of various interferon-stimulated genes (ISGs), including ISGF3 components STAT1, STAT2 and IRF9 (Gough et al., 2012; Hu et al., 2002). Stimulation of WT BMDMs with IFNβ for varying time intervals over the course of 14 hours resulted in a gradual increase in STAT1 and STAT2 levels over time (Fig. 27A). Interestingly, STAT1 and STAT2 expression peaked around the time when macrophages begin to die by necroptosis (Fig. 27A). Weakened IFN-I signaling from IFNAR1 deficiency (Fig. 27A,B) or ISGF3 impairment (Fig. 28A-C), resulted in severely reduced expression of STAT1 and STAT2 even after stimulation with LPS/zVAD Taken together these results highlight the importance of IFN-I signaling for necroptotic cell death of macrophages.

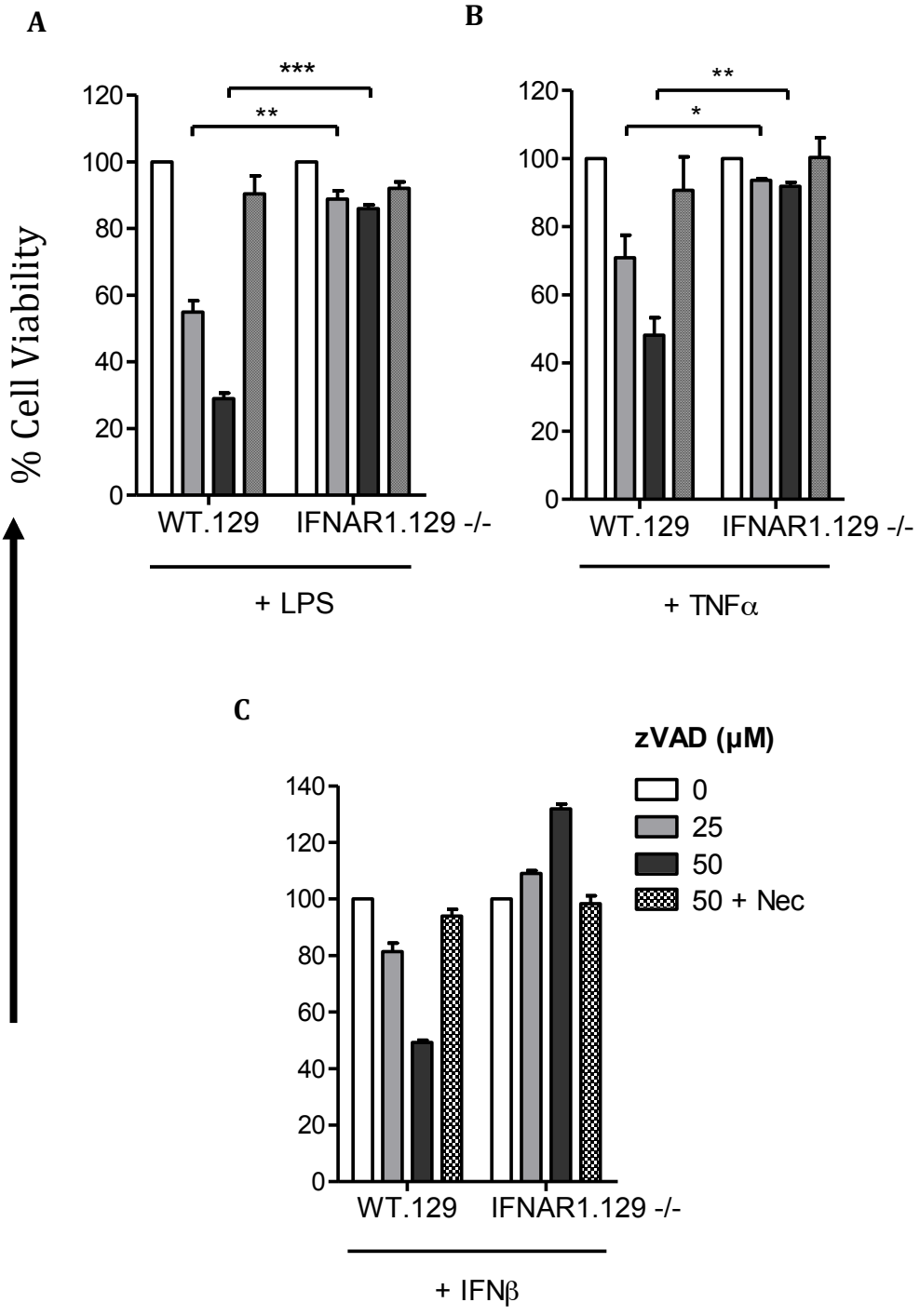
A
B
C
% Cell Viability
***
**
*
120
100
80
60
40
20
0
WT.129
IFNAR1.129 -/-
+ LPS
+ TNFα
+ IFNβ
zVAD (μM)
0
25
50
50 + Nec
140

Figure 24. *IFNAR1-/- mice on a 129S6 genetic background are resistant to necroptosis.* BMDMs from WT 129S6 and IFNAR1-/- mice on a 129S6 background were treated with LPS/zVAD, TNFα/zVAD and IFNβ/zVAD, all with and without Nec-1, for 24 hours before measuring cell viability by MTT assay (**A-C**). LPS was used at a concentration of 100 ng/ml, zVAD at 25-50 μM, TNFα at 50 ng/ml, IFNβ at 100 U/ml and Nec-1 at 30 μM. Graphs show % cell viability mean ± SEM relative to cells treated with corresponding stimuli in the absence of zVAD and are representative of at least 3 independent experiments performed in triplicate. Statistical analyses done by unpaired students t-test *P<0.05, **P<0.001 and ***P<0.0001.

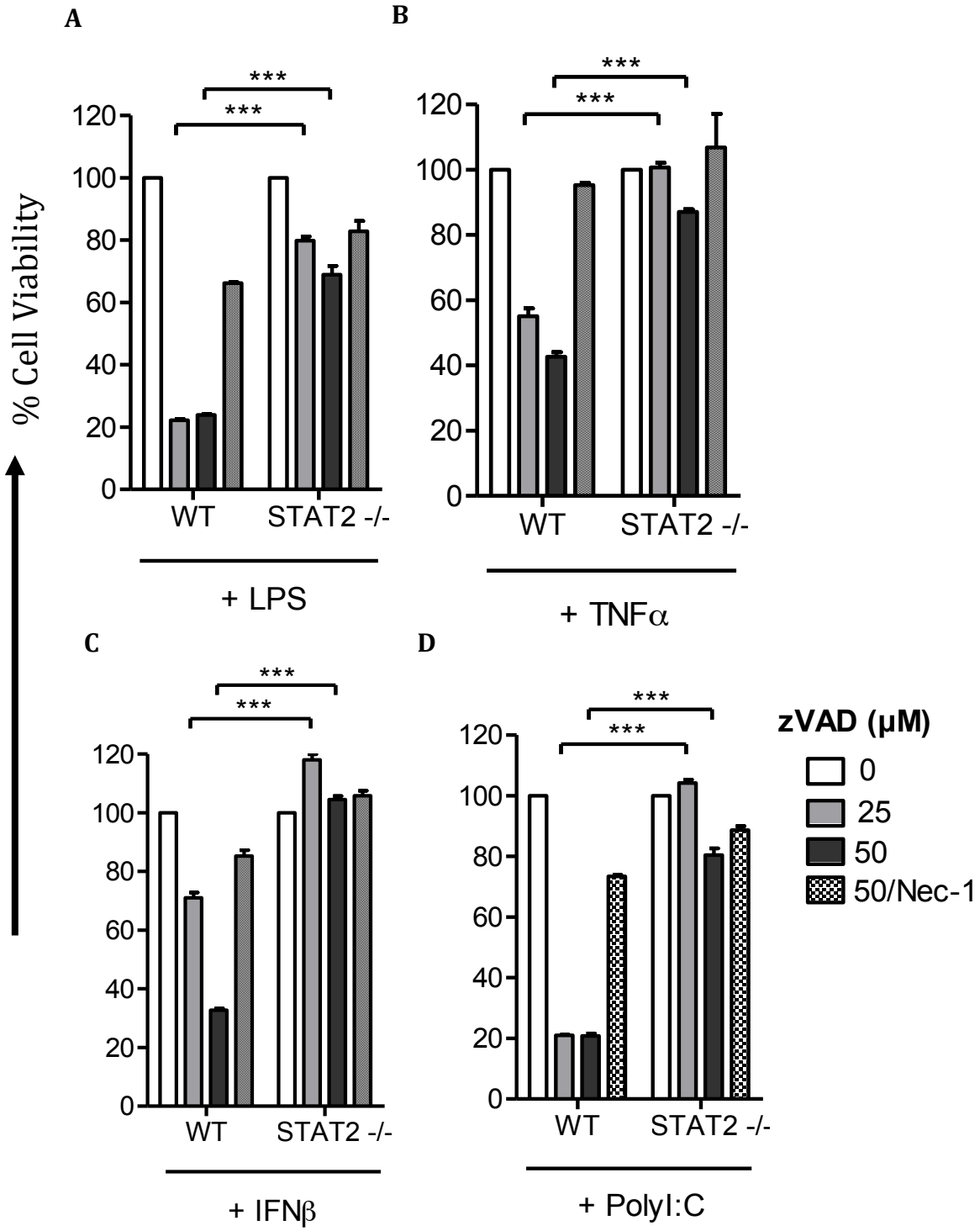
A
B
C
D
% Cell Viability
***
***
120
100
80
60
40
20
0
WT
STAT2 -/-
+ LPS
+ TNFα
+ IFNβ
+ PolyI:C
zVAD (μM)
0
25
50
50/Nec-1

Figure 25. *STAT2 is needed for necroptosis.* WT and STAT2-/- BMDMs were treated with LPS/zVAD, TNFα/zVAD, IFNβ/zVAD and PolyI:C/zVAD, all with and without Nec-1, for 24 hours before measuring cell viability by MTT assay (**A-D**). LPS was used at a concentration of 100 ng/ml, zVAD at 25-50 μM, TNFα at 50 ng/ml, IFNβ at 100 U/ml, PolyI:C at 20 μg/ml and Nec-1 at 30 μM. Graphs show % cell viability mean ± SEM relative to cells treated with corresponding stimuli in the absence of zVAD and are representative of at least 3 independent experiments performed in triplicate. Statistical analyses done by unpaired students t-test ***P<0.0001.

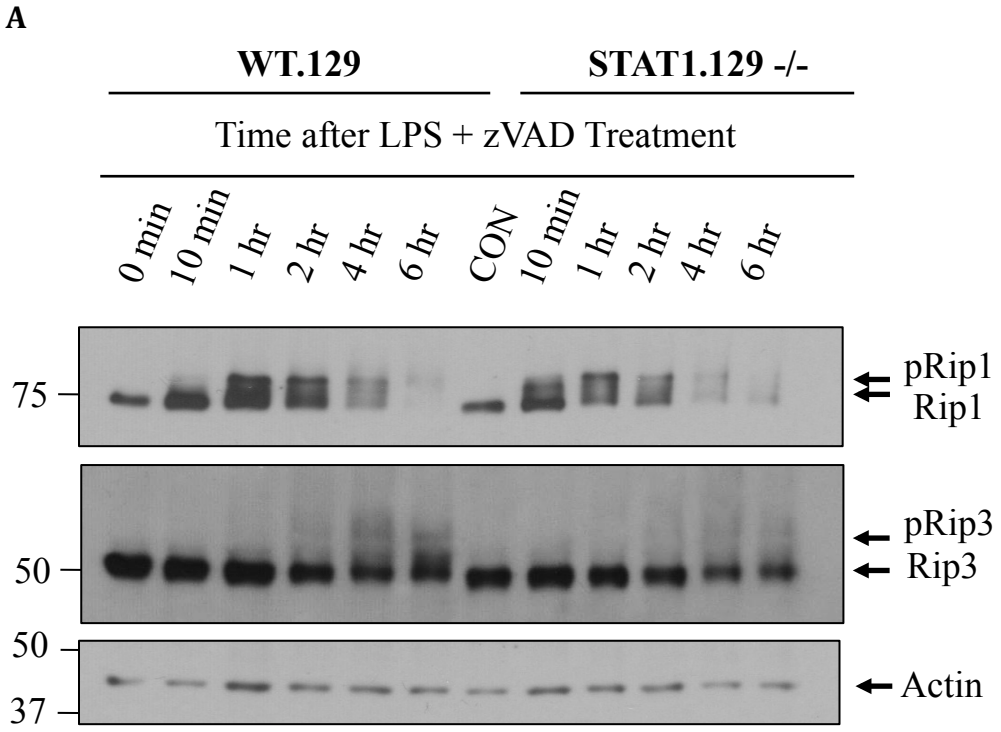
A
WT.129
STAT1.129 -/-
Time after LPS + zVAD Treatment
0 min
10 min
1 hr
2 hr
4 hr
6 hr
CON
10 min
1 hr
2 hr
4 hr
6 hr
75
pRip1
Rip1
50
pRip3
Rip3
50
37
Actin

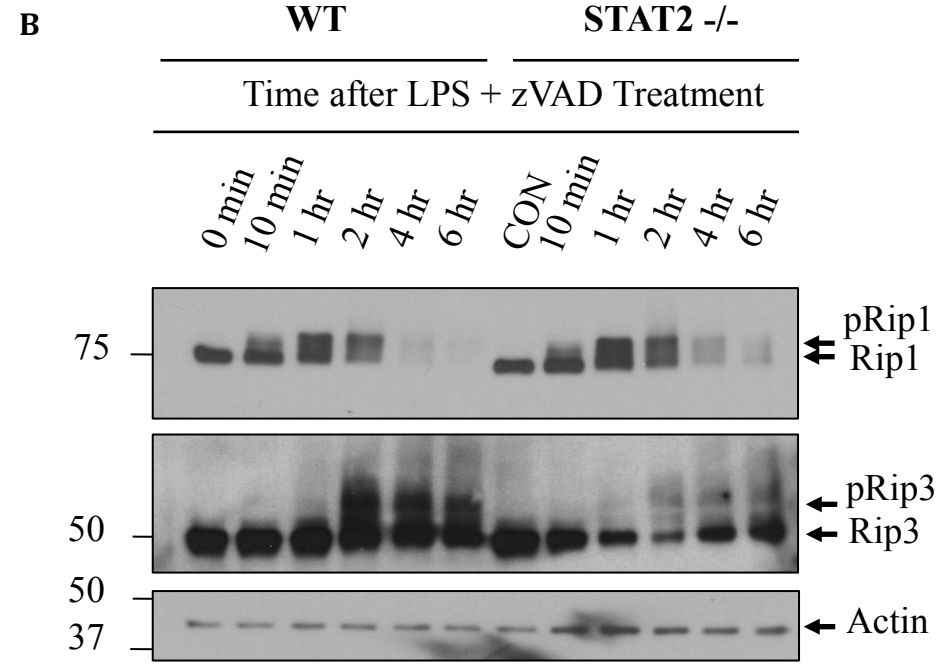
B
WT
STAT2 -/-
Time after LPS + zVAD Treatment
0 min
10 min
1 hr
2 hr
4 hr
6 hr
CON
10 min
1 hr
2 hr
4 hr
6 hr
75
pRip1
Rip1
50
pRip3
Rip3
50
37
Actin

Figure 26. *Impairment to ISGF3 components diminishes Rip3 activation.* Lysates for western blot analysis were collected from WT and STAT1-/- macrophages treated with LPS (100 ng/ml)/zVAD (50 μM) for different time intervals up to 6 hours (**A**). WT and STAT2-/- BMDMs were treated as described above and lysates were collected to examine by western blot (**B**). Data representative of at least three independent experiments.

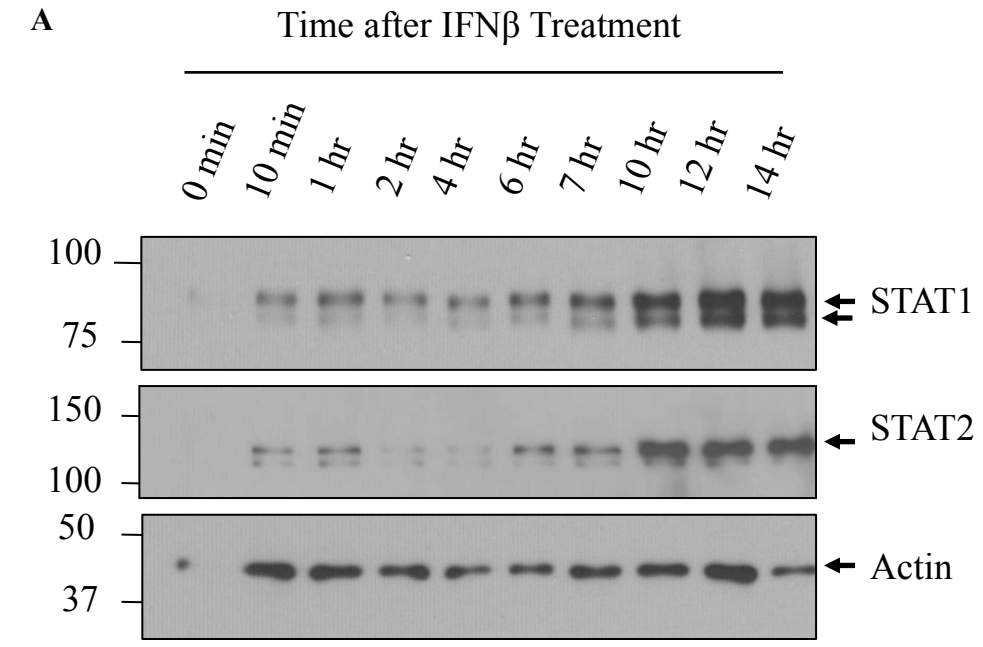
A
Time after IFNβ Treatment
0 min
10 min
1 hr
2 hr
4 hr
6 hr
7 hr
10 hr
12 hr
14 hr
100
75
150
100
50
37
STAT1
STAT2
Actin

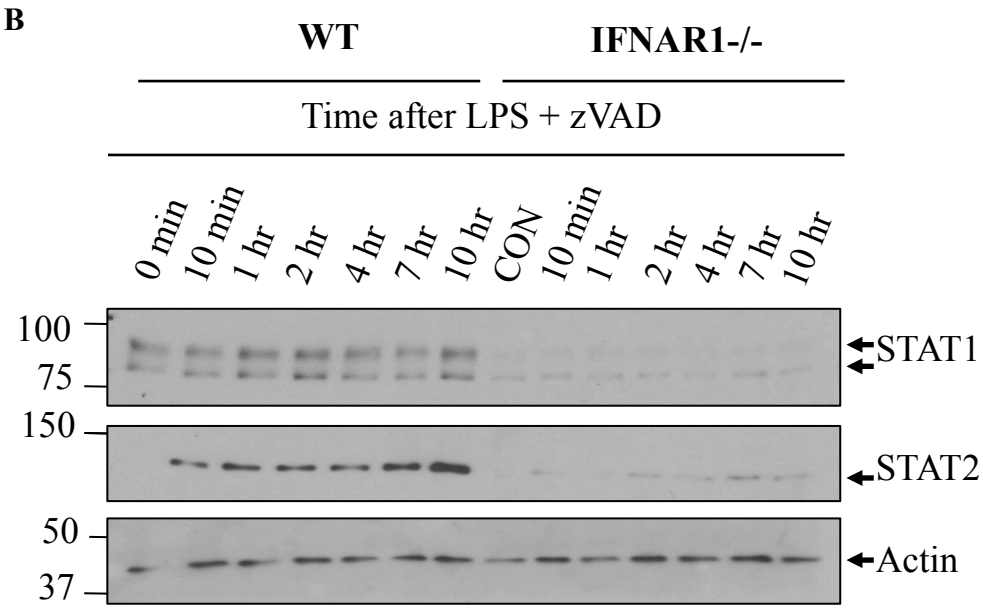
B
WT
IFNAR1-/-
Time after LPS + zVAD
0 min
10 min
1 hr
2 hr
4 hr
7 hr
10 hr
CON
10 min
1 hr
2 hr
4 hr
7 hr
10 hr
100
75
150
50
37
STAT1
STAT2
Actin

Figure 27. Constitutive IFNβ signaling regulates *STAT1 and STAT2 expression.* WT macrophages were treated with IFNβ (100 U/ml) for varying time intervals over the course of 14 hours before lysates were collected to measure STAT1 and STAT2 expression by western blot (**A**). Lysates from WT and IFNAR1-/- BMDMs treated with LPS (100ng/ml)/zVAD (50 μM) for different time intervals were collected for western blot examination of STAT1 and STAT2 (**B)**. Data representative of at least 3 independent experiments.

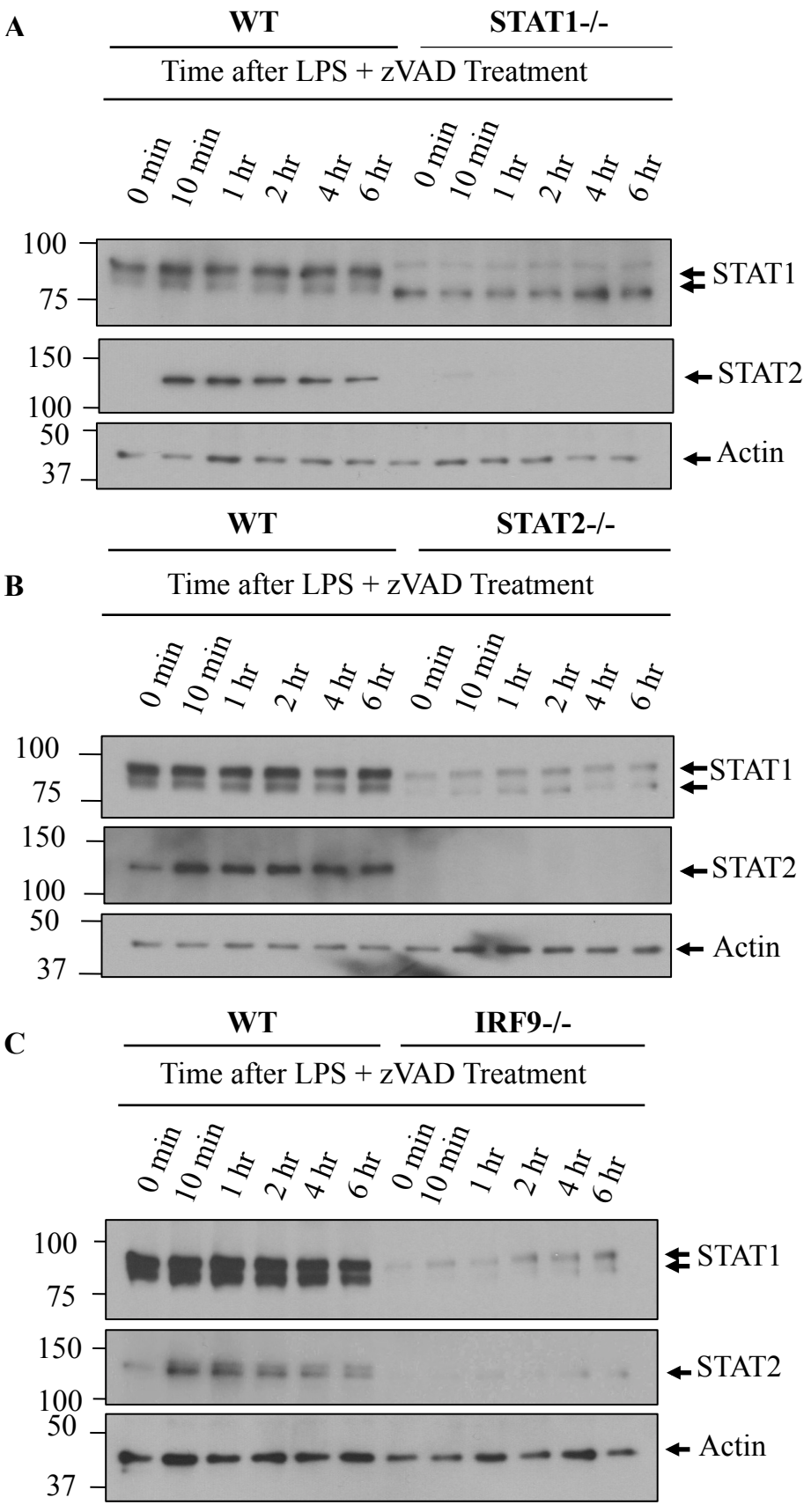
A
WT
STAT1-/-
Time after LPS + zVAD Treatment
0 min
10 min
1 hr
2 hr
4 hr
6 hr
0 min
10 min
1 hr
2 hr
4 hr
6 hr
100
75
150
100
50
37
STAT1
STAT2
Actin
B
WT
STAT2-/-
Time after LPS + zVAD Treatment
0 min
10 min
1 hr
2 hr
4 hr
6 hr
0 min
10 min
1 hr
2 hr
4 hr
6 hr
100
75
150
100
50
37
STAT1
STAT2
Actin
C
WT
IRF9-/-
Time after LPS + zVAD Treatment
0 min
10 min
1 hr
2 hr
4 hr
6 hr
0 min
10 min
1 hr
2 hr
4 hr
6 hr
100
75
150
100
50
37
STAT1
STAT2
Actin

Figure 28. *Impairment to ISGF3 strongly reduces STAT1 and STAT2 expression.* Lysates from WT, STAT1-/-, STAT2-/- and IRF9-/- BMDMs treated with LPS (100ng/ml)/zVAD (50 μM) for different time intervals were collected for western blot examination of STAT1 and STAT2 (**A-C**). Data representative of at least 3 independent experiments.

4.2.8 LPS/zVAD treatment induces proteasomal degradation of Rip1

Interestingly, relative expression levels of Rip1 declined following an LPS/zVAD time course in WT BMDMs (Fig. 29A). I therefore wanted to evaluate the mechanism behind Rip1 degradation post LPS/zVAD stimulation. Intriguingly, Rip3 levels remained relatively stable and did not show the same decrease as was observed with Rip1 (Fig. 29A). To investigate whether or not Rip1 was being degraded by the proteasome, I performed a time course with LPS/zVAD with and without pretreatment of lactacystin, a proteasomal inhibitor (Fig. 29B). Interestingly, inhibition of the proteasome resulted in maintenance of Rip1 expression for longer periods of LPS/zVAD treatment (Fig. 29B). These results suggest that Rip1 is being degraded by the proteasome, which is possibly mediated via ubiquitination (Fig. 29B).

Several pieces of evidence support the notion that Rip1 is being actively targeted and degraded by the proteasome as oppose to generally degrading as a result of cellular breakdown driven by necroptotic death. First, other protein levels in WT macrophages, such as actin, Rip3 and STAT1, remained consistent over a 12-hour LPS/zVAD time course (Fig. 16A). Second, degradation of Rip1 still occurred during an LPS/zVAD time course in IFNAR1-/- macrophages (Fig. 16A). Similar degradation of Rip1 in WT and IFNAR1-/- macrophages therefore negates the possibility of passive Rip1 degradation since IFNAR1-/- macrophages are highly resistant to necroptosis (Fig. 13). Lastly, experiments testing the kinetics of LPS-mediated necroptosis were performed by lactate dehydrogenase (LDH) release (as described in experimental methods), using supernatants from an LPS/zVAD time course in WT BMDMs, and an 8- and 24-hour MTT assay comparison from WT BMDMs treated with LPS/zVAD (Fig. 29C,D). Importantly, the timing of Rip1 degradation,

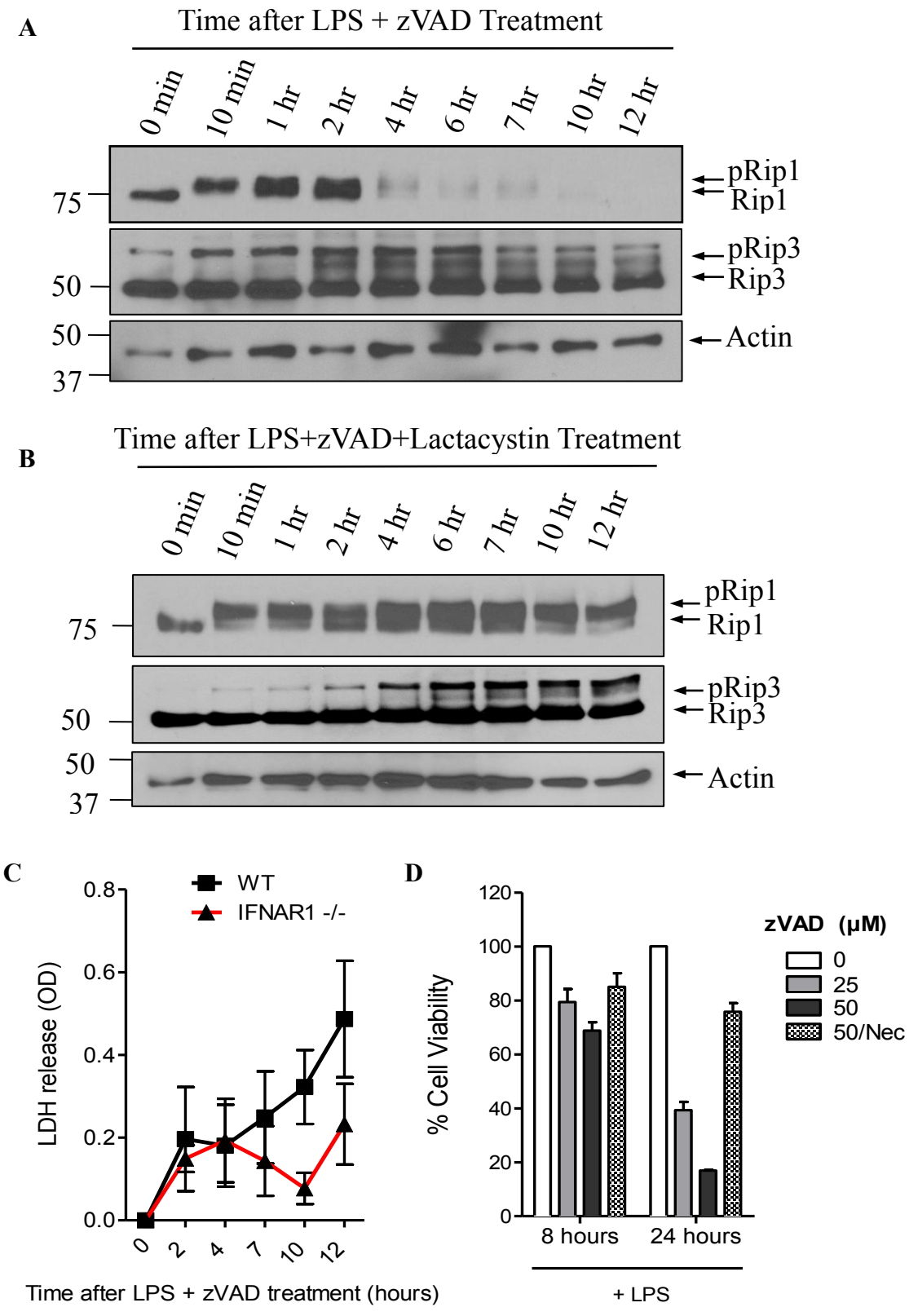
A
Time after LPS + zVAD Treatment
0 min
10 min
1 hr
2 hr
4 hr
6 hr
7 hr
10 hr
12 hr
75
50
50
37
pRip1
Rip1
pRip3
Rip3
Actin
B
Time after LPS+zVAD+Lactacystin Treatment
0 min
10 min
1 hr
2 hr
4 hr
6 hr
7 hr
10 hr
12 hr
75
50
50
37
pRip1
Rip1
pRip3
Rip3
Actin
C
WT
IFNAR1 -/-
LDH release (OD)
0.8
0.6
0.4
0.2
0.0
0
2
4
7
10
12
Time after LPS + zVAD treatment (hours)
D
% Cell Viability
120
100
80
60
40
20
0
8 hours
24 hours
+ LPS
zVAD (μM)
0
25
50
50/Nec

Figure 29. *Rip1 is degraded by the proteasome in response to LPS/zVAD treatment.* WT BMDMS were treated with LPS (100ng/ml)/zVAD (50 μM) with and without a 30 minute pretreatment with lactacystin (10 μg/ml) for varying time intervals before lysates were collected to measure Rip1 and Rip3 expression by western blot (**A,B**). LPS-mediated necroptosis kinetics were measured by LDH release and an 8- and 24-hour MTT assay comparison in WT and IFNAR1-/- BMDMs treated with LPS (100 ng/ml)/zVAD (50 μM) (**C,D**). Data representative of at least 3 independent experiments.

commencing after 2 hours of LPS/zVAD treatment, long precedes the timing of necroptotic death, which begins around 12 hours post LPS/zVAD treatment (Fig. 29C,D).

4.2.9 Proteasomal degradation of Rip1 is not mediated by cIAP1/2 and is driven by activated Rip3

To test whether Rip1 was being targeted to the proteasome by cIAP1/2-mediated K48-linked ubiquitination I treated WT BMDMs with LPS/zVAD and SMAC mimetic 164 (SM-164), which is known to induce rapid degradation of cIAPs, at varying time intervals over the course of 12-hours. Depletion of cIAPs by SM-164 treatment had no effect on Rip1 degradation (Fig. 30A). Instead, cIAP1/2 were degraded even without SM-164 treatment in response to LPS/zVAD stimulation (Fig. 30B). To further explore the mechanisms driving Rip1 degradation I performed an LPS/zVAD time course with and without Nec-1 in WT BMDMs (Fig. 31A). Interestingly, Rip1 activation still occurred however degradation was prevented (Fig. 31A). The key difference with the addition of Nec-1 was the prevention of Rip3 phosphorylation (Fig. 31A). After observing that Rip1 degradation was prevented in the absence of active Rip3, I performed an LPS/zVAD time course in Rip3-/- BMDMs and observed that Rip3 deficiency prevented Rip1 degradation (Fig. 31A). Lastly I evaluated the impact of LPS treatment on Rip1 levels and noted that LPS stimulation in the absence of zVAD did not cause degradation of Rip1 or activation of Rip3 (Fig. 31A). Collectively, these results indicate that active Rip3 is needed to induce proteasomal degradation of Rip1.

A

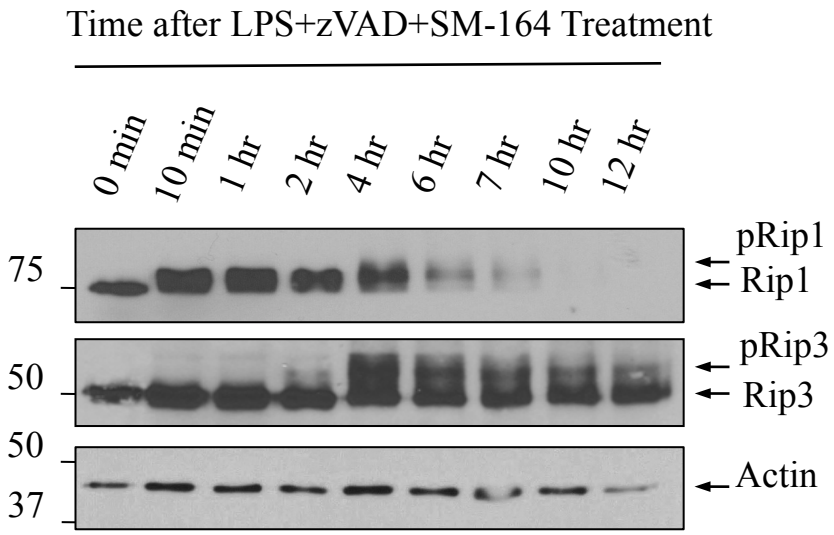
Time after LPS+zVAD+SM-164 Treatment
0 min
10 min
1 hr
2 hr
4 hr
6 hr
7 hr
10 hr
12 hr
75
50
50
37
pRip1
Rip1
pRip3
Rip3
Actin

B

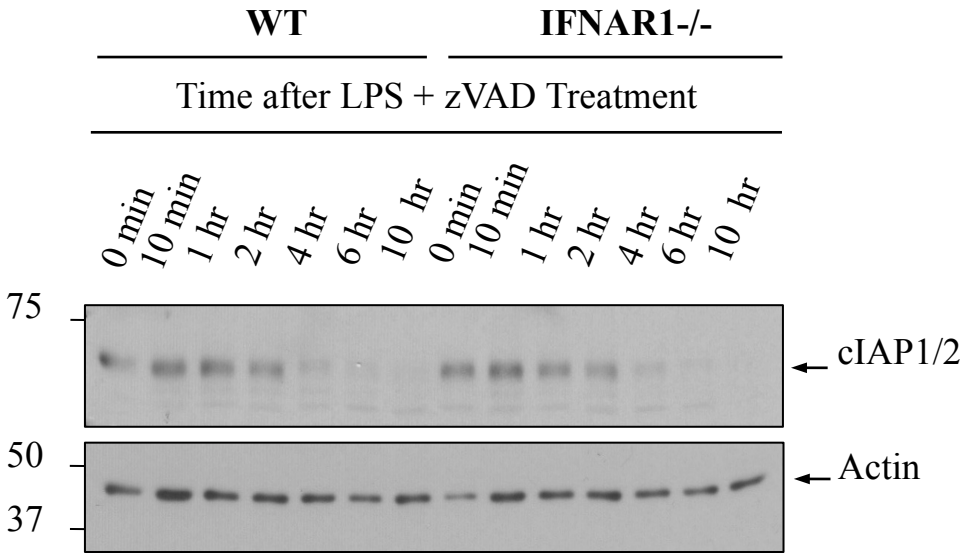
WT
IFNAR1-/-
Time after LPS + zVAD Treatment
0 min
10 min
1 hr
2 hr
4 hr
6 hr
10 hr
0 min
10 min
1 hr
2 hr
4 hr
6 hr
10 hr
75
50
37
cIAP1/2
Actin

Figure 30. *Proteasomal degradation of Rip1 is independent of cIAP1/2 E3 ligase activity.* Lysates from WT BMDMs treated with LPS (100ng/ml), zVAD (50 μM) and SM (5000 nM) for varying time intervals were examined by western blot (**A**). An LPS/zVAD time course, using the same concentrations as mentioned above, was performed in WT and IFNAR1-/- macrophages to collect lysates for western blot analysis of cIAP1/2 expression (**B**). Data representative of at least 3 independent experiments.

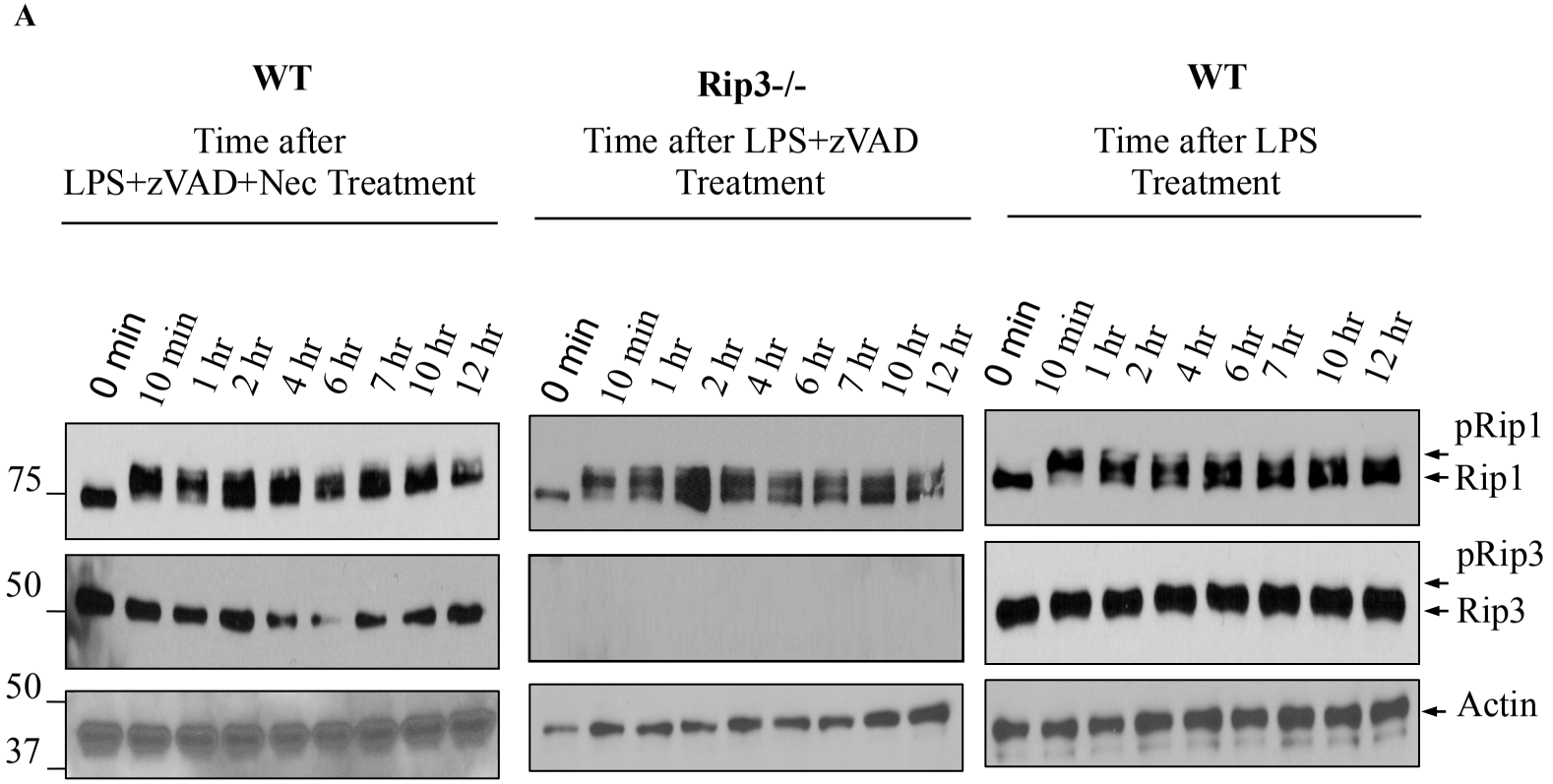
A
WT
Time after
LPS+zVAD+Nec Treatment
Rip3-/-
Time after LPS+zVAD
Treatment
WT
Time after LPS
Treatment
0 min
10 min
1 hr
2 hr
4 hr
6 hr
7 hr
10 hr
12 hr
75
50
50
37
pRip1
Rip1
pRip3
Rip3
Actin

Figure 31. *Activated Rip3 drives the proteasomal degradation of Rip1 in response to LPS/zVAD treatment.* WT and Rip3-/- BMDMs were treated with different combination of LPS (100 ng/ml), zVAD (50 μM) and Nec-1 (30 μM) for varying time intervals prior to collecting cell extracts for western blot analysis of Rip kinase activation (**A**). Data representative of at least 3 independent experiments.

5.0 DISCUSSION

Necroptosis is a fascinating, highly inflammatory programmed mode of cell death. In direct contrast to apoptosis, necroptosis proceeds specifically in the absence of caspase activity. Not only does necroptosis equip cells with an alternative mechanism of death, but it also provides a mechanism to rapidly and robustly alert the immune system to the threat of infection or tissue injury. The understanding of programmed necrosis has advanced rapidly over the last 15 years, particularly in regard to ligands, receptors and proteins involved in the signaling events leading to necroptotic death. It is now very well established that necroptotic death of a variety of cell types requires the kinase activity of receptor interacting protein kinase 3 (Rip3) (Cho et al., 2009; He et al., 2009; Zhang et al., 2009). In my own experiments using Rip3 knockout (KO) mice, I have also observed that in the absence of Rip3, murine bone marrow derived macrophages (BMDMs) are highly resistant to all necroptotic stimuli (Fig. 14A-D).

More recently in the context of TNF signaling it was discovered that Rip3 functions to phosphorylate a pseudokinase known as mixed lineage kinase domain like (MLKL) protein, which contains a kinase-like domain lacking two of the three conserved catalytic residues needed for functional kinase activity (Murphy et al., 2013; Wang et al., 2012). Further research examining MLKL found that similar to Rip3, MLKL plays an indispensible role in necroptosis (Wu et al., 2013). More specifically, MLKL appears to be a key necroptotic executioner protein as it forms homo-oligomers following Rip3-mediated phosphorylation that localize at the plasma membrane via interactions with phosphatidylinositol phosphates (PIPs) (Dondelinger et al., 2014) Once at the plasma membrane, the specific action of MLKL is not yet understood, however its ultimate function appears to be associated with disruption

of ionic homeostasis, resulting in oncosis and subsequent plasma membrane rupture (Dondelinger et al., 2014).

Research investigating the mechanisms of necroptosis has predominantly focused on the pleiotropic TNF pathway via stimulation of cells with TNFα and the pan-caspase inhibitor benzyloxycarbonyl-Val-Ala-Asp-fluoromethylketone (zVAD). The strong emphasis placed on TNF-mediated necroptosis is likely due to the fact that the majority of studies on necroptosis, including the founding preliminary studies by Vercammen and colleagues (1998) that discovered necroptosis, have focused on nonimmune cells, such as fibroblasts. Importantly, in my own studies I have observed that murine embryonic fibroblasts (MEFs) succumb to TNF-mediated necroptosis but are resistant to LPS- and IFNβ-mediated necroptosis (Fig. 10A). It was not until studies began examining the mechanisms of necroptosis in different cell types, particularly immune cells known to mediate inflammation, such as bone marrow derived macrophages (BMDMs), that greater insight into necroptotic inducers was gained (He et al., 2011). More specifically, engagement of toll-like receptor 3 (TLR3) and TLR4 with polyinosinic-polycytidylic acid (PolyI:C) and lipopolysaccharide (LPS) respectively was shown to drive programmed necrosis via phosphorylation and subsequent activation of receptor-interacting protein kinase 3 (RIP3) (He et al., 2011). It is currently unclear if the downstream MLKL signaling events that occur in response to TNF/zVAD stimulation also occur in response to LPS/zVAD, IFNβ/zVAD or PolyI:C/zVAD stimulation, however it is highly likely that MLKL acts as a common executioner mechanism for all necroptotic signaling pathways.

The difference between nonimmune and immune cells in terms of susceptibility to necroptotic stimuli, particularly LPS/zVAD and IFNβ/zVAD treatment, is intriguing. Physiologically it is understandable that inflammatory mediators and pathogen controllers,

such as macrophages, would be highly responsive to pattern-associated molecular patterns (PAMPs), like LPS, and inflammatory cytokines, like TNFα and IFNβ. Necroptotic death of macrophages not only aids in the clearance of certain pathogens, particularly those microorganisms containing apoptotic inhibitors, but also recruits additional immune cells to the site of infection or injury thereby making macrophages a more interesting and physiologically relevant cellular model to study necroptosis.

5.1 The role of dynamin-mediated endocytosis in macrophage necroptosis

Currently very little is known about the initial upstream signaling events that occur directly after ligand-receptor and eventually result in necroptosis. Understanding how the necroptotic signal is being transmitted, whether it is at the cell surface directly after engagement of a necroptotic receptor or intracellularly following endocytosis, is an important aim in my thesis. I first wanted to examine the impact of cytokine and PAMP signaling, which in macrophages happens at the cell surface, in the absence of zVAD to analyze initial signaling events. To ensure that cytokine or PAMP treatment was not inducing death of macrophages I performed several experiments without zVAD treatment. Importantly, I observed that treatment of BMDMs with LPS, TNFα, IFNβ or PolyI:C did not induce cell death (Fig. 5B,C). Instead, macrophages stimulated with cytokines or PAMPs displayed enhanced metabolic activity as a result of entering an activated state (Mosser and Edwards, 2008) (Fig. 5A). Only when macrophages were stimulated in the presence of zVAD was massive death observed, a phenotype that was rescuable when co-treated with the Rip1 kinase inhibitor necrostatin-1 (Nec-1) (Fig. 5B,C, 6A). In addition, similar to what was observed with cytokine or PAMP stimulation, treatment with zVAD alone did not induce necroptosis (Fig. 6A).

Knowing the importance of Rip1 and Rip3 for necroptosis I was interested in examining their expression levels. In particular, I wanted to measure activate phosphorylated Rip1 and Rip3 levels in response to LPS/zVAD. Previous studies using the same Rip1 and Rip3 antibodies have shown that phosphorylated Rip1 and phosphorylated Rip3 can be detected by western blot from a slower migrating, slightly heavier band found just above the unphosphorylated Rip1 or Rip3 band (McComb et al., 2012; Robinson et al., 2012). In my own experiments I confirmed this finding via lambda phosphatase treatment (Fig. 7B). In addition, I observed rapid phosphorylation of Rip1 followed by later phosphorylation of Rip3 in response to varying durations of LPS/zVAD treatments thus providing a model to examine necroptotic signaling events over time (Fig. 7A).

Cytokine signaling is an important aspect of necroptotic death (discussed further in section 5.2). To delve into the upstream signaling events of necroptosis I wanted to explore the impact of dynasore, a dynamin-mediated endocytosis inhibitor, on cytokine production. Endocytosis is an important cellular mechanism used to process signals from the extracellular milieu (Sorkin and Von Zastrow, 2002). For a long time, endocytosis was largely regarded as a mechanism to switch off membrane receptor signaling, however more recent studies have demonstrated that endocytosis can play an upstream role in signal transduction (Schneider-Brachert et al., 2004). Understanding the relationship between endocytosis, signal transduction and formation of intracellular signaling complexes is an important area of study, especially in the context of necroptosis. More specifically, it is important to understand whether or not receptors are able to signal intracellularly from endosomes and if they are, what is the physiological relevance (Sorkin and Von Zastrow, 2002). Interestingly, inhibition of dynasore-mediated endocytosis resulted in significantly reduced IL-6 and IL-10 production relative to macrophages treated with necroptotic stimuli

in the absence of dynasore (Fig. 8A-C). Furthermore, dynasore treatment dramatically impaired phosphorylation of STAT1 in response to LPS/zVAD stimulation (Fig. 8D). These findings support a previous study by Kagan et al., (2008), which focused on elucidating the mechanisms of TLR4 signaling. In short, Kagan et al., (2008) demonstrated that TLR4 signaling through MyD88 occurs at the cell surface, while TLR4 signaling through TRIF occurs intracellularly following dynamin-mediated endocytosis. In addition, Kagan and colleagues (2008) reported that macrophages treated with LPS and dynasore showed a dramatic decrease in phosphorylated IRF3 and production of IL-6 relative to macrophages treated with only LPS. In the context of necroptotic stimulation, intracellular signaling following dynamin-mediated endocytosis is important for facilitating the production of cytokines and also transducing signals needed for STAT1 activation.

Having identified a clear role for dynamin-mediated endocytosis in signal transduction and cytokine production in response to necroptotic stimuli I next wanted to elucidate the role of dynamin-mediated endocytosis in programmed necrosis of macrophages. Interestingly, inhibition of dynamin-mediated endocytosis did not seem to affect LPS-mediated necroptosis, rather slighting exacerbating death (Fig. 9A,D). In stark contrast, prevention of dynamin-mediated endocytosis rendered macrophages significantly resistant to TNFα and IFNβ induced necroptosis (Fig 9B,C,E,F). With respect to PolyI:C-mediated necroptosis, blocking dynamin-mediated endocytosis had no effect on death due to the fact that TLR3 already resides in endosomal vesicles and therefore does not require dynamin-mediated endocytosis for signal transduction (Kawai and Akira, 2006) (Fig. 9D). In regards to TNFα/zVAD and IFNβ/zVAD treatment, it appears that the necroptotic signal is transmitted intracellularly following endocytosis rather than at the cell surface. Why exactly LPS-mediated necroptosis

does not similarly rely on dynamin-mediated endocytosis is still an important question that needs answering and is currently under investigation in our lab.

As mentioned previously, the MEF cell line I tested was only susceptible to TNFα induced necroptosis (Fig. 10A). Importantly, MEFs have previously been shown to express high levels of mRNA for various TLRs, including TLR3 and TLR4 (Kurt-Jones et al., 2004). Furthermore, MEFs are reportedly highly responsive to TLR agonists and secrete high levels of IL-6 and monocyte chemoattractant protein-1 (MCP-1) in response to TLR stimulation (Kurt-Jones et al., 2004). In addition to expressing TLRs, MEFs also express IFNAR and TNFR (Chen et al., 2009; Wong et al., 2010). Collectively the findings from these studies rule out the possibility that the differential response to necroptotic stimuli, such as LPS/zVAD, observed in MEFs is a result of diminished or absent expression of necroptotic receptors. Interestingly, another striking difference between MEF and macrophage necroptosis was observed when dynamin-mediated endocytosis was inhibited. More specifically, necroptosis of MEFs occurred independently of dynamin-mediated endocytosis, as dynasore treatment did not rescue fibroblasts from death (Fig. 10B). It is possible that this difference is a result of differing functionality amongst cell types. In particular, macrophages are highly active professional phagocytes, which are constantly surveying the environment by endocytosis and phagocytosis (see section 1.1), while fibroblasts are non-inflammatory cells of the connective tissue known for their role in synthesizing extracellular matrix and providing the structural framework for animal tissues (Kalluri and Zeisberg, 2006). A comprehensive comparison of important endocytic proteins, such as dynamin, between BMDMs and MEFs may reveal why inhibition of dynamin-mediated endocytosis prevents necroptosis of macrophages and does not affect necroptosis of MEFs.

After observing that inhibition of dynamin-mediated endocytosis prevented TNFα induced necroptosis from occurring in macrophages I wanted to explore the role of dynamin-mediated endocytosis in Rip1 and Rip3 activation. Previous work has demonstrated that within minutes of TNF binding TNFR1, clathrin-mediated endocytosis of the ligand-receptor complex occurs, resulting in the formation of a multi-protein receptosome and activation of a death-inducing signaling complex (DISC) that can signal for apoptotic death (Schneider-Brachert et al., 2004). In addition, Schneider-Brachert and colleagues (2004) demonstrated that TNF receptosomes are important for establishing which TNF pathway is initiated (i.e. NFκB pathway or apoptotic pathway), which provides support for a role of TNFR internalization in necroptosis of macrophages. Interestingly, Rip1 activation in response to various necroptotic stimuli was unimpaired, thereby demonstrating that Rip1 activation occurs at the cell surface following ligand-receptor binding (Fig. 11A,B). Similar to this finding, Schneider-Brachert et al., (2004) also observed that Rip1 was recruited to TNFR1 at the plasma membrane. In contrast to Rip1, Rip3 activation was strongly impaired when dynamin-mediated endocytosis was inhibited, suggesting that Rip3 phosphorylation is induced from within an endosome (Fig. 11A,C). It would be interesting to delineate how Rip3 gets activated from an endosome following necroptotic activation and dynamin-mediated endocytosis.

In addition to impaired Rip3 activation, the maintenance of NFκB signaling was also strongly attenuated when dynamin-mediated endocytosis was blocked (Fig. 11A,D). Initial phosphorylation of NFκB protein p65 was similar to dynasore and non-dynasore treated groups, however in the presence of dynasore, phosphorylated p65 levels were transient and rapidly decreased after initial activation (Fig. 11A,D). Collectively these results provide a novel window into the initial signaling events involved in the induction of necroptotic death

of macrophages. Understanding upstream mechanisms is important to gain a thorough understanding of necroptosis and may also open up new therapeutic avenues to target various inflammatory pathologies.

5.2 The role of IFN-I signaling in macrophage necroptosis

Previous work from our lab has demonstrated that type I interferons (IFN-Is) play an important role in macrophage necroptosis during *Salmonella enterica* serovar Typhimurium (ST) infection (Robinson et al., 2012). More specifically, ST was able to drive Rip3-mediated necroptosis in macrophages via the upregulation of IFN-Is as a mechanism to evade immune detection (Robinson et al., 2012). Building upon this work, I have sought to investigate the underlying intracellular mechanisms of IFN-I signaling in macrophage necroptosis. Fascinatingly, macrophages lacking the IFNAR1 subunit of the IFN-I receptor were highly resistant to LPS, TNFα, IFNβ and PolyI:C induced necroptosis, ultimately highlighting the absolute importance of IFN-I signaling for Rip3-mediated necroptotic death (Fig. 12A-E, 14A-D). IFNAR1-/- mice have been shown to be resistant to TNFα induced septic shock, which supports our finding of a critical role for IFN-Is in necroptosis and its influence on inflammatory pathology (Huys et al., 2009). Huys and colleagues (2009) demonstrated that IFN-Is act as essential mediators in TNF-induced lethal inflammatory shock, however this study did not provide mechanistic insight into how IFN-I signaling leads to septic shock, which is potentially by driving highly inflammatory necroptotic death. The resistance of IFNAR1-/- macrophages to TNFα/zVAD induced necroptosis was surprising since TNFα has generally been considered to be the canonical inducer of necroptosis (Christofferson and Yuan, 2010). Furthermore, macrophages deficient in TNFR1/2 remained susceptible to LPS, IFNβ and PolyI:C induced necroptosis (Fig. A,C,D). These results

support the notion that TNF signaling is dispensable and not necessarily required for necroptosis of macrophages to occur. In contrast, these findings demonstrate that IFN-Is play an indispensible role in macrophage necroptosis, regardless of the particular necroptotic signaling pathway initiated.

To elucidate the role of IFN-Is on necrosome activation, Rip1 and Rip3 expression was examined in response to LPS/zVAD stimulation. Interestingly, the initial activation of Rip1 and Rip3 was similar in WT and IFNAR1-/- macrophages, however macrophages with impaired IFN-I signaling demonstrated a significant decrease in activated Rip1 and Rip3 expression after only a few hours of treatment (Fig. 15A,B). In contrast to Rip1 activation, where the difference between WT and IFNAR1-/- macrophages was less appreciable, the difference in Rip3 activation was consistently greater over at least five biological replicates. Based on these findings it appears that IFN-I signaling is needed to sustain Rip3 activation long enough for necroptosis to be executed.

Previous studies focusing on Rip kinases have demonstrated that genetic ablation of Rip1 results in early postnatal lethality since Rip1 is needed to prevent excessive apoptotic, necroptotic and NFκB signaling during critical developmental stages (Dillon et al., 2014; Kelliher et al., 1998). In contrast, Rip3 deficient mice are viable and appear phenotypically normal, making it much easier to examine the role of Rip3 in a variety of different models including atherosclerosis, brain injury and septic shock (Khan et al., 2014). The importance of Rip3 for necroptosis is undisputed, however the importance of Rip1 is currently a topic of debate. Initially, Rip1 was considered to be a fundamental protein in which necroptosis could not proceed without, however studies have now reported that necroptosis can occur independently of Rip1 (Dillon et al., 2014; Moujalled et al., 2013). More specifically, studies have demonstrated that TNF-mediated necroptosis of MEFs requires the presence of Rip1

and its kinase activity, a result I also observed when I treated MEFs with TNF/zVAD and Nec-1 (Vandenabeele et al., 2010) (Fig. 10A). Interestingly, other inducers of necroptosis, such as interferons, have been suggested to activate Rip3 independently of Rip1 via TRIF binding (Dillon et al., 2014). In my own findings however, Rip1 kinase activity does appear to have a role in necroptosis of macrophages, as Nec-1 treatment rescues cells from necroptosis (Fig.6A). It is possible that Rip1 is needed for the initial activation of Rip3, however IFN-I signaling is required to sustain this activation leading to necroptosis.

In addition to examining Rip1 and Rip3 activation, I also evaluated the activation of signal transducer and activator of transcription 1 (STAT1), a key protein involved in IFN-I signaling (see Fig. 2), and RNA-responsive protein kinase R (PKR), a protein recently implicated in type II IFN-mediated necroptosis of MEFs (Cheon et al., 2013; Thepa et al., 2014). PKR and phosphorylated PKR levels were similar between WT and IFNAR1-/- macrophages, suggesting that PKR does not necessarily play an important role in necroptosis of macrophages (Fig. 15A). Data from our lab has also shown that PKR-/- BMDMs are susceptible to all necroptotic stimuli providing further support for the notion that PKR is not required for necroptosis of macrophages (McComb et al., 2014). In the case of STAT1, phosphorylation occurred quite rapidly in WT BMDMs after only a few hours of LPS/zVAD stimulation. Interestingly, the timing of STAT1 phosphorylation correlated with robust activation of Rip3, providing further support for the importance of IFN-I signaling in Rip3 activation (Fig. 15A). As mentioned previously, studies have demonstrated that LPS signaling through TLR4 and TRIF induces the production of IFN-Is, which can autocrine signal back through IFNAR (Kagan et al., 2008). Importantly, rapid IFN-I production in response to LPS/zVAD treatment was confirmed in an L929 cell line with a luciferase

reporter gene cloned under the regulation of an interferon stimulated response element (ISRE) promoter (Fig. 15D).

To further characterize the mechanisms of LPS-mediated necroptosis, I examined necroptotic susceptibility in BMDMs deficient in either TRIF or MyD88; the two key adaptor proteins needed for TLR4 signal transduction. Recently it has been suggested that TRIF plays an important role in necroptosis via Rip homotypic interaction motif (RHIM) domain interactions with Rip3 (Kaiser et al., 2013). Providing further support for a necroptotic role of TRIF, I observed that macrophages lacking TRIF were significantly resistant to LPS and PolyI:C induced necroptosis (Fig. 16A,D). TRIF is well known for its role in IFN-I production in response to LPS, thus in the absence of TRIF, IFN-I production is strongly attenuated, Rip3 phosphorylation is abolished and subsequent necroptotic death is prevented (Fig. 16A, 17A,B). When stimulated with IFNβ/zVAD, TRIF-/- macrophages underwent necroptotic death similar to WT macrophages due to the fact that cells were being supplemented with IFNβ resulting in the activation of IFNAR signaling, effectively bypassing the need for TRIF-mediated production of IFN-Is (Fig. 16C). A role for TRIF in the context of TNF signaling has not been identified and in response to TNFα/zVAD treatment TRIF-/- macrophages showed similar susceptibility to necroptosis relative to WT macrophages (Fig.16B).

In terms of MyD88 deficiency, no substantial effect on necroptosis of macrophages was observed, however a slight resistance to PolyI:C-mediated necroptosis was detected (Fig. 16A-D). Unlike TRIF-/- BMDMS, Rip3 phosphorylation was unaffected in MyD88-/- macrophages (Fig. 17A,B). Additionally, MyD88 null macrophages displayed a lag in the initial activation of Rip1 (Fig. 17B). In contrast, TRIF deficient macrophages showed robust initial Rip1 phosphorylation (Fig. 17B). Collectively, these results suggest that LPS signaling

through TLR4 activates Rip1 via TRIF and MyD88 dependent pathways, which may involve multiple kinases or converge upon a common pathway. Previous studies have reported that Rip1 is able to autophosphorylate following stimulation of Jurkat T cells, however in my own findings, I have observed Rip1 phosphorylation in the presence of Nec-1, suggesting that this may not necessarily be the case in macrophages (Christofferson and Yuan, 2010; Degterev et al., 2008; Ting et al., 1996). Inquiry into functions of MyD88 outside of NFκB signaling revealed that MyD88 is capable of activating IRF1, IRF5 and IRF7, which may aid in the production of IFN-Is needed for necroptotic death (O'Neil and Bowie, 2007). Further investigation into converging and diverging kinases that are downstream targets of MyD88, such as interleukin-1 receptor-associated kinases 1 and 2 (IRAK1/2), and TRIF, such as TANK-binding kinase 1 (TBK1) and Akt, may provide a clearer picture into the early events of Rip1 activation (Joung et al., 2011; Muzio et al., 1997; Warner and Núñez, 2013). In contrast to the modest differences in Rip1 phosphorylation observed in TRIF null and MyD88 null macrophages, Rip3 activation is largely dependent on TRIF and less so MyD88. More specifically, TRIF is needed to induce IFN-Is in response to LPS, which autocrine signals through IFNAR and promotes sustained Rip3 phosphorylation leading to eventual necroptotic demise.

After observing an imperative role for IFN-I signaling in necroptosis of macrophages, I wanted to better understand the mechanism involved. To evaluate the downstream effects of IFNAR signaling on necroptosis, I examined a variety of interferon regulatory factor (IRF) knockout mice. Consistent with previous findings, various IRFs showed redundancy in activating and releasing IFN-Is in response to TLR stimulation (Schmid et al., 2010). More specifically, impairment to one or even two IRFs only resulted in partial resistance to necroptosis unlike the dramatic resistance observed in IFNAR1-/- macrophages. Partial

resistance to LPS-mediated necroptosis was observed in macrophages lacking IRF1, IRF3, IRF7 or IRF3/7 (Fig. 18A, 19A). In addition, IRF3, IRF7 and IRF3/7 macrophages also displayed resistance to treatment with TNF/zVAD and IFN/zVAD (Fig. B,C). A cumulative effect was not observed in the IRF3/7 double KO, thus providing support for a redundant role of IRFs in necroptosis. Previous work has demonstrated that TNF induces IFN-I production through IRF1 activation (Yarilina et al., 2008). Interestingly and consistent with this finding, IRF1 was particularly important for TNFα induced necroptosis (Fig. 18B). No significant effect was observed in IRF1 null macrophages treated with IFNβ/zVAD since macrophages were being supplemented with IFNβ rather than depending on IRF1-mediated production of IFN-Is (Fig. 18C).

In contrast to the results observed in various IRF KO macrophages, IRF9 deficiency resulted in significant resistance to all necroptotic stimuli, which was similar to the resistance observed in IFNAR1-/- macrophages (Fig. 20A-D). Importantly, rather than promoting IFN-I production, IRF9 has a unique role in facilitating the response to IFN-I signaling through IFNAR (Honda and Taniguchi, 2006). More specifically, IRF9 is able to associate with STAT1 and STAT2 to form a heterotrimeric transcription complex known as interferon-stimulated gene factor 3 (ISGF3) (Tsuno et al., 2009). IRF9 is particularly important for the recognition of an ISRE site in the nucleus, thereby allowing ISGF3 to bind and activate the transcription of targeted ISGs (Tsuno et al., 2009). In terms of necrosome activation, Rip1 phosphorylation was not affected by the lack of IRF9 expression, however Rip3 phosphorylation was strongly attenuated as a result of IRF9 deficiency (Fig. 21A-C). To my knowledge, the impact of IRF9 deficiency on various inflammatory pathologies has not been evaluated. Taken together, these results convincingly demonstrate a key role of downstream IFNAR signaling component IRF9 in inflammatory necroptotic death of macrophages.

To decipher whether IRF9 was exclusively important or if instead ISGF3 as a whole was needed for necroptosis I evaluated the impact of STAT1 and STAT2 deficiency. In addition to IRF9, STAT1 and STAT2 deficiency also resulted in significant resistance to necroptosis, supporting a view that ISGF3 has a pro-necroptotic role in macrophages (Fig. 22A-D, 24A-D). It is important to mention that STAT1-/- mice were maintained on a 129S6 genetic background. To ensure that the STAT1-/- results were comparable to the C57BL/6 model I evaluated necroptosis in IFNAR1-/- macrophages on a 129S6 background. Importantly, I found a similar resistant phenotype in IFNAR1-/- macrophages on a 129S6 background to that observed in IFNAR1-/- macrophages on a C57BL/6 genetic background (Fig. 23A-C). Interestingly, STAT1 and STAT2 deficiency also resulted in strongly attenuated Rip3 activation, suggesting that ISGF3 mediates necroptotic death through the late activation of Rip3 (Fig. 25A,B). Consistently, Rip1 activation has been unaffected by various knockouts or treatments, providing support for the concept that Rip1 phosphorylation is an upstream event that follows rapidly after necroptotic stimulation. Rip3 activation, however, is hindered with impairment to IFNAR signaling through ISGF3. Further work is required to unveil the exact mechanism of how IFN-I signaling through ISGF3 influences Rip3 and also MLKL, the effectors of necroptosis.

Previous work examining IFN-I signaling hypothesized that macrophages constitutively secrete low levels of IFNβ as a priming mechanism to ensure adequate subsequent responses to other cytokines or pathogens (Gough et al., 2012). Interestingly, macrophages stimulated with IFNβ for varying time intervals over the course of 14 hours showed a time-dependent increase in STAT1 and STAT2 levels (Fig. 26A). Fascinatingly, both STAT1 and STAT2 expression levels peaked at approximately 12-14 hours, which is around the timing of programmed necrotic death (Fig. 26A). Previous studies have suggested that tonic IFNβ

signaling is needed to maintain basal levels of various proteins, such as STAT1 and STAT2 (Gough et al., 2012). Supporting this view, I observed significantly lower basal STAT1 and STAT2 levels, which remained low even after stimulation with LPS/zVAD, in IFNAR1-/- macrophages (Fig. 26B). Furthermore, impairment to ISGF3 components also resulted in dramatically reduced basal STAT1 and STAT2 levels (Fig. 26C-E). Unfortunately I was unable to examine IRF9 protein expression due to the poor quality of anti-IRF9 antibodies. Subsequent work in our lab did notice that IRF9 transcript levels, both basal and LPS/zVAD stimulated, were substantially lower in IFNAR1-/- macrophages relative to WT (McComb et al., 2014). Collectively these results indicate that tonic low level IFNβ signaling through ISGF3 is needed to maintain adequate basal levels of ISGF3 components. Furthermore, sustained IFNβ signaling is needed to gradually increase STAT1 and STAT2 levels such that protein expression eventually peaks around 12-14 hours, ultimately correlating with the timing of necroptosis.

To date, many questions surrounding the necrosome and its formation remain unanswered. It is well known that Rip1/Rip3 necrosome formation is dependent upon necroptotic receptor stimulation and impaired caspase activity. Previous work examining the mechanisms of TNF-mediated necroptosis reported that Rip1 and Rip3 associate via their RHIM domains to form heterodimeric filamentous structures characteristic of β-amyloids (Li et al., 2012). This study provided novel insight into the structural changes that occur following Rip kinase activation specifically in response to TNF induced necroptotic death (Li et al., 2012). Whether or not this phenotype occurs during LPS-, IFNβ- or PolyI:C-mediated necroptosis is unclear.

Interestingly, in my own experiments evaluating necrosome activation I observed a progressive decrease in Rip1 expression in response to LPS/zVAD treatment (Fig. 27A). In

contrast, Rip3 levels were fairly stable and decreased ever so slightly at a much later time point. This curious observation promoted further investigating to determine how Rip1 was being degraded in response to LPS/zVAD treatment. Fascinatingly, Rip1 degradation was prevented in the presence of lactacystin, a proteasomal inhibitor, thereby demonstrating that Rip1 is being actively degraded by the proteasome in response to necroptotic stimulation (Fig. 27B). Importantly, several pieces of data rule out the possibility that Rip1 is being passively released from the cell due to a loss of membrane integrity resultant from necroptotic death. First, it is important to note the timing of Rip1 degradation, which begins after 2 hour of LPS/zVAD treatment (Fig. 27A). The timing of Rip1 degradation long precedes the timing of necroptotic death, which occurs after approximately 12-14 hours of LPS/zVAD treatment (Fig. 27C,D). Furthermore, Rip1 degradation was also observed in IFNAR1-/- macrophages, which are highly resistant to necroptosis displaying only marginal amounts of cell death (Fig. 15A, 12A,B) Finally, the expression levels of other proteins, including STAT1 and PKR, remain consistent in response to LPS/zVAD treatment (Fig. 15A).

I was next interested in understanding the mechanism driving proteasomal degradation of Rip1 in response to LPS/zVAD stimulation. In particular, I wanted to determine whether or not Rip1 was being targeted to the proteasome via ubiquitination. Considered to be one of the most common post-translational regulatory processes within a eukaryote, ubiquitination of substrate proteins can have a variety of different functions ranging from degradation to signal transduction (Ben-Neriah, 2012). The process of protein ubiquitination is mediated by the activity of three enzymes (Liu et al., 2005). First E1 ligases activate ubiquitin in the presence of ATP (Liu et al., 2005). Next activated ubiquitin is transferred to a ubiquitin-conjugating enzyme, which is referred to as E2 (Liu et al., 2005). Lastly E3 ligases bring the

E2-ubiquitin complex together with the targeted protein and aid in the transfer of ubiquitin from E2 to the substrate protein (Liu et al., 2005). Previous studies have demonstrated an important relationship between E3 ligases cIAP1/2 and Rip1 in TNF-mediated NFκB signaling (Beug et al., 2012). More specifically, cIAP1/2 polyubiquitinate Rip1 with K68-linked ubiquitin chains that act as a docking site for proteins needed to transduce the NFκB signal (Shih et al., 2011). In addition, work from our lab has shown that cIAP1 and cIAP2 limit macrophage necroptosis via inhibition of Rip1 and Rip3 activation (McComb et al., 2012). Using SMAC mimetic 164 (SM-164) to degrade cIAP1/2, I wanted to determine if Rip1 was being selectively targeted to the proteasome via cIAP1/2-mediated K48-linked ubiquitination. Interestingly, degradation of cIAP1/2 had no effect on Rip1 degradation, demonstrating that Rip1 is being targeted to the proteasome independent of cIAPs (Fig. 29A). Instead of mediating Rip1 degradation, I found that cIAP1/2 are degraded in a similar fashion to Rip1 following LPS/zVAD treatment (Fig. 29B). Further experimentation is needed to clarify how Rip1 is being targeted to the proteasome. Other potential E3 ligase candidates that could be mediating the proteasomal degradation of Rip1 include TRAF2/6, important E3 ligases that facilitates NFκB signaling, or A20, which functions as both an E3 ligase and a deubiquitinating enzyme (DUB) in macrophage NFκB signaling (Liu et al., 2005).

Interestingly, I next observed that in the presence of Nec-1, LPS/zVAD no longer induced Rip1 degradation (Fig. 29C). As mentioned prior, Nec-1 disrupts the association of Rip1 and Rip3 thereby preventing Rip3 activation (Degterev et al., 2008; He et al., 2009). Building on this finding I next observed that Rip1 degradation was prevented in Rip3-/- macrophages stimulated with LPS/zVAD (Fig. 29C). Finally, in response to LPS stimulation in the absence of zVAD, Rip1 degradation was also prevented (Fig. 29C). Studies have

shown that functional caspase-8 is able to cleave Rip1 and Rip3, preventing necroptosis from occurring (Feng et al., 2007; Lin et al., 1999). Since cells were only stimulated with LPS and caspase activity was still intact, Rip3 activation was prevented (Fig. 29C). Collectively, these data reveal that Rip1-induced activation of Rip3 concurrently leads to a previously unidentified mechanism of Rip1 degradation. Since proteasomal degradation of Rip1 and cIAP1/2 occurs early on during necroptotic activation, this may act as a protective mechanism where the necrosome self-regulates to prevent death until a sustained necroptotic signal, such as IFN-I signaling then results in the execution of necroptosis. Further exploration into the role of protein degradation in necroptosis is being continued in the lab.

6.0 CONCLUSION

In this Masters thesis I have presented novel insights into the mechanisms of necroptotic cell death. Exploration into the induction of necroptosis of macrophages has unveiled an important role for dynamin-mediated endocytosis. More specifically, in response to TNFα/zVAD or IFNβ/zVAD stimulation my work has revealed that dynamin-mediated endocytosis is required to transmit the necroptotic signal intracellularly rather than at the cell surface, which is particularly important for Rip3 activation. Furthermore, cytokines produced in response to necroptotic stimuli are significantly attenuated in the absence of dynamin-mediated endocytosis, highlighting the importance of intracellular signal transduction for necroptosis and immune signaling. Interestingly, LPS-mediated necroptosis did not rely on dynamin-mediated endocytosis, suggesting that there are some vital underlying differences between cytokine and PAMP induced necroptosis. Understanding how macrophages initiate necroptosis and communicate these upstream signals to culminate in necroptotic suicide is

hugely important. In particular, piecing together the puzzle of necroptotic signaling is crucial to gain a better understanding of this inflammatory form of death, while at the same time shedding light on novel potential drug targets for various inflammatory pathologies. This work is currently ongoing in the lab and these findings should be published in the near future.

Building upon previous work by Robinson et al., (2012) in Dr. Sad's lab, I next investigated the mechanistic relationship between type I interferon (IFN-I) signaling and necroptosis. Remarkably, my results revealed that IFN-Is act as a fundamental mediator of necroptosis of macrophages. In addition, the importance of TNF signaling for necroptotic death of immune cells has been redefined. The results detailed in this thesis suggest that TNF, LPS and PolyI:C signaling indirectly promote necroptosis by facilitating the production of IFN-Is through IRF1, IRF3, IRF7 and TRIF, as oppose to directly driving necroptotic death. Following the production of IFN-Is, autocrine signaling through IFNAR and ISGF3 sustains Rip3 activation necessary for necroptosis of macrophages (Fig. 32). Collectively, these results have illuminated IFN-Is as a central, indispensible mechanism of necroptosis of macrophages (McComb et al., 2014). These findings may provide an alternative therapeutic target for acute inflammatory pathologies, such as sepsis.

Lastly, a proteasomal mechanism that leads to autoregulation of necrosome activation was identified. In response to LPS/zVAD stimulation Rip1 is rapidly degraded by the proteasome, which is independent of cIAP1/2 E3 ligase activity. In contrast to mediating Rip1 degradation, LPS/zVAD treatment induces cIAP1/2 degradation similar to Rip1. Furthermore, activated Rip3 mediates the proteasomal degradation of Rip1. Proteasomal degradation of necrosome components is an important regulator of cell death signaling, potentially acting as a protective cellular mechanism to prevent unwanted necroptosis from occurring. Furthermore, sustained Rip3 activation by IFN-I signaling may counterbalance

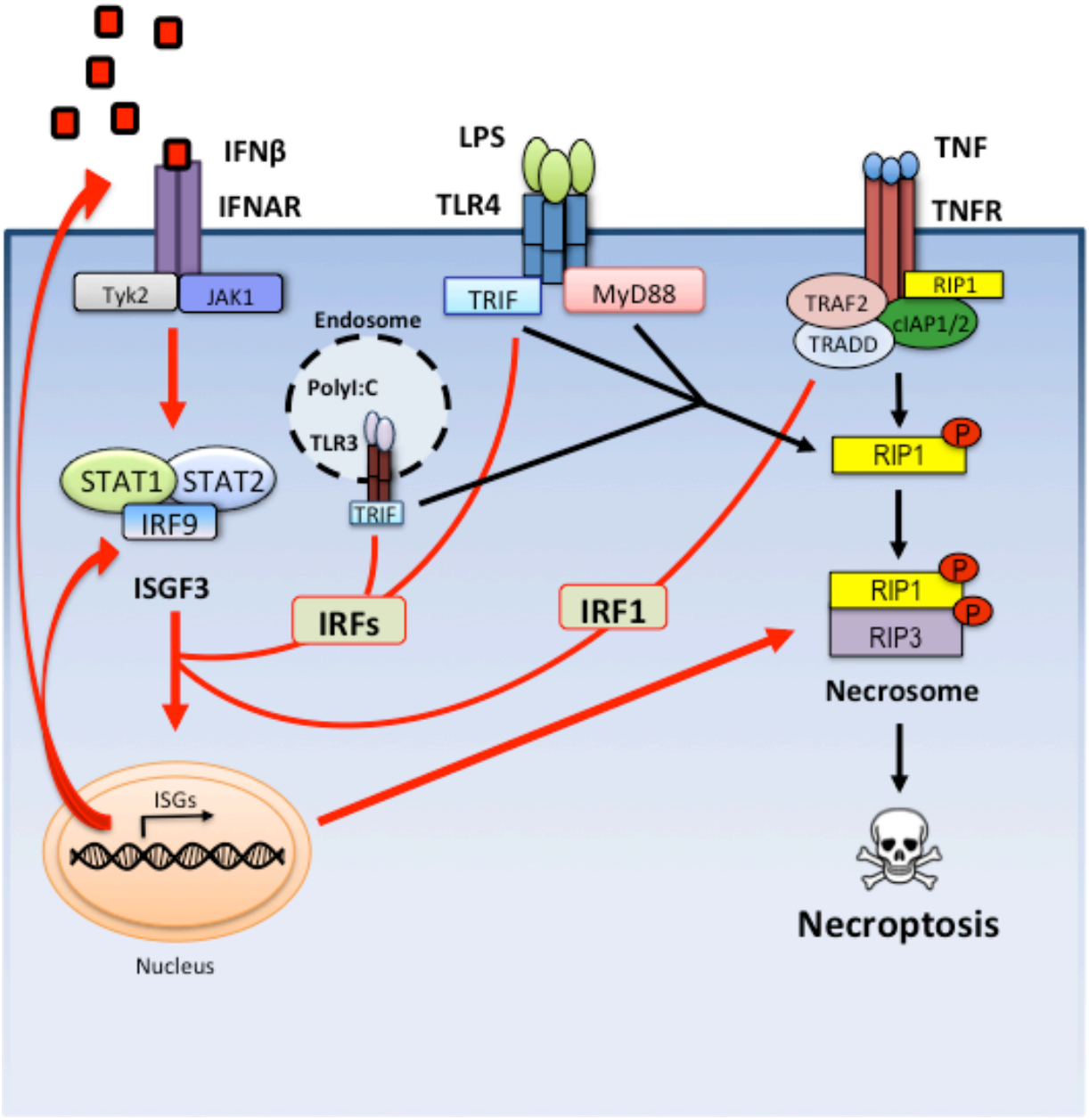
IFNβ
IFNAR
Tyk2
JAK1
LPS
TLR4
TRIF
MyD88
TNF
TNFR
TRAF2
RIP1
cIAP1/2
TRADD
Endosome
Poly I:C
TLR3
TRIF
STAT1
STAT2
IRF9
ISGF3
IRFs
IRF1
RIP1
P
RIP1
P
RIP3
Necrosome
ISGs
Nucleus
Necroptosis

Figure 32. *Model of the role of IFN-I signaling in necroptosis of macrophages.* Induction of necroptosis can occur through various cell surface receptors, such as TNFR, TLR4 and IFNAR, and endosomal receptor TLR3. Initial activation of Rip1 occurs directly after receptor stimulation, however IFN-I signaling is needed to drive sufficient Rip3 activation. Importantly, these necroptotic receptors are able to promote the production of IFN-Is through the activation of various IRFs. Once production, IFN-Is autocrine signal through IFNAR and ISGF3 to sustain Rip3 phosphorylation. Prolonged Rip3 phosphorylation and necrosome activation subsequently results in the execution of necroptosis.

this degradative regulation to promote necroptosis.

Collectively, the results presented in this thesis have uncovered previously unidentified mechanisms of necroptotic death of macrophages (Fig. 33). Inflammatory pathologies, such as sepsis, affect millions of individuals worldwide each year (Husak et al., 2010; Van der Poll and Opal, 2008). Specifically in Canada, sepsis mortality rates range from 30-50% and account for the majority of in-hospital mortalities (Husak et al., 2010). Simply put, by gaining a better understanding of necroptotic death we are taking steps towards preventative measures and perhaps cures to combat harmful inflammation. I hope that the findings presented in this thesis can in some way, small or large, aid in the development of therapies for a variety of inflammatory pathologies, including sepsis.

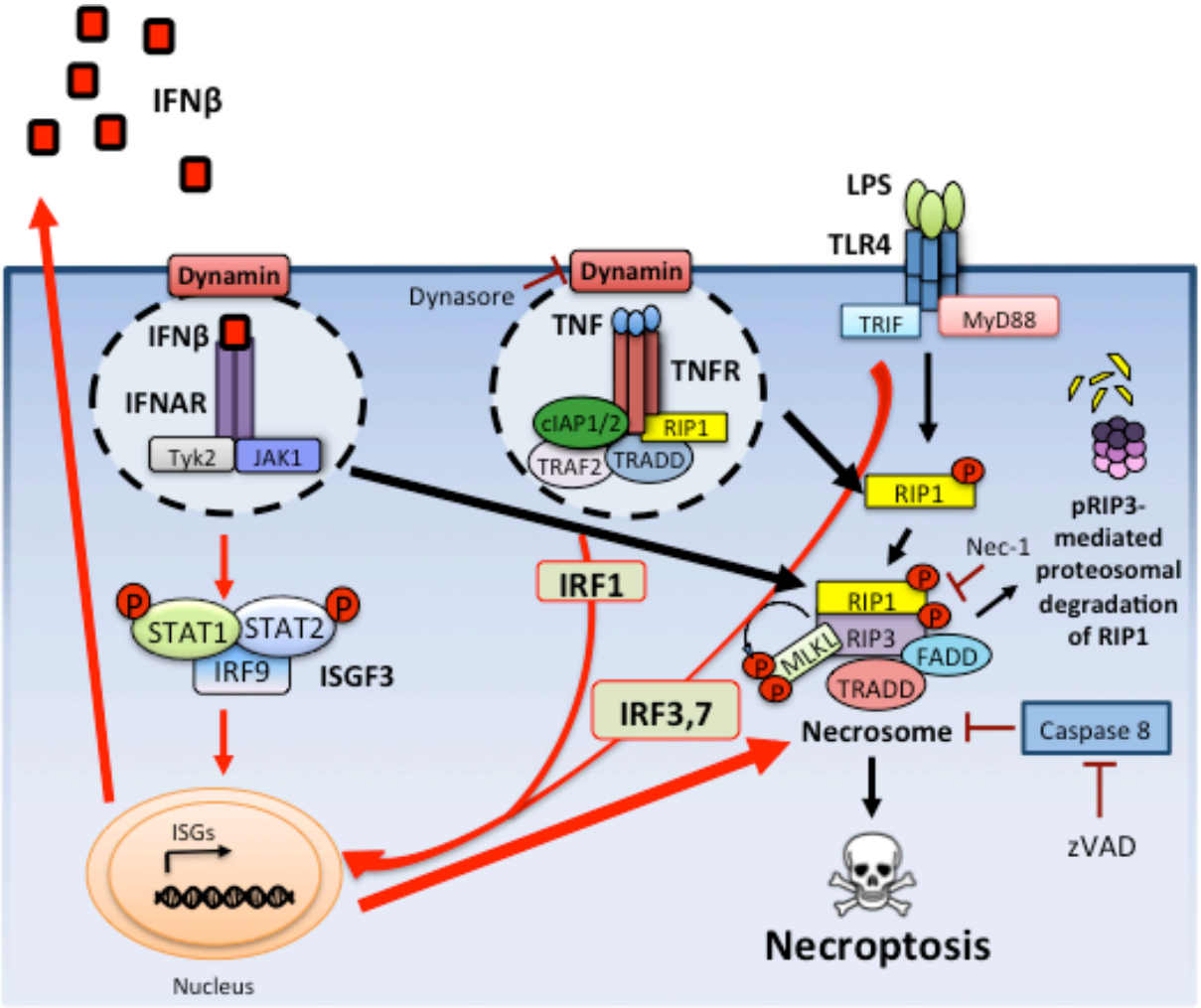
IFNβ
Dynamin
IFNβ
IFNAR
Tyk2
JAK1
Dynasore
Dynamin
TNF
TNFR
cIAP1/2
RIP1
TRAF2
TRADD
LPS
TLR4
TRIF
MyD88
RIP1
pRIP3-
mediated
proteosomal
degradation
of RIP1
Nec-1
RIP1
RIP3
MLKL
FADD
TRADD
Necrosome
Caspase 8
zVAD
IRF1
IRF3,7
STAT1
STAT2
IRF9
ISGF3
ISGs
Nucleus
Necroptosis

Figure 33. *Thesis model of the mechanisms of necroptosis.* Induction of necroptosis begins upon engagement of necroptotic receptors with corresponding ligands in the absence of caspase activity. Rapidly after stimulation, Rip1 is phosphorylated at the cell surface. In order to activate Rip3, dynamin-mediated endocytosis is required, however, LPS-mediated necroptosis specifically does not depend on this internalization process. Once phosphorylated, Rip3 drives the proteasomal degradation of Rip1 to prevent unwanted necroptosis from occurring. For necroptosis to occur, IFN-I signaling is needed to counter this protective degradative mechanism. Importantly, necroptosis inducing receptors are also able to promote IFN-I production through the activation of various IRFs. Once produced, IFN-I is able to autocrine signal through IFNAR and ISGF3 to prolong Rip3 activation. Sustained necrosome activation via Rip3 ultimately leads to the execution of necroptosis resulting in oncosis, plasma membrane rupture, release of intracellular content into the environment and a subsequent potent inflammatory response.

7.0 REFERENCES

1. Aderem, A., and Underhill, D.M. (1999). Mechanisms of phagocytosis in macrophages. Annual Review of Immunology *17*, 593–623.
2. Ajami, B., Bennett, J.L., Krieger, C., McNagny, K.M., and Rossi, F.M. (2011). Infiltrating monocytes trigger EAE progression, but do not contribute to the resident microglia pool. Nature Neuroscience *14*, 1142–1149.
3. Ameisen, J.C. (2002) On the origin, evolution, and nature of programmed cell death: a timeline of four billion years. Cell Death and Differentiation *9*, 367–393.
4. Ameisen, J.C. (2009) The origin and evolution of programmed cell death (Wiley & Sons).
5. Baxter, D. (2007). Active and passive immunity, vaccine types, excipients and licensing. Occupational Medicine (Oxford, England) *57*, 552–556.
6. Ben-Neriah, Y. (2002). Regulatory functions of ubiquitination in the immune system. Nature Immunology *3*, 20–26.
7. Buckley, C.D., Gilroy, D.W., Serhan, C.N., Stockinger, B., and Tak, P.P. (2013). The resolution of inflammation. Nature Reviews. Immunology *13*, 59–66.
8. Cai, Z., Jitkaew, S., Zhao, J., Chiang, H.-C.C., Choksi, S., Liu, J., Ward, Y., Wu, L.-G.G., and Liu, Z.-G.G. (2014). Plasma membrane translocation of trimerized MLKL protein is required for TNF-induced necroptosis. Nature Cell Biology *16*, 55–65.
9. Chen, C.J., Kono, H., Golenbock, D., Reed, G., and Akira…, S. (2007). Identification of a key pathway required for the sterile inflammatory response triggered by dying cells. Nature Medicine *13*, 851–856.
10. Chen, X., Li, W., Ren, J., Huang, D., He, W.-T.T., Song, Y., Yang, C., Li, W., Zheng, X., Chen, P., et al. (2014). Translocation of mixed lineage kinase domain-like protein to plasma membrane leads to necrotic cell death. Cell Research *24*, 105–121.
11. Chen, H, Tanaka, N, Mitani, Y, Oda, E, and Nozawa, H (2009). Critical role for constitutive type I interferon signaling in the prevention of cellular transformation. Cancer Science *100*, 449–456.
12. Chen, G.Y., and Nuñez, G. (2010). Sterile inflammation: sensing and reacting to damage. Nature Reviews. Immunology *10*, 826–837.
13. Cheon, H., Holvey-Bates, E.G., Schoggins, J.W., Forster, S., Hertzog, P., Imanaka, N., Rice, C.M., Jackson, M.W., Junk, D.J., and Stark, G.R. (2013). IFNβ-dependent increases in STAT1, STAT2, and IRF9 mediate resistance to viruses and DNA damage. The EMBO Journal *32*, 2751–2763.
14. Christofferson, D.E., and Yuan, J. (2010). Necroptosis as an alternative form of programmed cell death. Current Opinion in Cell Biology *22*, 263–268.
15. Cho, Y.S., Challa, S., Moquin, D., Genga, R., Ray, T.D., Guildford, M., and Chan, F.K. (2009). Phosphorylation-driven assembly of the RIP1-RIP3 complex regulates programmed necrosis and virus-induced inflammation. Cell *137*, 1112–1123.
16. Chow, S.C., Weis, M., Kass, G.E., Holmström, T.H., Eriksson, J.E., and Orrenius, S. (1995). Involvement of multiple proteases during Fas-mediated apoptosis in T lymphocytes. FEBS Letters *364*, 134–138.
17. Clarke, P.G., and Clarke, S. (1996). Nineteenth century research on naturally occurring cell death and related phenomena. Anatomy and Embryology *193*, 81–99.

18. Clarke, P.G., and Clarke, S. (2012). Nineteenth century research on cell death. Experimental Oncology *34*, 139–145.
19. Coussens, L.M., and Werb, Z. (2002). Inflammation and cancer. Nature *420*, 860–867.
20. Cusson-Hermance, N., Khurana, S., Lee, T.H., Fitzgerald, K.A., and Kelliher, M.A. (2005). Rip1 mediates the Trif-dependent toll-like receptor 3- and 4-induced NF-κB activation but does not contribute to interferon regulatory factor 3 activation. The Journal of Biological Chemistry*280*, 36560–36566.
21. Daffis, S., Suthar, M.S., Szretter, K.J., Gale, M., and Diamond, M.S. (2009). Induction of IFN-beta and the innate antiviral response in myeloid cells occurs through an IPS-1-dependent signal that does not require IRF-3 and IRF-7. PLoS Pathogens *5*, e1000607.
22. Danial, N.N., and Korsmeyer, S.J. (2004). Cell death: critical control points. Cell *116*, 205–219.
23. Degterev, A., Huang, Z., Boyce, M., Li, Y., Jagtap, P., Mizushima, N., Cuny, G.D., Mitchison, T.J., Moskowitz, M.A., and Yuan, J. (2005). Chemical inhibitor of nonapoptotic cell death with therapeutic potential for ischemic brain injury. Nature Chemical Biology *1*, 112–119.
24. Degterev, A., Hitomi, J., Germscheid, M., Ch'en, I.L., Korkina, O., Teng, X., Abbott, D., Cuny, G.D., Yuan, C., Wagner, G., et al. (2008). Identification of RIP1 kinase as a specific cellular target of necrostatins. Nature Chemical Biology *4*, 313–321.
25. De Weerd, N.A., and Nguyen, T. (2012). The interferons and their receptors–distribution and regulation. Immunology and Cell Biology *90*, 483–491.
26. Dickens, L.S., Powley, I.R., Hughes, M.A., and MacFarlane, M. (2012). The "complexities" of life and death: death receptor signalling platforms. Experimental Cell Research *318*, 1269–1277.
27. Dillon, C.P., Weinlich, R., Rodriguez, D.A., Cripps, J.G., Quarato, G., Gurung, P., Verbist, K.C., Brewer, T.L., Llambi, F., Gong, Y.-N.N., et al. (2014). RIPK1 blocks early postnatal lethality mediated by caspase-8 and RIPK3. Cell *157*, 1189–1202.
28. Dondelinger, Y., Declercq, W., Montessuit, S., Roelandt, R., Goncalves, A., Bruggeman, I., Hulpiau, P., Weber, K., Sehon, C.A., Marquis, R.W., et al. (2014). MLKL compromises plasma membrane integrity by binding to phosphatidylinositol phosphates. Cell Reports *7*, 971–981.
29. Dranoff, G. (2004). Cytokines in cancer pathogenesis and cancer therapy. Nature Reviews. Cancer *4*, 11–22.
30. Duprez, L., Takahashi, N., Van Hauwermeiren, F., Vandendriessche, B., Goossens, V., Vanden Berghe, T., Declercq, W., Libert, C., Cauwels, A., and Vandenabeele, P. (2011). RIP kinase-dependent necrosis drives lethal systemic inflammatory response syndrome. Immunity *35*, 908–918.
31. Duprez, L., Wirawan, E., Vanden Berghe, T., and Vandenabeele, P. (2009). Major cell death pathways at a glance. Microbes and Infection *11*, 1050–1062.
32. Ekert, P.G., Silke, J., and Vaux, D.L. (1999). Caspase inhibitors. Cell Death and Differentiation*6*, 1081–1086.
33. Ellis, H.M., and Horvitz, R.H. (1986). Genetic control of programmed cell death in the nematode C. elegans. Cell *44*, 817–829.
34. Elmore, S. (2007). Apoptosis: A review of programmed cell death. Toxicologic Pathology *35*, 495–516.
35. Evan, G., and Littlewood, T. (1998). A matter of life and cell death. Science (New York, N.Y.) *281*, 1317–1322.

36. Feng, S., Yang, Y., Mei, Y., Ma, L., Zhu, D.E., Hoti, N., Castanares, M., and Wu, M. (2007). Cleavage of RIP3 inactivates its caspase-independent apoptosis pathway by removal of kinase domain. Cellular Signalling *19*, 2056–2067.
37. Feoktistova, M., Geserick, P., Kellert, B., Dimitrova, D., Langlais, C., Hupe, M., Cain, K., MacFarlane, M., Häcker, G., and Leverkus, M. (2011) cIAPs block ripoptosome formation, a RIP1/caspase-8 containing intracellular cell death complex differentially regulated by cFLIP isoforms. Molecular Cell *43*, 449–463.
38. Feoktistova, M., Geserick, P., Panayotova-Dimitrova, D., and Leverkus, M. (2012) Pick your poison: The ripoptosome, a cell death platform regulating apoptosis and necroptosis. Cell Cycle *11*, 460–467.
39. Fink, S.L., and Cookson, B.T. (2005). Apoptosis, pyroptosis, and necrosis: mechanistic description of dead and dying eukaryotic cells. Infection and Immunity *73*, 1907–1916.
40. Fink, K., Martin, L., Mukawera, E., Chartier, S., De Deken, X., Brochiero, E., Miot, F., and Grandvaux, N. (2013). IFNβ/TNFα synergism induces a non-canonical STAT2/IRF9-dependent pathway triggering a novel DUOX2 NADPH oxidase-mediated airway antiviral response. Cell Research *23*, 673–690.
41. Frazier, W.J., Wang, X., Wancket, L.M., Li, X.A, Meng, X., Nelin, L.D., Cato, A.C.B., and Liu, Y. (2009). Increased inflammation, impaired bacterial clearance and metabolic disruption after Gram-negative sepsis in Mkp-1 deficient mice. Journal of Immunology (Baltimore, Md. : 1950) *182*, 7411–7419.
42. Fujiwara, N., and Kobayashi, K. (2005). Macrophages in inflammation. Current Drug Targets Inflammation Allergy *4*, 281–286.
43. Gad, H.H., Dellgren, C., Hamming, O.J., Vends, S., Paludan, S.R., and Hartmann, R. (2009). Interferon-lambda is functionally an interferon but structurally related to the interleukin-10 family. The Journal of Biological Chemistry *284*, 20869–20875.
44. Gaestel, M., Kotlyarov, A., and Kracht, M. (2009). Targeting innate immunity protein kinase signalling in inflammation. Nature Reviews. Drug Discovery *8*, 480–499.
45. Gao, J.J., Filla, M.B., Fultz, M.J., Vogel, S.N., Russell, S.W., and Murphy, W.J. (1998). Autocrine/paracrine IFN-alphabeta mediates the lipopolysaccharide-induced activation of transcription factor Stat1alpha in mouse macrophages: pivotal role of Stat1alpha in induction of the inducible nitric oxide synthase gene. Journal of Immunology (Baltimore, Md. : 1950) *161*, 4803–4810.
46. Gillet, G., and Brun, G. (1996). Viral inhibition of apoptosis. Trends in Microbiology *4*, 312–317.
47. González-Navajas, J.M., Lee, J., David, M., and Raz, E. (2012). Immunomodulatory functions of type I interferons. Nature Reviews. Immunology*12*, 125–135.
48. Gorbunova, V., Hine, C., Tian, X., Ablaeva, J., Gudkov, A.V., Nevo, E., and Seluanov, A. (2012). Cancer resistance in the blind mole rat is mediated by concerted necrotic cell death mechanism. Proceedings of the National Academy of Sciences of the United States of America *109*, 19392–19396.
49. Gordon, S., and Taylor, P.R. (2005). Monocyte and macrophage heterogeneity. Nature Reviews. Immunology *5*, 953–964.
50. Gough, D.J., Messina, N.L., Clarke, C.J., Johnstone, R.W., and Levy, D.E. (2012). Constitutive type I interferon modulates homeostatic balance through tonic signaling. Immunity *36*, 166–174.
51. Green, D.R., and Victor, B. (2012). The pantheon of the fallen: why are there so many forms of cell death? Trends in Cell Biology *22*, 555–556.

52. Hakem, R., Hakem, A., Duncan, G.S., and Henderson…, J.T. (1998). Differential requirement for caspase 9 in apoptotic pathways in vivo. Cell *94,* 339–352.
53. Han, C.Z., and Ravichandran, K.S. (2011). Metabolic connections during apoptotic cell engulfment. Cell *147*, 1442–1445.
54. Han, J., Zhong, C.-Q.Q., and Zhang, D.-W.W. (2011). Programmed necrosis: backup to and competitor with apoptosis in the immune system. Nature Immunology *12*, 1143–1149.
55. Hayden, M.S., and Ghosh, S. (2008). Shared principles in NF-kappaB signaling. Cell *132*, 344–362.
56. He, S., Liang, Y., Shao, F., and Wang, X. (2011). Toll-like receptors activate programmed necrosis in macrophages through a receptor-interacting kinase-3-mediated pathway. Proceedings of the National Academy of Sciences of the United States of America *108*, 20054–20059.
57. He, S., Wang, L., Miao, T., Wang, T., Du, F., Zhao, L., and Wang, X. (2009) Receptor interacting protein kinase-3 determines cellular necrotic response to TNF-α. Cell *137*, 1100–1111.
58. Hitomi, J., Christofferson, D.E., Ng, A., Yao, J., Degterev, A., Xavier, R.J., and Yuan, J. (2008). Identification of a molecular signaling network that regulates a cellular necrotic cell death pathway. Cell *135*, 1311–1323.
59. Holler, N., Zaru, R., Micheau, O., Thome, M., Attinger, A., Valitutti, S., Bodmer, J.L., Schneider, P., Seed, B., and Tschopp, J. (2000). Fas triggers an alternative, caspase-8-independent cell death pathway using the kinase RIP as effector molecule. Nature Immunology *1*, 489–495.
60. Honda, K., and Taniguchi, T. (2006). IRFs: master regulators of signalling by Toll-like receptors and cytosolic pattern-recognition receptors. Nature Reviews. Immunology *6*, 644–658.
61. Hopkins, W.G. and Hüner, N.P.A. (2008) Introduction to plant physiology (Wiley, Hoboken, NJ).
62. Hu, X., Herrero, C., Li, W.-P., Antoniv, T.T., Falck-Pedersen, E., Koch, A.E., Woods, J.M., Haines, K.G., and Ivashkiv, L.B. (2002). Sensitization of IFN-Jak-STAT signaling during macrophage activation. Nature Immunology *3*, 859–866.
63. Husak, L, Marcuzzi, A, Herring, J, Wen, E, Yin, L, Capan, DD, and Cernat, G (2010). National analysis of sepsis hospitalizations and factors contributing to sepsis in-hospital mortality in Canada. Healthcare Quarterly (Toronto, Ont.) *13*, 35–41.
64. Huys, L., Van Hauwermeiren, F., Dejager, L., Dejonckheere, E., Lienenklaus, S., Weiss, S., Leclercq, G., and Libert, C. (2009). Type I interferon drives tumor necrosis factor-induced lethal shock. The Journal of Experimental Medicine *206*, 1873–1882.
65. Imre, G., Larisch, S., and Rajalingam, K. (2011). Ripoptosome: a novel IAP-regulated cell death-signalling platform. Journal of Molecular Cell Biology *3*, 324–326.
66. Isaacs, A., and Lindenmann, J. (1957). Virus interference. I. The interferon. Proceedings of the Royal Society B. Biological Sciences *147*, 258–267.
67. Ivashkiv, L.B., and Donlin, L.T. (2014). Regulation of type I interferon responses. Nature Reviews. Immunology *14*, 36–49.
68. Jaeschke, H. (2006). Mechanisms of Liver Injury. II. Mechanisms of neutrophil-induced liver cell injury during hepatic ischemia-reperfusion and other acute inflammatory conditions. American Journal of Physiology. Gastrointestinal and Liver Physiology *290*, G1083–8.

69. Joung, SM, Park, ZY, Rani, S, and Takeuchi, O (2011). Akt contributes to activation of the TRIF-dependent signaling pathways of TLRs by interacting with TANK-binding kinase 1. The Journal of Immunology *186* 499–507.
70. Kaczmarek, A., Vandenabeele, P., and Krysko, D.V. (2013). Necroptosis: The release of damage-associated molecular patterns and its physiological relevance. Immunity *38*, 209–223.
71. Kagan, J.C., Su, T., Horng, T., Chow, A., Akira, S., and Medzhitov, R. (2008). TRAM couples endocytosis of Toll-like receptor 4 to the induction of interferon-beta. Nature Immunology *9*, 361–368.
72. Kaiser, W.J., Sridharan, H., Huang, C., Mandal, P., Upton, J.W., Gough, P.J., Sehon, C.A., Marquis, R.W., Bertin, J., and Mocarski, E.S. (2013). Toll-like receptor 3-mediated necrosis via TRIF, RIP3, and MLKL. The Journal of Biological Chemistry*288*, 31268–31279.
73. Kalluri, R., and Zeisberg, M. (2006). Fibroblasts in cancer. Nature Reviews. Cancer *6*, 392–401.
74. Kawai, T., and Akira, S. (2006). TLR signaling. Cell Death and Differentiation *13*, 816–825.
75. Kelliher, M.A., Grimm, S., Ishida, Y., Kuo, F., Stanger, B.Z., and Leder, P. (1998). The death domain kinase RIP mediates the TNF-induced NF- B signal. Immunity *8*, 297–303.
76. Kerr, J.F., Wyllie, A.H., and Currie, A.R. (1972). Apoptosis: a basic biological phenomenon with wide-ranging implications in tissue kinetics. British Journal of Cancer *26*, 239–257.
77. Keskitalo, J., Bergquist, G., and Gardeström…, P. (2005). A cellular timetable of autumn senescence. American Society of Plant Biologists *139*, 1635–1648.
78. Khan, N., Lawlor, K.E., Murphy, J.M., and Vince, J.E. (2014). More to life than death: molecular determinants of necroptotic and non-necroptotic RIP3 kinase signaling. Current Opinion in Immunology *26*, 76–89.
79. Kim, S.J., and Li, J. (2013). Caspase blockade induces RIP3-mediated programmed necrosis in Toll-like receptor-activated microglia. Cell Death & Disease *4*, e716.
80. Kimura,T., Kadokawa, Y., Harada, H., Matsumoto, M., Sato, M., Kashiwazaki, T., Tarutani, M., Tan, R.S., Takasugi, T., Matsuyama, T., et al. (1996) Essential and non-redundant roles of p48 (ISGF3 gamma) and IRF-1 in both type I and type II interferon responses, as revealed by gene targeting studies. Genes Cells *1*, 115–124.
81. Kolumam, G.A., Thomas, S., Thompson, L.J., Sprent, J. and Murali-Krishna, K. (2005) Type I interferons act directly on CD8 T cells to allow clonal expansion and memory formation in response to viral infection. Journal of Experimental Medicine *202*, 637–650.
82. Komander, D, and Rape, M (2012). The ubiquitin code. Annual Review of Biochemistry *81*, 203–229.
83. Kroemer, G., Galluzzi, L., and Vandenabeele…, P. (2008). Classification of cell death: recommendations of the Nomenclature Committee on Cell Death 2009. Cell Death and Differentiation *16*, 3–11.
84. Kumari, S., Mg, S., and Mayor, S. (2010). Endocytosis unplugged: multiple ways to enter the cell. Cell Research *20*, 256–275.
85. Kuroda, M.J. (2010). Macrophages: do they impact AIDS progression more than CD4 T cells? Journal of Leukocyte Biology *87*, 569–573.

86. Kurt-Jones, E.A., Sandor, F., Ortiz, Y., Bowen, G.N., Counter, S.L., Wang, T.C., and Finberg, R.W. (2004). Use of murine embryonic fibroblasts to define Toll-like receptor activation and specificity. Journal of Endotoxin Research *10*, 419–424.
87. Lawen, A. (2003). Apoptosis—an introduction. BioEssays *25*, 888–896.
88. Laukens, B., Jennewein, C., Schenk, B., Vanlangenakker, N., Schier, A., Cristofanon, S., Zobel, K., Deshayes, K., Vucic, D., Jeremias, I., et al. (2011). Smac mimetic bypasses apoptosis resistance in FADD- or caspase-8-deficient cells by priming for tumor necrosis factor α-induced necroptosis. Neoplasia (New York, N.Y.) *13*, 971–979.
89. Lemaire, C., Andréau, K., Souvannavong, V., and Adam, A. (1998). Inhibition of caspase activity induces a switch from apoptosis to necrosis. FEBS Letters *425*, 266–270.
90. Levy, M.M., Dellinger, R.P., Townsend, S.R., Linde-Zwirble, W.T., Marshall, J.C., Bion, J., Schorr, C., Artigas, A., Ramsay, G., Beale, R., et al. (2010). The Surviving Sepsis Campaign: results of an international guideline-based performance improvement program targeting severe sepsis. Intensive Care Medicine *36*, 222–231.
91. Li, J., McQuade, T., Siemer, A.B., Napetschnig, J., Moriwaki, K., Hsiao, Y.-S.S., Damko, E., Moquin, D., Walz, T., McDermott, A., et al. (2012). The RIP1/RIP3 necrosome forms a functional amyloid signaling complex required for programmed necrosis. Cell *150*, 339–350.
92. Lin, Y., Devin, A., Rodriguez, Y., and Liu, Z.G. (1999). Cleavage of the death domain kinase RIP by caspase-8 prompts TNF-induced apoptosis. Genes & Development *13*, 2514–2526.
93. Linkermann, A., and Green, D.R. (2014). Necroptosis. The New England Journal of Medicine *370*, 455–465.
94. Liu, Y.C., Penninger, J., and Karin, M. (2005). Immunity by ubiquitylation: a reversible process of modification. Nature Reviews. Immunology *5*, 941–952.
95. Liu, B., Xu, N., Man, Y., Shen, H., Avital, I., Stojadinovic, A., and Liao, D.J. (2013). Apoptosis in Living Animals Is Assisted by Scavenger Cells and Thus May Not Mainly Go through the Cytochrome C-Caspase Pathway. Journal of Cancer *4*, 716–723.
96. Lockshin, R.A., and Zakeri, Z. (2001). Programmed cell death and apoptosis: origins of the theory. Nature Reviews. Molecular Cell Biology *2*, 545–550.
97. Maeda, A., and Fadeel, B. (2014). Mitochondria release by cells undergoing TNF-α-induced necroptosis acts as danger signals. Cell Death and Disease *5*, e1312; doi: 10.1038/cddis.2014.277.
98. Macia, E., Ehrlich, M., Massol, R., Boucrot, E., Brunner, C., and Kirchhausen, T. (2006). Dynasore, a cell-permeable inhibitor of dynamin. Developmental Cell *10*, 839–850.
99. Mancuso, G., Midiri, A., Biondo, C., Beninati, C., Zummo, S., Galbo, R., Tomasello, F., Gambuzza, M., Macri, G., Ruggeri, A., Leanderson, T., and Teti, G. (2007) Type I interferon signalling is crucial for host resistance to different species of pathogenic bacteria. Journal of Immunology (Baltimore, Md. : 1950) *178*, 3126–3133.
100. Majno, G., and Joris, I. (1995). Apoptosis, oncosis, and necrosis. An overview of cell death. The American Journal of Pathology *146*, 3–15.
101. Martin, S.J. (1993). Apoptosis: suicide, execution or murder? Trends in Cell Biology *3*, 141–144.
102. McCall, K. (2010). Genetic control of necrosis - another type of programmed cell death. Current Opinion in Cell Biology *22*, 882–888.

103. McComb, S., Cessford, E., Alturki, N.A., Joseph, J., Shutinoski, B., Startek, J.B., Gamero, A.M., Mossman, K.L., and Sad, S. (2014). Type-I interferon signaling through ISGF3 complex is required for sustained Rip3 activation and necroptosis in macrophages. Proceedings of the National Academy of Sciences of the United States of America. *111*, E3206–13.
***SCOTT MCCOMB AND ERIN CESSFORD ARE CO-FIRST AUTHORS**

104. McComb, S., Cheung, H.H., Korneluk, R.G., Wang, S., Krishnan, L., and Sad, S. (2012). cIAP1 and cIAP2 limit macrophage necroptosis by inhibiting Rip1 and Rip3 activation. Cell Death and Differentiation *19*, 1791–1801.

105. McComb, S., Shutinoski, B., Thurston, S., Cessford, E., Kumar, K., and Sad, S. (2014). Cathepsins Limit Macrophage Necroptosis through Cleavage of Rip1 Kinase. Journal of Immunology (Baltimore, Md. : 1950) *192*, 5671–5678.

106. Medzhitov, R. (2001). Toll-like receptors and innate immunity. Nature Reviews. Immunology *1*, 135–145.
107. Medzhitov, R. (2007). Recognition of microorganisms and activation of the immune response. Nature *449*, 819–826.
108. Medzhitov, R. (2008). Origin and physiological roles of inflammation. Nature *454*, 428–435.
109. Medzhitov, R., and Horng, T. (2009). Transcriptional control of the inflammatory response. Nature Reviews. Immunology *9*, 692–703.
110. Medzhitov, R., and Janeway, C.A. (1997). Innate immunity: the virtues of a nonclonal system of recognition. Cell *91*, 295–298.
111. Meier, P., Finch, A., and Evan, G. (2000). Apoptosis in development. Nature *407*, 796–801.
112. Meraz, M.A., White, J.M., Sheehan, K.C., Bach, E.A., Rodig, S.J., Dighe, A.S., Kaplan, D.H., Riley, J.K., Greenlund, A.C., Campbell, D., et al. (1996). Targeted disruption of the Stat1 gene in mice reveals unexpected physiologic specificity in the JAK-STAT signaling pathway. Cell *84*, 431–442.
113. Morrissette, N., Gold, E., and Aderem, A. (1999). The macrophage--a cell for all seasons. Trends in Cell Biology *9*, 199–201.
114. Mosser, DM, and Edwards, JP (2008). Exploring the full spectrum of macrophage activation. Nature Reviews. Immunology *8*, 958–969.
115. Moujalled, D.M., Cook, W.D., Okamoto, T., Murphy, J., Lawlor, K.E., Vince, J.E., and Vaux, D.L. (2013). TNF can activate RIPK3 and cause programmed necrosis in the absence of RIPK1. Cell Death & Disease *4*, e465.
116. Murphy, J.M., Czabotar, P.E., Hildebrand, J.M., Lucet, I.S., Zhang, J.-G.G., Alvarez-Diaz, S., Lewis, R., Lalaoui, N., Metcalf, D., Webb, A.I., et al. (2013). The pseudokinase MLKL mediates necroptosis via a molecular switch mechanism. Immunity *39*, 443–453.
117. Müller, U., Steinhoff, U., Reis, L.F., Hemmi, S., Pavlovic, J., Zinkernagel, R.M. and Aguet, M. (1994) Functional role of type I and type II interferons in antiviral defense. Science *264***,** 1918–1921.
118. Murphy, K.P., Travers, P., Walport, M. and Janeway, C. (2008) Janeway's immunobiology (Garland Science).
119. Muzio, M., Ni, J., Feng, P., and Dixit, V. (1997). IRAK (Pelle) Family Member IRAK-2 and MyD88 as Proximal Mediators of IL-1 Signaling. Science *278*, 1612–1615.

120. Newton, K., and Dixit, V.M. (2012) Signaling in innate immunity and inflammation. Cold Spring Harbor Perspectives in Biology *4*:a006049.
121. Newton, K., Sun, X., and Dixit, V.M. (2004). Kinase RIP3 is dispensable for normal NF-kappa Bs, signaling by the B-cell and T-cell receptors, tumor necrosis factor receptor 1, and Toll-like receptors 2 and 4. Molecular and Cellular Biology*24*, 1464–1469.
122. Northington, F.J., Chavez-Valdez, R., Graham, E.M., Razdan, S., Gauda, E.B., and Martin, L.J. (2011). Necrostatin decreases oxidative damage, inflammation, and injury after neonatal HI. Journal of Cerebral Blood Flow and Metabolism : Official Journal of the International Society of Cerebral Blood Flow and Metabolism *31*, 178–189.
123. Ofengeim, D., and Yuan, J. (2013). Regulation of RIP1 kinase signalling at the crossroads of inflammation and cell death. Nature Reviews. Molecular Cell Biology *14*, 727–736.
124. O'Neill, L., and Bowie, AG (2007). The family of five: TIR-domain-containing adaptors in Toll-like receptor signalling. Nature Reviews. Immunology *7*, 353–364.
125. Palecanda, A., Paulauskis, J., Al-Mutairi, E., Imrich, A., Qin, G., Suzuki, H., Kodama, T., Tryggvason, K., Koziel, H., and Kobzik, L. (1999). Role of the scavenger receptor MARCO in alveolar macrophage binding of unopsonized environmental particles. The Journal of Experimental Medicine *189*, 1497–1506.
126. Park, C., Li, S., Cha, E. and Schindler, C. (2000). Immune response in Stat2 knockout mice. Immunity *13*, 795–804.
127. Pearse, B.M. (1976). Clathrin: a unique protein associated with intracellular transfer of membrane by coated vesicles. Proceedings of the National Academy of Sciences of the United States of America *73*, 1255–1259.
128. Pestka, S., Krause, C.D., and Walter, M.R. (2004). Interferons, interferon-like cytokines, and their receptors. Immunological Reviews *202*, 8–32.
129. Peter, M.E., and Krammer, P.H. (2003). The CD95 (APO-1/Fas) DISC and beyond. Cell Death and Differentiation *10*, 26–35.
130. Pettigrew, C.A., and Cotter, T.G. (2009). Deregulation of cell death (apoptosis): implications for tumor development. Discovery Medicine *8*, 61–63.
131. Qin, H., Srinivasula, S.M., Wu, G., and Fernandes-Alnemri…, T. (1999). Structural basis of procaspase-9 recruitment by the apoptotic protease-activating factor 1. Nature *399*, 549–557.
132. Rauert, H., Wicovsky, A., Muller, N., Siegmund, D., Spindler, V., Waschke, J., Kneitz, C., and Wajant, H. (2009). Membrane Tumor Necrosis Factor (TNF) Induces p100 Processing via TNF Receptor-2 (TNFR2). Journal of Biological Chemistry *285*, 7394–7404.
133. Riedl, S.J., and Salvesen, G.S. (2007). The apoptosome: signalling platform of cell death. Nature Reviews Molecular Cell Biology *8*, 405–413.
134. Robinson, N., McComb, S., Mulligan, R., Dudani, R., Krishnan, L., and Sad, S. (2012). Type I interferon induces necroptosis in macrophages during infection with Salmonella enterica serovar Typhimurium. Nature Immunology *13*, 954–962.
135. Ross, R. (1999). Atherosclerosis--an inflammatory disease. The New England Journal of Medicine *340*, 115–126.
136. Rothberg, K.G., Heuser, J.E., Donzell, W.C., Ying, Y.S., Glenney, J.R., and Anderson, R.G. (1992). Caveolin, a protein component of caveolae membrane coats. Cell *68*, 673–682.

137. Russel, P.J., Hertz, P.E., McMillan, B., Fenton, B., Addy, H., Maxwell, D., Haffie, T., and Milson, B. (2013) Biology: Exploring the diversity of life (Nelson Eduction Ltd).
138. Saelens, X., Festjens, N., Vande Walle, L., van Gurp, M., van Loo, G., and Vandenabeele, P. (2004). Toxic proteins released from mitochondria in cell death. Oncogene *23*, 2861–2874.
139. Safa, A.R., Day, T.W., and Wu, T.H. (2008) Cellular FLICE-like inhibitory protein (c-FLIP): a novel target for cancer therapy. Current Cancer Drug Targets *8*, 37–46.
140. Sato, M., Suemori, H., Hata, N., Asagiri, M., Ogasawara, K., Nakao, K., Nakaya, T., Katsuki, M., Noguchi, S., Tanaka, N., et al. (2000). Distinct and essential roles of transcription factors IRF-3 and IRF-7 in response to viruses for IFN-alpha/beta gene induction. Immunity *13*, 539–548.
141. Schmid, S., Mordstein, M., Kochs, G., García-Sastre, A., and Tenoever, B.R. (2010). Transcription factor redundancy ensures induction of the antiviral state. The Journal of Biological Chemistry *285*, 42013–42022.
142. Schmitz, I., Kirchhoff, S., and Krammer, P.H. (2000). Regulation of death receptor-mediated apoptosis pathways. The International Journal of Biochemistry and Cell Biology *32*, 1123–1136.
143. Schneider-Brachert, W., Tchikov, V., Neumeyer, J., Jakob, M., Winoto-Morbach, S., Held-Feindt, J., Heinrich, M., Merkel, O., Ehrenschwender, M., Adam, D., et al. (2004). Compartmentalization of TNF receptor 1 signaling: internalized TNF receptosomes as death signaling vesicles. Immunity*21*, 415–428.
144. Serhan, C.N., Chiang, N., and Van, T.E. (2008). Resolving inflammation: dual anti-inflammatory and pro-resolution lipid mediators. Nature Reviews. Immunology *8*, 349–361.
145. Shi, Y. (2004). Caspase activation: revisiting the induced proximity model. Cell *117*, 855–858.
146. Shih, V.F., Tsui, R., Caldwell, A., and Hoffmann, A. (2011). A single NFκB system for both canonical and non-canonical signaling.
147. Silva, M.T. (2010). Secondary necrosis: the natural outcome of the complete apoptotic program. FEBS Letters *584*, 4491–4499.
148. Slee, E.A., Zhu, H., Chow, S.C., MacFarlane, M., Nicholson, D.W., and Cohen, G.M. (1996). Benzyloxycarbonyl-Val-Ala-Asp (OMe) fluoromethylketone (Z-VAD.FMK) inhibits apoptosis by blocking the processing of CPP32. The Biochemical Journal *315 (Pt 1)*, 21–24.
149. Smythies, L.E., Sellers, M., Clements, R.H., Mosteller-Barnum, M., Meng, G., Benjamin, W.H., Orenstein, J.M., and Smith, P.D. (2005). Human intestinal macrophages display profound inflammatory anergy despite avid phagocytic and bacteriocidal activity. The Journal of Clinical Investigation *115*, 66–75.
150. Sorkin, A., and Von Zastrow, M. (2002). Signal transduction and endocytosis: close encounters of many kinds. Nature Reviews. Molecular Cell Biology *3*, 600–614.
151. Stuart, L.M., and Ezekowitz, R.A. (2008). Phagocytosis and comparative innate immunity: learning on the fly. Nature Reviews. Immunology *8*, 131–141.
152. Sun, L., Wang, H., Wang, Z., He, S., Chen, S., Liao, D., and Wang…, L. (2012). Mixed lineage kinase domain-like protein mediates necrosis signaling downstream of RIP3 kinase. Cell *148*, 213–227.
153. Takeuchi, O., and Akira, S. (2010). Pattern recognition receptors and inflammation. Cell *140*, 805–820.

154. Taylor, P.R., Brown, G.D., Reid, D.M., Willment, J.A., Martinez-Pomares, L., Gordon, S., and Wong, S.Y. (2002). The beta-glucan receptor, dectin-1, is predominantly expressed on the surface of cells of the monocyte/macrophage and neutrophil lineages. Journal of Immunology (Baltimore, Md. : 1950) *169*, 3876–3882.
155. Tenev, T., Bianchi, K., Darding, M., Broemer, M., Langlais, C., Wallberg, F., Zachariou, A., Lopez, J., MacFarlane, M., Cain, K., et al. (2011). The Ripoptosome, a signaling platform that assembles in response to genotoxic stress and loss of IAPs. Molecular Cell *43*, 432–448.
156. Thapa, R.J., Nogusa, S., Chen, P., Maki, J.L., Lerro, A., Andrake, M., Rall, G.F., Degterev, A., and Balachandran, S. (2013). Interferon-induced RIP1/RIP3-mediated necrosis requires PKR and is licensed by FADD and caspases. Proceedings of the National Academy of Sciences of the United States of America *110*, E3109–18.
157. Ting, A.T., Pimentel-Muiños, F.X., and Seed, B. (1996). RIP mediates tumor necrosis factor receptor 1 activation of NF-kappaB but not Fas/APO-1-initiated apoptosis. The EMBO Journal *15*, 6189–6196.
158. Tsuno, T., Mejido, J., Zhao, T., Schmeisser, H., Morrow, A., and Zoon, K.C. (2009). IRF9 is a key factor for eliciting the antiproliferative activity of IFN-alpha. Journal of Immunotherapy (Hagerstown, Md. : 1997) *32*, 803–816.
159. Upton, J.W., Kaiser, W.J., and Mocarski, E.S. (2010). Virus inhibition of RIP3-dependent necrosis. Cell Host & Microbe *7*, 302–313.
160. Van der Poll, T., and Opal, S.M. (2008). Host-pathogen interactions in sepsis. The Lancet Infectious Diseases *8*, 32–43.
161. Vanden Berghe, T., Vanlangenakker, N., Parthoens, E., Deckers, W., Devos, M., Festjens, N., Guerin, C.J., Brunk, U.T., Declercq, W., and Vandenabeele, P. (2010). Necroptosis, necrosis and secondary necrosis converge on similar cellular disintegration features. Cell Death and Differentiation *17*, 922–930.
162. Vandenabeele, P., Galluzzi, L., Vanden Berghe, T., and Kroemer, G. (2010). Molecular mechanisms of necroptosis: an ordered cellular explosion. Nature Reviews. Molecular Cell Biology *11*, 700–714.
163. Vanlangenakker, N., Bertrand, M.J., Bogaert, P., Vandenabeele, P., and Vanden Berghe, T. (2011). TNF-induced necroptosis in L929 cells is tightly regulated by multiple TNFR1 complex I and II members. Cell Death & Disease *2*, e230.
164. Vanlangenakker, N., Vanden Berghe, T., and Vandenabeele, P. (2012). Many stimuli pull the necrotic trigger, an overview. Cell Death and Differentiation *19*, 75–86.
165. Vercammen, D., Beyaert, R., Denecker, G., Goossens, V., Van Loo, G., Declercq, W., Grooten, J., Fiers, W., and Vandenabeele, P. (1998). Inhibition of caspases increases the sensitivity of L929 cells to necrosis mediated by tumor necrosis factor. The Journal of Experimental Medicine *187*, 1477–1485.
166. Vercammen, D., Brouckaert, G., Denecker, G., Van de Craen, M., Declercq, W., Fiers, W., and Vandenabeele, P. (1998). Dual signaling of the Fas receptor: initiation of both apoptotic and necrotic cell death pathways. The Journal of Experimental Medicine *188*, 919–930.
167. Volkman, A., and Gowans, J.L. (1965). The origin of macrophages from bone marrow in the rat. British Journal of Experimental Pathology *46*, 62–70.
168. Wallach, D., Varfolomeev, E.E., Malinin, N.L., Goltsev, Y.V., Kovalenko, A.V., and Boldin, M.P. (1999). Tumor necrosis factor receptor and Fas signaling mechanisms. Annual Review of Immunology *17*, 331–367.

169. Wang, H., Sun, L., Su, L., Rizo, J., Liu, L., Wang, L.F., and Wang…, F.S. (2014). Mixed lineage kinase domain-like protein MLKL causes necrotic membrane disruption upon phosphorylation by RIP3. Molecular Cell *54*, 133–146.
170. Wang, Z., Jiang, H., Chen, S., Du, F., and Wang, X. (2012). The mitochondrial phosphatase PGAM5 functions at the convergence point of multiple necrotic death pathways. Cell *148*, 228–243.
171. Warner, N., and Núñez, G. (2013). MyD88: a critical adaptor protein in innate immunity signal transduction. The Journal of Immunology *190*, 3–4.
172. Wiersinga, W.J., Leopold, S.J., Cranendonk, D.R., and van der Poll, T. (2014). Host innate immune responses to sepsis. Virulence *5*, 36–44.
173. Wong, W., Gentle, I.E., and Nachbur, U. (2010). RIPK1 is not essential for TNFR1-induced activation of NF-κB. Cell Death and Differentiation *17*, 482–487.
174. Wu, J., Huang, Z., Ren, J., Zhang, Z., He, P., Li, Y., Ma, J., Chen, W., Zhang, Y., Zhou, X., et al. (2013). Mlkl knockout mice demonstrate the indispensable role of Mlkl in necroptosis. Cell Research *23*, 994–1006.
175. Wullaert, A., Bonnet, M.C., and Pasparakis, M. (2011). NF- B in the regulation of epithelial homeostasis and inflammation. Cell Research *21*, 146–158.
176. Wyllie, A.H., Kerr, F.R., and Currie, A.R. (1980). Cell death: the significance of apoptosis. International Review of Cytology *68*, 251–306.
177. Wynn, T.A., Chawla, A., and Pollard, J.W. (2013). Macrophage biology in development, homeostasis and disease. Nature *496*, 445–455.
178. Yarilina, A., Park-Min, K.-H.H., Antoniv, T., Hu, X., and Ivashkiv, L.B. (2008). TNF activates an IRF1-dependent autocrine loop leading to sustained expression of chemokines and STAT1-dependent type I interferon-response genes. Nature Immunology *9*, 378–387.
179. Zhang, D.-W.W., Shao, J., Lin, J., Zhang, N., Lu, B.-J.J., Lin, S.-C.C., Dong, M.-Q.Q., and Han, J. (2009). RIP3, an energy metabolism regulator that switches TNF-induced cell death from apoptosis to necrosis. Science (New York, N.Y.) *325*, 332–336.
180. Zhao, J., Jitkaew, S., Cai, Z., Choksi, S., Li, Q., Luo, J., and Liu, Z.-G.G. (2012). Mixed lineage kinase domain-like is a key receptor interacting protein 3 downstream component of TNF-induced necrosis. Proceedings of the National Academy of Sciences of the United States of America *109*, 5322–5327.
181. Zhu, H., Fearnhead, H.O., and Cohen, G.M. (1995). An ICE-like protease is a common mediator of apoptosis induced by diverse stimuli in human monocytic THP.1 cells. FEBS Letters *374*, 303–308.

8.0 CONTRIBUTION OF COLLABORATORS

Collaborator	Affiliation(s)	Contribution to Thesis Work
Dr. Subash Sad	University of Ottawa	Supervisor
Dr. Kathryn Wright	University of Ottawa	Thesis Advisory Committee Member
Dr. Robert G. Korneluk	University of Ottawa	Thesis Advisory Committee Member
Dr. Karen L. Mossman	McMaster University	Provided bones from IRF3-/-, IRF7 -/-, IRF3/7-/- and IRF9-/- mice
Dr. Ana M. Gamero	Temple University School of Medicine	Provided bones from WT and STAT2 -/- mice
Dr. Shaomeng Wang	University of Michigan	Synthesized and provided SMAC mimetic 164

ERIN CESSFORD

EDUCATION

MSc. Microbiology and Immunology Candidate **September 2012 - Present**
(University of Ottawa, Ottawa, ON)

- Research-based thesis under the supervision of Dr. Subash Sad at the University of Ottawa to be completed in Fall 2014
- Investigating the mechanistic relationship between type I interferon signaling and necroptosis in the innate immune response
- Techniques used include western blotting, immunofluorescence, cell culture, cell viability assays and animal work using a mouse model

Bachelor of Science, Honours Specialization in Biology **September 2008 – August 2012**
(The University of Western Ontario, London, ON)

- Course and laboratory based undergraduate program with heavy interest in organismal physiology
- Deans Honour List

PUBLICATIONS

***Cessford, E.,** *McComb, S., Alturki, N.A., Joseph, J., Shutinoski, B., Startek, J.B., Gamero, A.M., Mossman, K.L., and Sad, S. (2014). Type-I interferon signaling through ISGF3 complex is required for sustained Rip3 activation and necroptosis in macrophages. Proceedings of the National Academy of Sciences of the United States of America *111*, E3206–13.

* Co-first authors

McComb, S., Shutinoski, B., Thurston, S., **Cessford, E.,** Kumar, K., and Sad, S. (2014). Cathepsins limit macrophage necroptosis through cleavage of Rip1 kinase. Journal of Immunology *192*, 5671–5678.

ACADEMIC AWARDS

1st place in the 2014 Annual Biochemistry, Microbiology and Immunology Seminar Day Competition

2nd place in the 2013 Annual University of Ottawa Biochemistry, Microbiology and Immunology Poster Day Competition

WORK EXPERIENCE

Server **May 2009 - May 2010, September 2010 – April 2012**

Malibu Restaurant (London, ON)

- Responsible for providing courteous, friendly customer service
- Opening and closing duties such as overall cleanliness of the restaurant
- Responsible for handling money transactions

Server **May 2010 - August 2010**

Montana's Restaurant (Kingston, ON)

- Responsible for providing courteous, friendly customer service
- Dealt with various forms of money transactions
- Responsible for designated shift cleaning duties, keeping a clean section and ensuring the overall cleanliness of the restaurant
- Occasional food expediting shifts

Weekend Barn Manager and Evening Night Checks **September 2006 - August 2008**

Dewmont Farms (Ashton, ON)

- In charge of the care, maintenance and well-being of 25 horses
- Responsible for maintaining a cleanly environment
- Responsible for the basic health care of the horses
- Weekly evening night check shifts where I was responsible for feeding and watering 25 horses, cleaning stalls and ensuring barn was clean before turning lights off and closing up

Summer Day Camp Counselor/Instructor **June - August in 2004-2006**

Swallow Creek Farms (Carp, ON)

- In charge of the well-being and safety of the children and horses
- Responsible for maintaining a cleanly environment
- Responsible for instructing theory lessons and riding lessons

VOLUNTEER WORK

Long Point Waterfowl Research Facility (Simcoe, ON)

- Spent a weekend in July, 2011 helping Dr. Scott Petrie at the Long Point Waterfowl research centre

Member of the Canadian Cancer Society Awareness Club at the University of Western Ontario

TECHNICAL SKILLS

- Level 1 and level 2 laboratory experience
- Laboratory animal experience (emphasis on mouse work)
- Data entry and analysis utilizing SPSS
- Microsoft word, excel and powerpoint skills, Graphpad Prism

EXTRACURRICULAR ACTIVITIES

- Horseback rider
- Volleyball player
- Snowboarder